NAVAL SHIP RESEARCH AND DEVELOPMENT CENTER
BETHESDA, MD 20034

EFFECTS OF MICROSTRUCTURE, COMPOSITION, AND STRENGTH ON THE NIL DUCTILITY TRANSITION (NDT) TEMPERATURE OF HY-80 STEEL

by

Marcel L. Salive

STRUCTURES DEPARTMENT
RESEARCH AND DEVELOPMENT REPORT

January 1972

Report 3722

Report 3722
EFFECTS OF MICROSTRUCTURE, COMPOSITION, AND STRENGTH ON THE NIL DUCTILITY TRANSITION (NDT) TEMPERATURE OF HY-80 STEEL

The Naval Ship Research and Development Center is a U. S. Navy center for laboratory effort directed at achieving improved sea and air vehicles. It was formed in March 1967 by merging the David Taylor Model Basin at Carderock, Maryland with the Marine Engineering Laboratory at Annapolis, Maryland. The Mine Defense Laboratory (now Naval Ship R & D Laboratory) Panama City, Florida became part of the Center in November 1967.

Naval Ship Research and Development Center

Bethesda, Md. 20034

MAJOR NSRDC ORGANIZATIONAL COMPONENTS

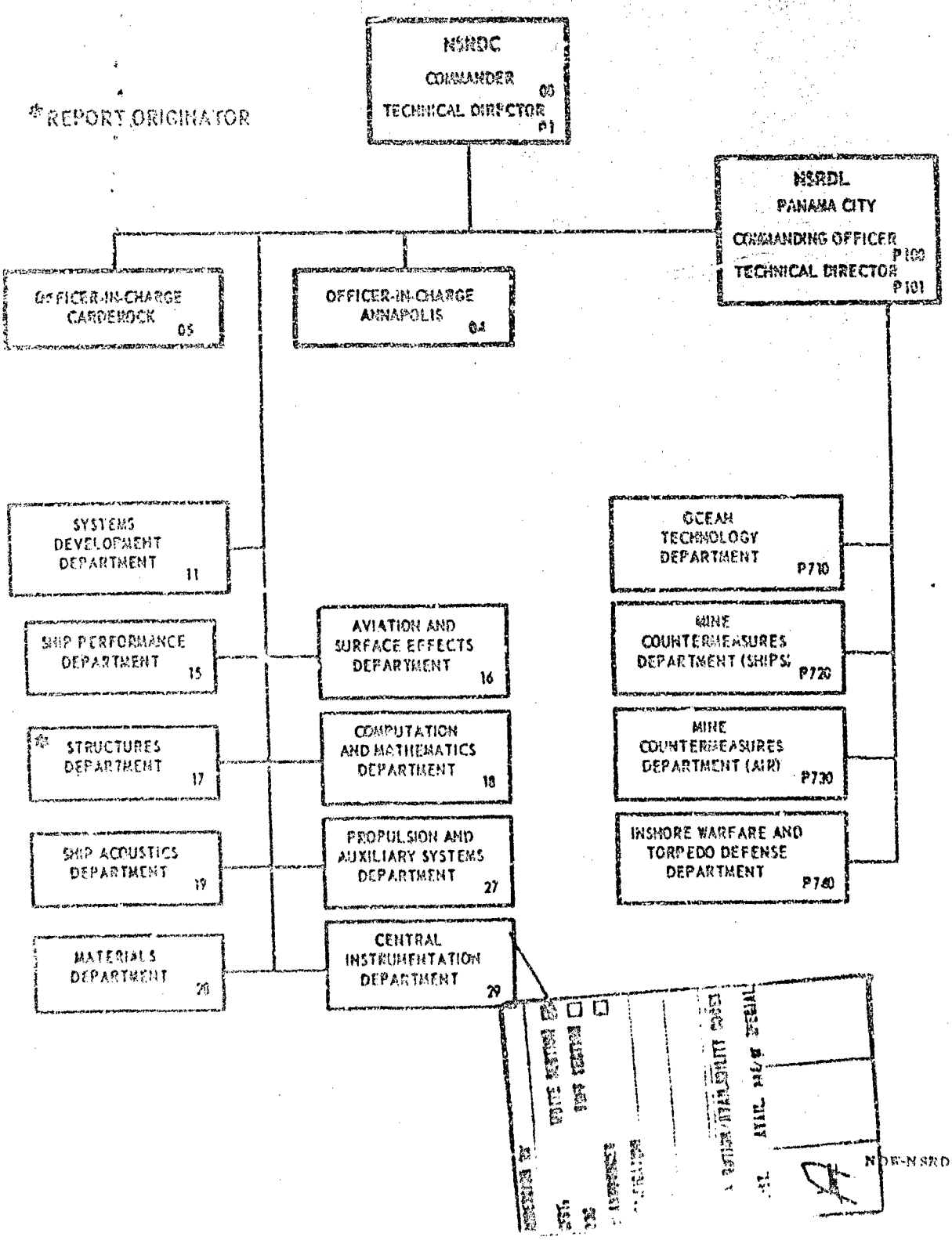

NAVSHIPS 3960/43 (8-71)

UNCLASSIFIED
Security Classification

DOCUMENT CONTROL DATA - R & D

Security classification of title, body of abstract and indexing annotation must be entered when the overall report is classified)

1 ORIGINATING ACTIVITY (Corporate author)

Naval Ship Research and Development Center
Bethesda, Maryland 20034

2a. REPORT SECURITY CLASSIFICATION

UNCLASSIFIED

2b. GROUP

3 REPORT TITLE

EFFECTS OF MICROSTRUCTURE, COMPOSITION, AND STRENGTH ON THE NIL DUCTILITY TRANSITION (NDT) TEMPERATURE OF HY-80 STEEL

4 DESCRIPTIVE NOTES (Type of report and inclusive dates)

Final Report

5 AUTHOR(S) (First name, middle initial, last name)

Marcel L. Salive

6 REPORT DATE	7a. TOTAL NO. OF PAGES	7b. NO. OF REFS
January 1972	131	54

8a CONTRACT OR GRANT NO.	9a. ORIGINATOR'S REPORT NUMBER(S)
b PROJECT NO SF 35.422.212 Program Element 62512N	3722
c.	9b. OTHER REPORT NO(S) (Any other numbers that may be assigned this report)
d.	

10 DISTRIBUTION STATEMENT

APPROVED FOR PUBLIC RELEASE: DISTRIBUTION UNLIMITED

11 SUPPLEMENTARY NOTES	12 SPONSORING MILITARY ACTIVITY
	Naval Ship Systems Command (NAVSHIPS)

13 ABSTRACT

Steel from 22 heats of low-carbon Ni-Cr-Mo steel, HY-80 (ASTM A543-65, and MIL-S-16216G (Ships)) was heat treated to study the effects on the drop weight nil ductility transition (NDT) temperature of (1) commercial variation in composition and inclusion content, (2) variation in microstructure such as prior austenitic grain size and the relative amount of isothermally produced ferrite or bainite in a tempered martensitic matrix, and (3) the observed variation in strength obtained after a one-hour 1150 F temper followed by water quench to prevent embrittlement while cooling from the tempering temperature.

Using a tempered 100 percent martensitic microstructure as a base line, the variables found to be most significant were linearly related to the measured Nil Ductility Transition (NDT) temperature. The range of the variable and its effect on the NDT temperature are as follows:

Variable	Range	Effect on NDT
Producer	(Coded 1 or 2)	- 21.9 F
Prior Austenitic Grain Size	(3 to 9.5)	- 19.2 F/ASTM G. S. No.
Percent Bainite	(0 to 76 percent)	0.62 F/Percent Bainite
Percent Ferrite	(0 to 69 percent)	- 0.23 F/Percent Ferrite
Percent Pearlite	(0 to 32 percent)	5.4 F/Percent Pearlite
Tensile Yield Strength	(61.5 to 124.7 ksi)	0.68 F/ksi

Higher order terms and interaction terms did not significantly improve the relationship, nor did consideration of inclusion content of the steel. Other than hydrogen, no alloying or trace elements were found to correlate with the measured NDT temperature of this steel.

DD FORM 1 NOV 68 1473 (PAGE 1)

S/N 0101-807-6801

UNCLASSIFIED
Security Classification

KEY WORDS	LINK A		LINK B		LINK C	
	ROLE	WT	ROLE	WT	ROLE	WT
Nil Ductility Transition Temperature						
NDT Temperature						
Ni-Cr-Mo Steel						
HY-80 Steel						
Composition						
Microstructure						
Austenite						
Bainite						
Ferrite						
Pearlite						
Grain Size						
Inclusions						
Strength						
Tensile Yield						

DEPARTMENT OF THE NAVY
NAVAL SHIP RESEARCH AND DEVELOPMENT CENTER
BETHESDA, MD 20034

EFFECTS OF MICROSTRUCTURE, COMPOSITION, AND STRENGTH ON THE NIL DUCTILITY TRANSITION (NDT) TEMPERATURE OF HY-80 STEEL

by

Marcel L. Salive

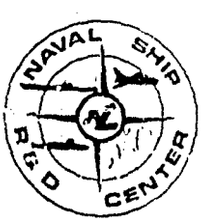

January 1972

Report 3722

TABLE OF CONTENTS

LIST OF FIGURES

APPENDIXES

Page

LIST OF TABLES

APPENDIX

ABSTRACT

Steel from 22 heats of low-carbon Ni-Cr-Mo steel, HY-80 (ASTM A543-65, and MIL-S-16216G (Ships)) was heat treated to study the effects on the drop weight nil ductility transition (NDT) temperature of (1) commercial variation in composition and inclusion content, (2) variation in microstructure such as prior austenitic grain size and the relative amount of isothermally produced ferrite or bainite in a tempered martensitic matrix, and (3) the observed variation in strength obtained after a one-hour 1150 F temper followed by a water quench to prevent embrittlement while cooling from the tempering temperature.

Using a tempered 100 percent martensitic microstructure as a base line, the variables found to be most significant were linearly related to the measured Nil Ductility Transition (NDT) temperature. The range of the variable and its effect on the NDT temperature are as follows:

Variable	Range	Effect on NDT
Producer	(Coded 1 or 2)	−21.9 F
Prior Austenitic Grain Size	(3 to 9.5)	−19.2 F/ASTM G. S. No.
Percent Bainite	(0 to 76 percent)	0.62 F/Percent Bainite
Percent Ferrite	(0 to 69 percent)	− 0.23 F/Percent Ferrite
Percent Pearlite	(0 to 32 percent)	5.4 F/Percent Pearlite
Tensile Yield Strength	(61.5 to 124.7 ksi)	0.68 F/ksi

Higher order terms and interaction terms did not significantly improve the relationship, nor did consideration of inclusion content of the steel. Other than hydrogen, no alloying or trace elements were found to correlate with the measured NDT temperature of this steel.

ADMINISTRATIVE INFORMATION

This work was performed under the sponsorship of the Naval Ship Systems Command (NAVSHIPS), as part of Research and Development Project SF 35.422.212 Program Element 62512N.

INTRODUCTION

At present there is a gap in the body of general metallurgical knowledge concerning the mechanisms that control the notch toughness, as measured by the drop weight nil ductility transition (NDT)* temperature of the low carbon, medium alloy, and quenched and tempered steels. Most prior studies have been limited to the process of characterizing specific classes of commercial steels by their expected NDT temperature frequency distribution range. No previous studies have been made of the interaction of chemical composition, mechanical properties and microstructure with the NDT temperature of any steel.

Studies of the notch toughness of higher alloy steels, such as those recently performed by U. S. Steel, have concerned themselves with the fracture mechanics or critical flaw size approach that is more appropriate for such higher strength, low toughness materials. Previous studies of the higher toughness steels, however, have always concerned themselves with the effect of variation in a single alloying element and usually only with its effect on strength or on some Charpy impact property. In addition, these previous studies have been concerned only with the effects on a normalized steel or on an oil quenched alloy steel of undetermined microstructure.

The normalized structural steels are gradually being replaced in critical, high toughness, low transition temperature applications by the medium alloy steels such as HY-80 and HY-100. Therefore, it is important that the mechanisms controlling the interaction of composition, mechanical properties, and microstructure with NDT temperature be determined. This is so, particularly since the NDT temperature is one of the most important criteria for the selection of a steel for structural application under severe service conditions.

There has long been an interest in the structural use of high toughness, low transition temperature steels, and more recently with the higher strength, quenched and tempered steels such as the ASTM A543-65 (Class I and Class II), MIL-S-16216G, HY-80, HY-100, and HY-130; these steels are currently being used for the shells of pressure vessels and hulls of oceanographic vehicles. The steel used in this study is a quenched and tempered medium alloy steel having an 85,000 psi yield strength and the following nominal percent composition: 0.16 C, 0.36 Mn, 0.015 P, 0.015 S, 0.25 Si, 2.75 Ni, 1.50 Cr and 0.35 Mo. This steel is commonly classed as a low carbon nickel-chrome-molybdenum alloy steel.

LITERATURE SURVEY

The impact transition temperature is some arbitrary point in the temperature range over which the fracture characteristics of a metal with a body centered cubic lattice, and sometimes with a hexagonal close packed lattice, exhibit a marked loss in ductility. This change is evidenced by (1) a large drop in the energy required to produce fracture, (2) a marked change in the fracture surface appearance from a dull, fibrous-looking transcrystalline shear fracture associated with high energy absorption to a bright, faceted cleavage or intercrystalline fracture associated with low energy absorption, and (3) a decrease in the amount of lateral contraction at the bottom of the notch used to initiate the crack, or a decrease in the amount of lateral expansion at the "hinge" point of the impact specimen opposite the notch. The temperature range over which this transition from ductile to brittle behavior occurs is sensitive to test conditions such as strain rate, notch acuity, and residual or applied stress levels, as well as the toughness of the material at the time of testing; as a result the transition range is usually determined by using a standardized impact specimen and test method to test the material at a series of temperatures.

*The NDT is the temperature of initial transition from plane strain to mixed-mode fracture and represents the temperature at which very small flaw sizes suffice for dynamic fracture initiation. The NDT temperature is generally not indexable to the sharply falling Charpy energy curve.

The "transition temperature" then is defined as that temperature in the transition range at which some specific condition occurs such as:

1. The fracture appearance transition temperature, FATT, is the temperature at which the specimen is 50 or 100 percent fibrous and is called the 50 percent FATT or the 100 percent FATT, respectively.

2. The fracture temperature is the temperature at which the Charpy V-notch (C_V) impact specimen absorbs some specific amount of energy. A common energy value used to characterize mild steel ship plate is 15 ft-lb; this criterion would be referred to as the Charpy V-notch 15 ft-lb transition temperature.

3. The temperature at which the drop weight impact test specimen exhibits no ductility is the NDT temperature, and is the temperature of initial transition from plane strain to mixed-mode fracture. The NDT temperature represents the temperature at which very small flaw sizes suffice for dynamic fracture initiation. The drop weight NDT temperature is not generally indexable to some specific point on the sharply falling Charpy energy curve.

An extensive body of literature exists on the effects of microstructure, composition, and strength on the impact transition temperature. The data are mainly concerned with the effects of alloy additions to plain carbon steels, or alloy steels having 0.30 percent or more carbon, whose microstructures are frequently not specified other than as resulting from a normalizing treatment, and these data often ignore the austenitic grain size of the steel prior to cooling. These studies are seldom based on the drop weight nil ductility transition temperature.

GRAIN SIZE EFFECT

Changes in grain size have been reported to have a detrimental effect on the ductile to brittle fracture transition temperature of steels.[1-32] Some authors report the effect of change in the average grain diameter, others in terms of the change in ASTM micrograin size. Some authors report grain size in terms of: (1) ferritic grain size as measured on a polished and etched section; (2) prior austenitic grain size, measured using the McQuaid-Ehn test method; (3) prior austenitic grain size as measured using an etheral picric acid etch to outline the prior austenitic grain boundaries on a polished specimen; and (4) fracture grain size as determined by comparing a specimen broken at low temperature and exhibiting a crystalline fracture appearance to the fracture grain size of a set of specially prepared specimens used as a standard.

The various methods of reporting grain size are not independent. The ASTM micrograin size is related to the average grain diameter as follows:

1. The ferritic grain size is highly dependent upon the prior austenitic grain size and to a lesser degree upon other factors[2, 4-7, 13, 17-19, 22, 24, 26, 28, 30, 31] such as:

   a. Cooling rate from the austenitizing temperature. The slower the cooling rate the coarser the resultant ferrite due to fewer nucleation sites and more time for these sites to grow.

   b. Temperature at which transformation from austenite to ferrite, or some other product, takes place. The higher the temperature the fewer nucleation sites and therefore larger grains.

   c. The amount of ferrite grain growth that takes place after transformation while cooling, tempering or stress relieving. Longer times allow growth of some grains at the expense of smaller or less favorably oriented neighbors.

[1] References are listed on page 119.

d. The quantity and dispersion of inclusions, oxides and nitrides that may inhibit ferritic as well as austenitic grain growth.

e. Deoxidation practice.

2. The fracture grain size of embrittled material is usually the same as the prior austenitic grain.[11, 12] The strong dependence on prior austenitic grain size, all other things being equal, is due to the fact that the austenite to ferrite reaction nucleates at the prior austenite, gamma, grain boundary. The finer the prior austenitic grain the greater the grain boundary surface area and thus the more nucleation sites available for the gamma to ferrite transformation. Slower cooling rates or longer times at temperature allow growth of existing grains either from existing gamma or at the expense of other smaller ferrite grains.

Most of the investigators who have reported on the effects of grain size have used the Charpy V-notch impact test to determine the fracture transition temperature;[1, 3, 4, 7–11, 13–21, 23, 24, 29–31] only a few have used the Charpy keyhole specimen,[2, 6] the drop weight impact test specimen,[21, 24, 32] or the crack or tear test specimen.[6] How the fracture transition temperature is defined has a marked effect on the magnitude of the shift in transition temperature caused by changes in grain size.[26] Some of the definitions of fracture transition temperature used in the literature are as follows:

1. For Charpy V-notch and keyhole specimens

a. Level of impact energy absorbed was frequently used to determine the transition temperature.[7, 8, 13, 14, 16, 20, 21, 24] The values used ranged from 8 to 40 ft-lb, with perhaps the most common value being 15 ft-lb. The 15 ft-lb level is commonly used for plain carbon steels because it is the level found by the National Bureau of Standards and the Ship Structures Committee to characterize the susceptibility of plain carbon steel ship plate to brittle fracture. The higher values are associated with quenched and tempered alloy steels.

b. A specific amount of fibrous fracture appearance on the broken surface of the impact specimen is sometimes used to define the fracture transition temperature.[4, 8, 16, 21, 23, 26, 27] This is usually referred to as the fibrous fracture appearance transition temperature (FATT), and 50 percent fibrous fracture is the most commonly used value.

c. An amount of lateral expansion or contraction in the deformed area of fracture is occasionally used to define the transition temperature.[21]

d. The inflection point or sharp drop in the energy absorbed versus temperature curve is used.[3, 20]

e. A mean energy level such as the mean energy absorbed at +100 and −196 C has set the transition temperature,[4] as has the temperature at which the Charpy energy absorbed is one-half the maximum energy absorbed at upper energy shelf,[24] and as ". . . the middle of the temperature range over which an impact value of 40 ft-lb was obtained."[2]

f. Sometimes just a visual comparison is made of energy absorption versus test temperature curves for one material or condition as opposed to another.[1]

2. For drop weight impact test specimens, the transition temperature is defined as the highest temperature at which the crack from the brittle crack starter weld will propagate across the surface of the specimen and around the edge on at least one side.[21, 24, 32]

3. The crack arrest or tear test transition temperature is the temperature at which a running crack is halted or arrested by the material. In a specimen having a thermal gradient, the crack runs toward the warm

Charpy Impact Tests

All Charpy V-notch impact tests were performed in accordance with ASTM Standard E 23-64 using a pendulum type of impact machine with 268 ft-lb capacity and a striking velocity of 16.85 ft/sec. Energy losses due to friction were negligible (less than 1.5 ft-lb) over the full range and therefore were disregarded. A Type A Charpy V-notch (simple-beam) impact test specimen 0.394 x 0.394 x 2.165 in. was used for these tests.

Most Charpy specimens were cut parallel to the 5 in. dimension of the drop weight test block and thus were transverse to the major direction of plate roll (see Figure 3). Transverse Charpy specimens were selected for this study so that if banding or nonmetallic inclusions were present in the test specimen, they would be oriented in such a way as to offer the least resistance to crack propagation and so as not to act as crack arresters and thus mask the properties being studied. However, a few coupons were large enough to provide extra material to make a few oversize 5/8 x 2 1/4 x 5 1/4 in. specimen blanks (see Figure 4). These blanks were heat treated and used to make a set of longitudinal, 2.165 in. dimension parallel to the major direction of plate roll, Charpy V-notch impact specimens. Each specimen was identified before notching on both 0.394 x 0.394 end faces with the drop weight specimen number, test direction and specimen number. All Charpy specimens were notched so that the notch was perpendicular to the plate surface through-the-thickness of the plate.

The Charpy V-notch specimens were machined to closer tolerances than recommended by the ASTM in order to minimize scatter in test results; the permissible variations used were as follows:

Adjacent sides	90 deg ±30 min
Cross-section dimension	±0.001 in.
Length of specimen (L)	±0.002 in.
Centering of the notch (L/2)	±0.001 in.
Angle of notch	45 deg ±22 1/2 min
Radius of notch	±0.005, −0.002 in.
Dimensions to bottom of notch	±0.001 in.
Finish requirements	32 μin. all over

Specimens were cooled to test temperature using a liquid bath in an insulated container. Specimens were removed from the bath and centered in the test machine using self-centering tongs similar to those shown in ASTM E 23; the tongs were chilled in the low temperature bath with the specimens for at least 15 min and were immediately returned to the bath each time after they were used. Bath temperatures were controlled using a dummy specimen with an embedded thermocouple. The values of energy absorbed by the specimen reported herein are usually the average of two specimens broken at the indicated temperature; individual specimen results are plotted on the energy absorbed versus test temperature curves.

METALLOGRAPHIC PROCEDURES

Metallographic specimens were cut from the undeformed areas of the drop weight test specimen blank and far enough from the crack starter bead to be sure that no alloying elements had diffused into the specimen. Longitudinal and transverse specimens were prepared and mounted in transoptic mounting resin. After the specimens were mounted, 1/8 in. of specimen surface was machined off in a lathe under coolant using a sharp cutting tool. The surface was progressively ground using 180-, 240-, and 600-grit silicon carbide papers.

least 45 minutes prior to test by manually stirring the bath and adding dry ice or liquid nitrogen as required. Gloves were used to handle the specimens by the heat treating loop welded to the end (5/8 x 2 in. face). Interpretation of the specimen fracture as to "Break" or "No Break" was as recommended in ASTM E208. The only "No-Test" specimens encountered in these tests were a few that were cut a little thin, less than the recommended 0.62 ± 0.02 in. thickness. These specimens were not included in the measurement of the NDT temperature.

Tensile Tests

All tensile tests were performed in accordance with ASTM Standard E 8-65T, Tension Testing of Metallic Materials. A small size specimen, 0.250-in. diameter with a 1-in. gage length, proportioned to the standard Type 1, 0.505-in. diameter tension test specimen was used. The specimens were taken parallel to the original direction of plate roll, thus the overall length of the specimen was limited to 2 in. since this is the size of the P-3 drop weight specimen in that direction (see Figure 3). The 2-in. overall length was achieved by slightly reducing the length of the threaded ends of the specimen.

The specimens were tested in hydraulically loaded universal testing machines calibrated in accordance with ASTM Standard E 4-64, Verification of Testing Machines, using proving rings. The testing machines were found to indicate the correct load within ±0.5 percent in the loading ranges used in these tests. Self aligning, spherical bearing devices were used to ensure axial loading of the test specimens. Load-strain curves were recorded for all specimens using an averaging, 1-in. gage length, microformer strain indicator (extensometer), and an autographic recording device calibrated over the range of the expected yield. Specimens were tested at a speed of 0.002 in./in./min or less, up to and slightly beyond the yield point. The 0.2 percent offset method was used to determine the yield strength. The values reported are the average of two specimens.

Compression Tests

All compression tests were performed in accordance with ASTM Standard E 9-61. The specimens tested were 1/2-in. diameter by 2-in. long cylinders made with special care to ensure that the ends were parallel to each other within 0.002 in. and perpendicular to the long axis of the specimen within 0.005 in. The specimens were taken parallel to the original direction of plate; thus they were machined parallel to the 2-in. dimension of the drop weight specimen they were cut from (see Figure 3).

The specimens were tested using hydraulically loaded testing machines calibrated in accordance with ASTM Standard E 4-64, Verification of Testing Machines. The testing machines were verified using proving rings and found to indicate the correct load within ±0.5 percent in the loading ranges used in these tests.

All compression tests were run using a subpress with a spherical seated bearing block at the end of its shaft to ensure full contact with the end of the specimen and to ensure true axial loading. Hardened steel bearing blocks with smooth, ground, parallel faces were used in contact with the ends of specimen to prevent possible damage to the faces of the subpress. The ends of the specimen were greased with lubriplate to eliminate end restraints. Because of the shape of the specimen it was not necessary to use a jig to prevent lateral buckling. Load-strain curves were recorded for all specimens using an averaging, 1-in. gage length, microformer strain indicator (compressometer) and an autographic recording device calibrated over the range of the expected yield. Specimens were tested at a speed of 0.002 in./in./min or less up to and slightly beyond the yield point. The 0.2 percent offset method was used to determine the yield strength. The values reported are the average of two specimens.

875 F Isothermal Treatment (Semi-Bainitic)

Specimen blanks that were treated isothermally at 875 F to ultimately give a microstructure consisting of a mixture of tempered bainite and tempered martensite were treated as follows: 1640 F – 1/2 hr – transferred to 875 F – held 152 (or 1600) sec-BQ; -110 F – 1/2 hr; temper 1150 F – 1 hr – BQ. Additional specimen blanks available from coupons *X*-12, *X*-13, and *X*-15–*X*-18 were treated as follows: 2000 F – 1 hr -- transferred to 1640 F held 5 min (minimum) – transferred to 875 F – held 1600 sec – BQ; – 110 F – 1/2 hr; 1150 F – 1 hr -- BQ.

1200 F Isothermal Treatment (Semi-Ferritic)

Specimen blanks from all coupons were isothermally treated at 1200 F to ultimately give a microstructure of tempered martensite and tempered ferrite. In several cases a little pearlite was found to have been formed during the isothermal treatment. These coupons were treated as follows: 1640 F – 1/2 hr – transferred to 1200 F – held for 3350 sec (or extra sets of specimen blocks from coupons *X*-1, *X*-2, *X*12, *X*-13, *X*-15– *X*-18 and *Y*-2, *Y*-4, and *Y*-11 were also held for 8500 sec) – BQ; – 110 F – 1/2 hr; 1150 F – 1 hr – BQ. There was insufficient material to give any specimens with a coarse austenitic grain size the 1200 F isothermal treatment.

TESTING PROCEDURES

In general an attempt was made to adhere to standard ASTM testing procedures. In a few cases it was necessary to make slight deviations from standard practice to take into account the specific conditions of these tests; any such deviations will be indicated below.

Drop Weight NDT Tests

All drop weight tests were performed in accordance with ASTM Method E 208-66T, using the type P-3 specimen which is 5/8 x 2 x 5 in. The specimens were supported as a simple beam and subjected to an impact load of 259 ft-lb produced by dropping a 223-lb weight 1 ft 2 in.; this drop energy was found to consistently crack the crack starter weld bead and to cause the specimen to consistently contact the anvil stop.

As stated previously, the specimens were prepared with one, as rolled, 2 x 5 in. face. The Hardex-N crack starter bead was deposited in the center of this face prior to heat treatment of the specimen so that the heat-affected zone created by deposition of the weld bead would not interfere with the correct measurement of the NDT temperature of the base material. After final heat treatment, the crack starter weld beads were notched as required in ASTM E 208, using a thin abrasive disk. The combination of the isothermal treatments and the subsequent 1150 F temper was not found to prevent proper functioning of the crack starter bead; upon impact, a good crack formed in the bead in every case.

A group of four or five, usually five, specimens was given a selected heat treatment and used to determine the NDT temperature. Since tests were conducted on a known material with a known thermal history, the NDT temperature was determined within 10 F by three to five tests, the usual number being four. Prior to testing each specimen was placed in a large insulated liquid, isopentane, low temperature bath with at least 1 in. of liquid all around the specimen. A thermocouple embedded in a dummy specimen was attached to an automatic recorder and used to control the bath temperature. The bath temperature was maintained for a period of at

the table lists the identification numbers assigned to each coupon. Coupons made by the largest producer have a number starting with an *X* and coupons made by the other producer have been assigned a number prefixed with a *Y*. To obtain the maximum use of each coupon and to make specimen location as uniform as possible for all specimens, specimens were taken from adjacent to the original plate surfaces (see Figure 1). In fact, to minimize machining costs, the original plate surface was made one of the 2 x 5 in. surfaces of the drop weight specimen blank. The specimen blanks were 5/8 x 2 x 5 in. with the 2-in. dimension in the direction of plate roll and the 5-in. dimension parallel to the plate surface and perpendicular to the direction of plate roll (see Figure 2). This is the size of specimen required for subsize drop weight NDT temperature tests in ASTM Method E 208. Each specimen blank was coded on the end with the appropriate number, location, test direction, and specimen number. These specimen blocks were used for drop weight tests, after that the broken specimens were used to make mechanical property test specimens.

HEAT TREATING PROCEDURES

The 5/8 x 2 x 5 in. drop weight specimen blanks were prepared for heat treatment by (1) welding handling loops onto one of the 5/8 x 2 in. faces, (2) depositing a brittle crack starter bead on the 2 x 5 in. surface of the specimen that represented the original plate surface of the specimen using a 3/16-in. diameter Hardex N hardfacing electrode, (3) normalizing the specimens by heating to 1650 F, holding for 1 hour and then air-cooling, and (4) sandblasting the specimen prior to final heat treatment.

The final heat treatment of the drop weight specimen blanks consisted of austenitizing in a neutral salt bath at 1640 F for 1/2 hour and then either water quenching in a brine solution or quenching into an isothermal neutral salt bath, holding for a prescribed time and then brine quenching. After quenching, all specimens were immediately given a low temperature (about – 110 F) treatment in a bath made of acetone and chunks of dry ice; all specimen blanks were given at least 1/2 hour in this bath to ensure that they came down to temperature and that all retained austenite was transformed to martensite by the treatment. All specimens were subsequently tempered in a circulating air furnace at 1150 F for 1 hour at temperature and then water quenched in a brine solution (BQ). In a few cases, where sufficient material was available, a few sets of drop weight specimen blanks were austenitized at 2000 F for 1 hour in a circulating air furnace, then transferred to the 1640 F salt bath for 5 minutes, minimum, to standardize the temperature differential between the isothermal bath and the specimen prior to immersion. All furnace and bath temperatures are manually controlled using potentiometers to within ±5 F. Specimens were heat treated by suspending them by their loop from a fixture that allowed them to be treated as a group. This fixture held the specimens 1 1/2 in. apart and suspended them vertically in the salt baths to permit circulation of the salt.

Fully Quenched (Martensitic)

Specimen blanks that were fully quenched to form a fine prior austenitic grain size to ultimately give a tempered martensitic microstructure were treated as follows: 1640 F – 1/2 hr – BQ; – 110 F – 1/2 hr; temper 1150 F – 1 hr – BQ. Specimen blanks from coupons *X*-12, *X*-13, and *X*-15–*X*-18 which were quenched from a coarse prior austenitic size were treated as follows: 2000 F – 1 hr – 1640 F 5 min (minimum) – BQ; – 110 F – 1/2 hr; temper 1150 F – 1 hr – BQ.

under a wide variety of conditions, and tempering treatment. Increases in strength produce corresponding increases in impact transition temperatures unless other parameters are adjusted to compensate for the increased strength level.[27,35] Conversely, a decrease in strength brought about by a long time temper is no guarantee that the impact transition temperature will improve, since for a wide variety of quenched and tempered steels a 100 hour stress relief will reduce the strength and at the same time increase the transition temperature; this is attributed to a susceptibility to temper embrittlement.[38]

In bainitic steels, increases in strength brought about by refining the bainitic-ferrite microstructure will have an adverse effect on impact transition temperature unless compensation is made by refining the prior austenitic grain size also.[27] The dependence of the impact transition temperature of bainitic steels on prior austenitic grain size is attributed to the fact that the upper limit on the size of the bainitic-ferrite plates is the prior austenite grain diameter.[27] Tempering bainitic steels at a temperature above the temperature at which the bainite formed improves its impact transition temperature by lowering the strength.[42]

EXPERIMENTAL PROCEDURES

SUMMARY

The general test program followed in this study can be summarized as follows. Test coupons were collected from commercially produced plates made by the two major producers of a low carbon, nickel-chrome molybdenum steel.* These coupons were selected to represent the broad range of chemical composition to which this steel is melted in commercial practice. These coupons were slabbed to convenient size, analyzed for chemical composition, heat treated, and tested. All heat treating and testing was performed on 5/8 × 2 × 5 in. drop weight blanks heat treated so as to eliminate the effects of variation in hardenability, plate thickness, and mill heat treatment. Isothermal heat treatments were used to produce controlled microstructures, and a uniform tempering temperature of 1150 F, slightly above the minimum value permitted by the specification, was used. The isothermal holding times and temperature were tentatively selected to produce approximately 25 percent ±10 percent of each nonmartensitic product, bainite or ferrite, for an average composition. Microstructures produced by a given heat treat were measured for each coupon using microspecimens taken from the broken drop weight test specimens; mechanical properties were measured on these same test specimens.

MATERIALS

Coupons were collected over a period of years from plates made during actual mill runs at the plants of the two major producers of this steel and represent only a small fraction of heats melted during this period. The coupons were obtained after final heat treatment from the end of the plate when the plate was cropped to ordered size. All coupons were cut from material adjacent to the ordered plate. The actual coupons selected were chosen by the investigator on the basis of the producer's chemical analysis to represent a fairly broad range of the chemical compositions used for this steel in commercial mill practice. A total of 27 coupons representing 22 heats were collected; 16 coupons were from one producer and 11 coupons from the other. Table 1 summarizes the heat numbers, mechanical properties, and chemical compositions reported by the producers; in addition,

*Commonly called HY-80 steel and made in accordance with ASTM Specification A543-65 and Military Specification MIL-S-16216G (SHIPS).

COMPOSITION

The effects of compositional changes in tempered martensitic and lower-bainitic microstructures on impact properties are threefold: first, the basic impact fracture transition temperature is shifted due to the presence of trace impurity elements;[23, 36, 37] second, the susceptibility to embrittlement at low tempering temperatures, 500 to 800 F, may be affected;[10, 37] and third, there may be susceptibility to temper embrittlement during either long time tempering treatments or slow cooling instead of quenching from the tempering temperatures.[9, 10, 22, 23, 34, 36, 37, 41] In addition, the composition changes may be detrimental to impact properties if they increase the strength markedly or if they tend to retard softening during tempering.[27, 35, 37]

Tests on special high purity quenched and tempered steels have shown that certain minor impurity elements, some of which are invariably present in commercial steels and for which many are not routinely analyzed, such as P, Sb, As, Sn, and N_2, are primarily responsible for embrittlement.[23, 36, 37] The high purity steels show very low impact transition temperatures and very little susceptibility to embrittlement as a result of usually detrimental tempering treatments. Susceptibility to low tempering temperature embrittlement is increased by Mn, P, Si, Cr, As, Sn, N_2, not affected much by Ni, Cr, and Mo, and seems to be inhibited by Al.[10, 37] The most detrimental effects were observed for P and N_2.[37]

Susceptibility to temper embrittlement due to either long tempering times in the region from 900 to 1100 F or slow cooling from the tempering temperature is increased by C,[9, 22] Mn,[34, 36, 37] P,[10, 23, 36, 37, 41] Si,[36, 37] Ni,[34] Cr,[34] As,[36, 37] Sb,[36, 37, 39, 41] and Sn,[23, 36, 37, 39] not affected much by N_2, Bi, Cu, Co, Ge, Ga, and Zr,[36, 37] and inhibited by Mo,[10, 34, 36, 39] and W.[39] There was no evidence in studies of a quenched and tempered Ni-Cr-Mo steel that there was any interaction between regular alloying additions and trace elements that exaggerated their total effect.[39, 41] For some hardened steels, there is evidence from the impact transition temperature and the fracture appearance that some embrittlement occurred during the initial tempering at an elevated (1112 to 1202 F) temperature.[37, 41]

A study of a quenched and tempered Ni-Cr-Mo steel that was not deliberately given an embrittling treatment shows that P, Sb, and Sn have a detrimental effect on impact transition temperature, As had little or no effect, and Al additions were actually beneficial.[39] Phosphorus was the most damaging, and the effect of As, which had been shown to be detrimental to deliberately embrittled steel, showed little effect in the not deliberately embrittled steel. The effect of Al shifted from detrimental in embrittled material to beneficial in non-embrittled material; the benefit of Al additions was attributed to a decrease in the prior gamma grain size. Other effects reported are that the optimum carbon content in quenched and tempered steels is about 0.38 percent and that this amount optimizes both NDT temperature and maximum Charpy V-notch shelf energy.[40] Sulphur is reported to have no effect on impact transition temperature but to lower the maximum Charpy shelf energy.[10]

B, C, Mn, Ni, and Cr additions can be detrimental to the impact properties of low-carbon bainitic steels if they reduce the austenite decomposition temperature and as a result either increase the strength excessively or produce a mixed microstructure of bainite and martensite.[27] Secondary hardening elements like Mo and V have a tendency to reduce impact properties of low-carbon bainites, in that they increase the hardness of the initial microstructure and they tend to precipitate carbides which retard softening during tempering.[27]

STRENGTH

The effect of strength level on impact transition temperature is complicated by the dependency of strength on the interaction between composition, grain size, microstructure produced by the transformation of austenite

In martensitic steels transgranular and intergranular fracture refer to austenitic grains present prior to quenching and not to the ferritic grain structure developed by tempering the martensite.[11,12,23,29,36,37,41] The relative amount of transgranular and intergranular fracture developed by the impact fracture of a tempered martensite depends on the following:

1. The relative temperature in the fracture transition region. The lowest temperatures tend to give more intergranular fracture.[11]

2. The amount of temper embrittlement. Certain combinations of temperatures and long holding times, will increase the tendency to intergranular fracture if the material is susceptible to temper embrittlement.[12]

3. Blue brittleness, associated with a 500 F tempering temperature. This tends to give an intergranular fracture and shows a brittle appearance over a considerable temperature range and which slowly disappears at higher temperatures without ever exhibiting an abrupt transition.[11]

4. Nonembrittling tempering causes fracture to show a progression from transgranular fracture after a 500 F temper, and a return to the transgranular fracture mode after a 1200 F temper. Tempers from 550 F to 1200 F exhibit brittle fractures composed of a mixture of intergranular and transgranular brittle partings.[11]

5. High purity tempered martensite will exhibit only transgranular cleavage when it breaks in a brittle way whereas steels containing 0.04 atomic percent phosphorus or tin showed at least some intergranular fracture along the prior austenitic grain boundaries with the proportion increasing with grain size and with embrittling treatments.[23] Phosphorus containing steel, 0.023 weight percent in a 0.3 C, 3.0 Ni, 0.75 Cr steel, tended to show more intergranular fracture than the same steel doped with 0.074 weight percent Sn.

Summarizing, the impact fracture path is characterized by the transgranular or intergranular mode relative to the ferritic grains in plain carbon steels having a microstructure consisting of ferrite or ferrite and pearlite, and to the prior austenitic grains in quenched and tempered martensite which shows some degree of temper embrittlement. The impact properties of bainitic steels are separated into two distinct types, with the high temperature bainitic structures behaving like ferrite-pearlite structures and low temperature bainitic structures behaving like martensitic structures; the impact properties of the low temperature bainite improve with decreasing prior austenitic grain sizes.[27]

MICROSTRUCTURE

The general effect reported in the literature is for tempered bainitic steels to have impact properties intermediate to those of tempered martensitic and tempered pearlitic steels of the same hardness, with the tempered martensitic steel having the lowest impact transition temperature and the highest level of energy absorbed above the transition temperature.[27, 33, 42] The fine bainitic structure responds to tempering like a quenched steel; the transition temperature steadily decreases with increasing tempering temperature.[27, 35] Composition of low carbon bainitic steels has little effect on the impact properties if similar microstructures having the same grain size and same hardness are compared.[27] In order to get adequate impact resistance in bainitic or martensitic steels, they must be tempered beyond the stage where maximum secondary hardening takes place; secondary hardening due to the presence of other alloying elements has a deleterious effect on impact resistance.[22] Even after tempering, a portion of upper bainite is more detrimental to the impact properties of an otherwise martensitic microstructure than is a portion of lower bainite.[42]

side of the specimen. These tests are not used extensively and apparently are seldom used to evaluate the effect of grain size on the transition temperature.

Other parameters associated with the material, and its treatment and microstructure have been reported to have an interaction with the grain size to change the magnitude of the shift in the impact transition temperature. These factors are: impurity level and composition changes;[5, 7, 8, 19, 23] commercial size heats as opposed to laboratory size heats or melts;[9, 31] straining or cold deformation;[5, 12, 26] thermal treatments that cause a secondary effect to overshadow grain size effects, retention of austenite,[3] temper embrittlement[10, 15, 20, 23, 26] and growth of grains;[2, 5, 7, 23] and microstructure changes.[1, 3, 14, 17, 20, 22, 26, 27] The effect of each on the apparent shift in transition temperature with grain size ($\Delta T/\Delta GS$) may either be positive or so negative in nature as to make grain size appear to have no effect.

As a result of these complications, each reported value of $\Delta T/\Delta GS$ must be evaluated in terms of the specimen used; the criterion defining transition temperature; the composition, including impruity levels; source of the material, lab versus production melts; thermal treatment; straining; microstructure; and the range over which grain size was actually varied. If this is done, a few general observations may be made on the specific effect of changes in grain size on the impact transition temperature. For convenience, this report will always refer to grain size as the ASTM micrograin size. The following equation represents the relationship between the number of grains per square inch (n) and ASTM micrograin size (N) : $n = 2^{(N-1)}$.

Ferritic Grain Size

The ferritic grain size is commonly used in the literature to report the effects of grain size on $\Delta T/\Delta GS$. There are three reasons for this: first, ferrite is the major room temperature equilibrium phase in the hypoeutectoid plain carbon steels used in most of the studies reported in the literature; second, ferrite with varying amounts of carbide is the primary room temperature microconstituent of quenched and tempered alloy steels; and third, the final ferritic grain size is readily measured using standard metallographic techniques.

Changes in the size of the ferrite subgrain size are reported to affect the impact transition temperature.[18, 31] An increase in the sub-boundaries, a decrease in the ferritic subgrain size, raises not lowers the Charpy V-notch 15 ft-lb transition temperature (20 F/per ferrite grain size number). The ferrite subgrain boundaries examined with an electron microscope show a lower dislocation density than the boundaries associated with the true ferrite grain boundary.[31] While these authors were puzzled by this effect, a possible explanation must be pointed out. Current dislocation theory says that the subgrain structure is caused by a preferential alignment of dislocations having like signs. As the number of dislocations increases, the subgrain size would be expected to decrease and the strain in the grain increase. The usual effect of straining is to raise the transition temperature for ductile to brittle fracture. In fact, temper embrittlement has even been attributed to strain developed across prior austenitic grain boundaries as a result of the contraction of the ferrite lattice when dissolved alloying elements are removed from solution in ferrite by a reaction with existing minor carbide phases.[12] Thus it is logical to expect that as the ferritic subgrain size gets smaller indicating increasing dislocation densities and higher strains in the lattice, the impact transition temperature would increase as opposed to the usual decrease in $\Delta T/\Delta GS$ associated with a finer true ferritic grain size.

References 2, 6, 7, 13, 17, 18, 24, 28, and 31 show that a decrease in the ferritic grain size of a plain carbon steel sufficient to increase the ASTM grain size number one unit will reduce the transition temperature 22 F on the average, the effect ranging from an increase of 9 F to a decrease of 39 F. The 9 F value,

Reference 31, is undoubtedly due to the normal variation in the measurement of transition temperature of ±10 F reported by Gross[21] and to the small variation in grain size, less than one unit.[31] The −39 F value for $\Delta T/\Delta GS$ is difficult to rationalize since the author reports neither the type of impact specimen he used nor the criterion used for determining the transition temperature.

These $\Delta T/\Delta GS$ values seem to be independent of carbon content in these plain carbon steels. It is reported that of the factors: ferrite grain size, pearlite island size, pearlite spacing and amount of proeutectoid ferrite, as it influences pearlite carbon content; only the ferrite grain size showed any degree of correlation with the Charpy V-notch 15 ft-lb transition temperature.[17] The $\Delta T/\Delta GS$ value's dependence on test method is seen in Reference 24 where the author reports a value of −18 F/ΔGS based on the Charpy V-notch 15 ft-lb energy transition temperature and −11 F/ΔGS based on drop weight NDT.

Austenitic Grain Size

Increases in the prior austenitic grain size have usually been associated with increasing impact transition temperatures.[1, 3, 4, 8–14, 16, 19, 23, 27] In fact, as temper brittleness increases in martensitic-ferrite, the fracture paths become increasingly intergranular and follow the prior austenitic grain boundaries.[11, 12, 29, 36, 37, 41] The relationship between the Charpy V-notch 10 ft-lb and 50 percent FATT transition temperatures and prior austenitic grain size was linear for hardened 0.84 and 0.95 C steels.[16]

It was reported for tests on SAE 1045, 2340 and 3140 having various microstructures and tempered to the same hardness, that increasing the prior austenitic grain size increased the impact transition temperature of air cooled and tempered (pearlitic) material ($\Delta T/\Delta\gamma GS$ from −25 to ≃−120 F) but had the opposite effect (+5 to +20 F) on quenched and tempered material.[3] The slight improvement in the quenched and tempered steels as austenitic grain size increased was attributed to the increase in hardenability as the grain size increased and to the resultant increase in the amount of martensite formed during quenching. The impact fracture transition temperature of the tempered martensitic structure was always better, i. e., lower than that of the tempered pearlitic structures. Increasing gamma grain size also increased the notch sensitivity of the pearlitic microstructure.[3] In a later study it was reported for 0.80 percent C plain carbon steel that as the hardness was increased, pearlite spacing decreased, the impact transition temperature went up, more so for fine than for coarse prior austenitic grain size material; in fact, there was a minimum in the pearlite spacing (hardness) versus impact transition temperature relation for coarse material whereas the finer prior gamma grain size material showed a continuous increase.[14]

Prior austenitic grain size is also reported to have a controlling effect on the mean impact energy absorbed transition temperature of 0.12 C bainitic steels, but the effect is lessened as the strength increases with increased dispersion of carbides.[27] The prior austenitic grain diameter, which is directly related to either the rolling finishing temperature or the reheating temperature used during austenitizing, has been shown to strongly affect the average Charpy energy impact transition temperature of 70,000 psi tensile strength bainitic steel, with the transition temperature increasing in an S shaped relationship with increasing prior austenitic grain diameter.[27] The transition temperature of the bainitic steels reportedly ranged from −76 F for an austenite grain diameter of 3.9×10^{-4} in. to 140 F for a 22.3×10^{-4} in. diameter.

Grain refiners are frequently cited as and demonstrated to have a beneficial effect on lowering the impact transition temperature[4, 5, 7] and even materials which are not specific grain refiners, such as lead, but which react to inhibit grain growth, will show a beneficial effect, especially when added to normally coarse grained steels.[8]

Petch is reported[30] to have shown that the Charpy V-notch 15 ft-lb transition temperature (T) of ferritic steels is linearly related to the natural logarithm of the square root of the reciprocal of the mean grain diameter (d) in the following way: $T = A + B \ln (D^{-1/2})$. If one uses $n = 2^{(N-1)}$ where n is the number of grains per square inch and N is the ASTM grain size number, and notes the fact that n is proportional to d^2, one can rewrite the Petch relationship in terms of the ASTM grain size and show that impact transition temperature should be a direct linear function of N, $T = A_1 + B_1 (N)$.

An investigation of unhardened C1095 and C1080 plain carbon steels shows that a coarser prior austenitic grain size raises the impact transition temperature, regardless of the temperature at which the austenite is transformed to pearlite.[8] In addition, it was shown that while lower transformation temperatures raised the ultimate tensile strength, it also lowered the impact transition temperatures by refining the microstructure. The data below shows the observed range of change in Charpy V-notch impact transition temperature ΔT per unit change in prior austenitic grain size, $\Delta T/\gamma GS$ and demonstrates the dependence of $\Delta T/\gamma GS$ on both the criteria used to measure ΔT and the steel composition.

Steel	C_V (10 ft-lb)	C_V (50 Percent FATT)
C1095	46–35 F/γGS	17–19 F/γGS
C1080	27–29 F/γGS	33–23 F/γGS

Studies of the effects of various factors on the impact transition temperature of plain carbon steel ship plate have shown that the higher transition temperatures associated with thicker plates are more closely related to differences in the ferrite grain size resulting from rolling finishing temperature and cooling rate than to differences in chemical composition.[13] The finer the grain size, the higher the ASTM grain size number, the lower the impact transition temperature. The magnitude of the effect of grain size on $\Delta T/\Delta GS$ depends on the method used to measure grain size; based on ferrite grain size the $\Delta T/\Delta GS$ for ship plate was −14 F/ΔGS and based on fracture, which may partially reflect prior austenitic grain size,[11, 12, 29, 36, 37, 41] $\Delta T/\Delta GS$ was −9 F/ΔGS.[13]

In a study of the effects of impurity level on the way changes in prior austenitic grain size influenced Charpy V-notch 100 percent FATT transition temperature of a 0.3 C, 3.0 Ni, 0.75 Cr steel, it was observed that the relative effect of grain size was strongly influenced by both impurity level and thermal treatment.[23]

	As Oil Quenched and Tempered at 1112 F	Oil Quenched and Tempered Plus 168 Hours at 842 F
High Purity	− 4.1 F/$\Delta\gamma GS$	− 5.9 F/$\Delta\gamma GS$
Plus 0.023 Percent *P**	−13.6 F/$\Delta\gamma GS$	−19.8 F/$\Delta\gamma GS$
Plus 0.074 Percent *Sn**	−28.5 F/$\Delta\gamma GS$	−42.3 F/$\Delta\gamma GS$

These data show that the impact transition temperature of high purity alloys is affected by changes in gamma grain size; that tin is more detrimental than phosphorus at equal atomic percents; and that the detrimental effect of increasing prior austenitic grain size is greater after an embrittling treatment than after a simple tempering treatment.

*Each about 0.04 atomic percent.

Microstructure

The interaction of microstructure and grain size appears to be rather straightforward; the finer the microstructure for any given prior austenitic grain size, the lower will be the impact transition temperature. The finer the ferrite grains in ferritic steels,[2, 4–7, 15, 18, 22, 24, 26, 28, 32] the finer the pearlite colonies and the finer the interlaminar ferrite-carbide spacing,[1, 3, 14, 16, 17] the finer the bainitic-ferrite[20, 22, 27] and the finer the martensitic-ferrite,[3, 22, 27] the lower will be the impact transition temperature. It should be remembered that the finer the prior austenitic grain size,[2, 6] the lower the rolling finishing temperature,[13] the faster the cooling rate,[2, 6, 28] and the lower the temperature of transformation from austenite,[8, 28] the finer will be the resultant final grain size.

Because of the increasingly acicular nature of the ferrite grain size as the microstructure is changed from polygonal ferrite to bainitic-ferrite and then to martensitic-ferrite, it becomes increasingly difficult to make a change in ferritic grain size and as a result, ferritic grain size can hardly be considered a variable.[22] As a result of the increasing acicular nature of the microstructure and the fracture path following the embrittled prior austenitic grain boundary,[11, 12, 29, 36, 37, 41] one finds the tendency is for researchers to report the effects of grain size on $\Delta T/\Delta GS$ in terms of prior austenitic grain size when dealing with tempered bainitic and martensitic steels.[3, 20, 22, 27] Researchers also tend to report ferritic grain sizes when dealing with plain carbon steels where the structure is essentially ferrite or some mixture of ferrite and pearlite.

For 0.02 percent carbon, plain carbon and alloy steels there is reported to be a slight increase in Charpy V-notch transition temperature due to the acicular shaped ferrite grains over what might otherwise be expected from simple changes in ferrite grain size alone.[20] This may be due to the fact that the identical grain sizes were developed by a combination of furnace and air cooling from different austenitizing temperatures, which means that prior gamma grain size differences or embrittlement during cooling may have caused the differences rather than simply the differences between polygonal and acicular ferrite grains.

For 0.32 percent carbon, plain carbon steel, it was found that of ferrite grain size, pearlite island size, pearlite spacing and amount of proeutectoid ferrite as it affects pearlite carbon content, only the ferrite grain size showed any degree of correlation with the Charpy V-notch 15 ft-lb transition temperature.[17] As the pearlite spacing is decreased in a 0.80 percent carbon, plain carbon steel, the hardness is increased and the Charpy V-notch 8 ft-lb transition temperature increased, more so for fine than for coarse prior austenitic grain size materials.[14] In tests on SAE 1045, 2340, and 3140 having various microstructures tempered to the same hardness, the Charpy V-notch transition temperature of tempered martensite was always lower than that of the tempered pearlitic structures.[3]

Fracture Path

The sudden decrease in impact energy shown by the truly ferritic, low carbon, little or no alloying steels is accompanied or brought about by a marked increase in the amount of cleavage fracture and by a marked reduction in the plastic deformation accompanying fracture.[6, 7, 13, 15, 20] The cleavage fracture of the ferrite grains initiates at the ferrite or ferrite-pearlite grain boundaries.[20] The properties of the ferrite rather than the pearlite control notch toughness in killed and semikilled steels.[31] The low temperature brittle fracture in these ferritic steels is primarily transcrystalline cleavage of the ferrite grains, though there has been reported an increased tendency to intergranular brittleness with increasingly coarse grains as the oxygen content is raised above 0.003 percent.[15, 18, 20]

Final polishing was performed in two stages using 60-cycle automatic vibratory polishers. The semifinal polishing bowl was covered with bleached silk cloth and a slurry of Linde A, distilled water, and aerosol wetting agent. The final polishing bowl was covered with Gamal cloth and a slurry of Linde B, distilled water, and aerosol. All specimens were lightly etched in 2 percent Nital and repolished several times during the final stages of polishing to ensure the removal of any smeared structure and correct development of the microstructure.

The inclusion content of the specimens was measured in both the longitudinal and transverse, through-the-thickness planes in accordance with ASTM Standard E 45-63, Determining the Inclusion Content of Steel. Microscopic Method B was used to determine the length of the longest inclusion, the number and average length of all inclusions over 0.005 in. long and the background rating including all inclusions less than 0.005 in. long. The vibratory polishing technique was found to leave the inclusions intact and in the specimen.

The prior austenitic grain size was measured on fully-quenched specimens taken from the quenched and tempered fully martensitic specimens in accordance with ASTM Standard E 112-63, Estimating the Average Grain Size of Metal, using the intercept or Heyn procedure. The prior austenitic grain size was revealed by the use of the etching reagents described in Appendix A. Comparisons made on several different specimens from different melts showed that both etches indicated the same prior austenitic grain size.

The percent of isothermal transformation product resulting from the isothermal treatments was measured for each treatment. The microspecimens were each etched in three reagents. Between each of the reagents, the specimens were rinsed and dried. The triple etch consisted of (1) a saturated picric acid solution to develop the prior austenitic grain boundaries, (2) a one percent nital solution to develop the structure in the areas of tempered martensite, and (3) a 20 percent solution of anhydrous sodium metabisulfite for staining (darkening) the tempered martensite areas. The last etch leaves the areas of the tempered bainite or ferrite white, in sharp contrast to the darker areas of stained tempered martensite. The details of these etching solutions and how they were used are given in Appendix B. The percent of transformation product was estimated by superimposing a grid on the specimen and determining the percentage of the grid intersections that fell over each microconstituent. Because of the finely banded nature of the transformation product and the high magnification (500X /1000X) needed to resolve the structure, extreme care was taken to systematically traverse the specimen and read at least 10 areas so as to get a representative average value to report.

EXPERIMENTAL RESULTS

CHEMICAL COMPOSITION

The actual chemical compositions of the coupons tested in this study are listed in Table 2. These analyses were made by a commercial testing laboratory on material located adjacent to the original plate surface of the coupon. The material analyzed came from the top 5/8 in. of the plate but did not include any heat treating scale or decarburized plate surface which would have influenced the analysis.

Wet chemical analyses were performed for percent Carbon (C), manganese (Mn), phosphorus (P), silicon (Si), nickel (Ni), chrome (Cr), molybdenum (Mo), copper (Cu), and acid soluble and total aluminum (Al).

Spectrographic analysis was performed to determine the percent present of the following trace elements: vanadium (V), lead (Pb), tin (Sn), magnesium (Mg), cobalt (Co) and titanium (Ti). No values are reported for Pb, Sn, and Mg in Table 2 since they were not found to be present in detectable amounts. After several samples had been analyzed it was found that V and Co were present in negligible amounts and therefore, analysis for these elements was discontinued. The producers informed the author that the Co was a tramp element

introduced by the nickel addition. The Co was left in with the nickel since it was too difficult to remove and since they found that it had essentially no effect on the hardenability or properties of the steel. The V was also present only as a tramp element but it came from a variety of sources that went into the make up of a given heat of steel.

Gaseous analysis was performed for oxygen (O_2), hydrogen (H_2), and nitrogen (N_2). O_2 and N_2 are reported as a percent and H_2 as parts per million (ppm) in Table 2.

A review of Table 2 shows that in general the range of the alloying elements found in the samples selected for this study almost completely cover the full composition range permitted for nickel-chrome-molybdenum steels such as ASTM A 543 and HY-80. The only element that falls outside the combined range for the two steels is Mn; coupons Y-8 and Y-10 have 0.49 percent Mn. This is only 0.04 percent over the 0.45 percent (0.40 upper limit plus the allowance of 0.05 percent variation over the upper limit) maximum allowed for these steels.

METALLOGRAPHIC ANALYSIS

The results of the metallographic analysis of coupons used in this study are given in Tables 3, 4, and 5. Table 3 presents the results of the inclusion analysis of these coupons at the mid-thickness and adjacent to the surface of each coupon in both the longitudinal and transverse directions on planes perpendicular to the plate surface through the thickness of the plate. The reporting method recommended in ASTM E 45-63 is used to describe the inclusion content. The length of the longest inclusion at 100X is reported in units equivalent to 0.005 in. on the specimen along with a superscript describing whether it is grouped (g), very disconnected (vd), or disconnected (d). The average length of all inclusions over one unit long and excluding the longest is reported with a superscript denoting the number of inclusions averaged. The background rating A, B, C or D corresponds to the sample photographs in E 45 with A being a rather clean steel and D a rather dirty steel. Figures 5 and 6 are photomicrographs (100X) of representative samples and will give the reader a better understanding of the significance of the data reported in Table 3.

The prior austenitic micro-grain size of each coupon is reported in Table 4. The grain size is reported for the as-received coupon and for the coupons after heat treatment. This table shows that the coupons austenitized at 1640 F had a slightly finer prior austenitic grain size than as-received coupons, and a slightly coarser grain size after the 2000 F treatment.

The percent of isothermal transformation products produced by the various isothermal treatments are summarized for each coupon in Table 5. The large variation in percent transformation product resulting from a given heat treatment reflects the large range in chemical composition and hardenability of these coupons. The high hardenability, rich composition coupons had the least transformation take place for a given isothermal treatment. Photomicrographs of typical areas of each coupon for each isothermal treatment are given in Appendix C. The dark areas are tempered martensite that has been darkened as described in Appendix B and the light areas are tempered isothermal products.

MECHANICAL PROPERTY TEST RESULTS

Table 6 summarizes the mechanical property test results for each heat treatment; the corresponding microstructures are also included for reader convenience. The table lists the longitudinal tensile and compressive

properties, the NDT temperature, and the transverse Charpy V-notch impact properties at the NDT temperature, − 120 F and + 212 F (representative of the maximum energy shelf). All values reported are the average of two specimens. Also longitudinal Charpy data are reported for the few cases where it was measured. Appendix D contains the full Charpy V-notch curves for most of the coupons.* The Charpy curves show the energy absorbed, the lateral expansion at the notch after fracture and the percent fibrous fracture appearance of the fracture surface.

DISCUSSION

A comparison of Tables 1 and 2 shows that there are some significant differences between the producer's reported chemical composition of the heats and the actual composition of the coupons. The biggest differences are in C, Mn, P, and S with the coupon values generally higher than the producer's values. These variations are slightly more than what might be expected from normal variation in analytical results and from variation caused by the differences in the position of the sample in the heat of steel, and point up the need to check the actual composition of coupons being evaluated in laboratory experiments rather than to rely on the producer's data. Table 2 shows a good compositional range for the usual alloying elements and a fair spread for most of the rest of them.

Table 3 shows the mid-thickness and surface inclusion content of the coupons. In general, the material adjacent to the surface is cleaner than at the mid-thickness of the coupon. Even though a good range of inclusion sizes is represented in these samples, it must be pointed out that no large continuous inclusions were found.

Table 4 compares the prior austenitic grain size of the as-received material at mid-thickness to the prior austenitic, gamma grain size that resulted from the austenitizing treatments used in this study. While the as-received gamma grain size was fairly coarse, ranging from ASTM 8 to 4, the treatments used in this study bracketed an equally wide range in gamma grain size of ASTM 9.5 to 3.0.

The isothermal holding times referred to in Tables 5 and 6 are time in the bath, not actual holding times at bath temperature. Appendix E gives a comparison of the actual time-temperature history of 5/8 x 2 x 5 in. drop weight specimens when they are transferred from 1640 F into either 875 or 1200 F salt baths and compares it to the cooling curves predicted using the method of Sinnott and Shyne.[47] The mid-thickness of the drop weight specimen is within 20 F of 875 F in about 120 seconds, a considerable portion of the 152 second treatment at 875 F but a reasonable fraction of the 1600 second treatment. The data indicate that the mid-thickness of the specimens is within 20 F of 1200 F in about 90 seconds, which is negligible compared to the 3350 and 8500 second holding times used at 1200 F. The important matter concerning holding times is that they produced a reasonable range in the amount of microconstituents.

Table 5 reports the amount of bainite produced during the 875 F isothermal treatments and the amount of ferrite and pearlite produced by the 1200 F treatments. The balance of the austenite that was untransformed at the end of the isothermal treatment was completely transformed to martensite by the brine-water quench and 120 F treatment. The amount of bainite produced by the 875 F treatment ranged from 0 to 76 percent and varied with the hardenability of the particular steel and the isothermal holding time. As would be expected, the

*A few coupons (X-4, X-6 and Y-5 and Y-6) only had a pair of Charpy specimens tested at each of the three indicated temperatures, NDT, − 120 F and + 212 F. This was not enough data to draw a meaningful Charpy data curve so they are not shown.

steels with the highest hardenabilities transformed the least. A similar effect was observed for the 1200 F isothermal treatment, the amount of ferrite ranging from 0 to 69 percent. Only four of the 1200 F treatments produced measurable amounts of pearlite, ranging from 4 to 32 percent; these steels were low hardenability, low Ni, and low Mn compositions. The fact that only four samples had pearlite in the microstructure must be considered during the subsequent discussion of the effects of microstructure on the NDT temperature. There are so few points that not much confidence should be placed on the estimated effect of pearlite as opposed to the other microconstituents. It must be pointed out that one normally would not find pearlite in the microstructure of this low-carbon, Ni-Cr-Mo alloy steel unless something were grossly wrong. Any discussion of the effect of pearlite is of academic rather than practical interest.

Table 6 gives a summary of the microstructure, tempered-bainite, -ferrite, -pearlite, and -martensite, longitudinal mechanical properties, the drop weight NDT temperature, and transverse and longitudinal Charpy V-notch impact properties resulting from the various heat treatments. Because of the uniform 1150 F temper, the strengths reported here are more characteristic of an HY-100 steel rather than an HY-80 steel. The variations in strength reflect the variety of chemistries studied and the different initial hardnesses, the slightly different responses to tempering, and the different microstructures. The mechanical property data in Table 6, the chemistry data in Table 2, the inclusion content data in Table 3, the prior austenitic grain size data in Table 4 and the microconstituent data in Table 5 were combined to form the set which is the basis of this analysis. In summary, the 115 data points represent the 27 different coupons and constitute the sample used in this analysis.

INDEPENDENCE OF VARIABLES

When performing a regression analysis to determine the functional relationship between a dependent variable and more than one independent variable (in this case NDT temperature and such things as composition, microstructure and strength), it is obvious that the magnitude of each independent variable must be randomly distributed relative to the magnitude of each other independent variable; otherwise it will be difficult if not impossible to apportion a part of the observed changes in the dependent variable to one or another independent variable. In experiments where the investigator is melting his own material he can ensure independence between the independent variable he wishes to study by careful randomization in statistically designed experiments. In this case we have 27 coupons with a wide variation in chemical composition and mechanical properties. In this study to ensure independence, or at least to ensure that there was not a strong correlation between the variables considered, the data making up the sample (115 data sets) were run on a correlation matrix as described in Reference 43.

The results from this correlation matrix are summarized in Table 7, showing the cross-correlated variables with a correlation coefficient from 0.85 to 0.999. Table 7 gives a numbered list of the 83 variables considered and indicates which variables are related to another for three ranges of correlation. The identification number of the variable having the indicated level of correlation is listed next to each. For example V1-Sample Number* is strongly related (correlation from 0.900 to 0.949) to variables 10 and 15 (amount of copper and amount of cobalt). A look at Table 2 shows that this is indeed the case. Producer *X* has much less copper in his melts than producer *Y* and cobalt was measured only on coupons from producer *X*.

*Sample number was derived by numbering the coupons from producer X in the one hundreds and those from producer Y as the two hundreds. For example, material from coupon X-3 was identified in the data set as 103 and material from coupon Y-11 as 211.

Of the individual alloying elements, V8–Amt. Cr is slightly related to V15–Amt. Co, related to V50–V7xV9–NixCr, the product of Amt. Ni times Amt. Cr, a variable representing an interaction effect, and highly related to V79–V8xV8–CrxCr, a second order effect in this variable itself. Table 7 shows that many of the interaction effects and higher order effects using a given variable are strongly correlated to that variable and may not be capable of being properly evaluated using these data. For example, the effect of total aluminum may not be separable from the effect of acid soluble Al in these data, V11 and V12. Similarly, ultimate tensile strength, V27, tensile yield strength, V28, and compressive yield strength, V31 are so strongly correlated as to be difficult to evaluate individually, and thus each must be regarded as just a different way of quantifying the "strength" of the sample.

Of interest in Table 7 is the failure of most of the Charpy V-notch properties at +210 F, –120 F and even at the NDT temperature itself to correlate with the NDT transition temperature of this steel. It is not surprising that Gross[21] was able to obtain only a ±50 F correlation between Charpy V-notch and drop weight NDT transition temperatures for the variety of steels he was using, since the Charpy transition properties measured in the present study did not correlate very well with NDT temperature. Of the Charpy impact properties, only V36 –120 F Pct Fiber has a correlation coefficient greater than 0.47, and it was 0.82. Gross did not try to correlate this with NDT. The present study was not able to relate Charpy and NDT transition temperatures even though this steel (a) was a single grade, (b) had carefully controlled heat treatments, (c) had the drop weight specimen crack starter bead deposited before heat treatment to eliminate the effects of a heat affected zone under the brittle bead, and (d) that the Charpy specimens were taken from the drop weight specimen used to measure NDT.

SINGULARLY SIGNIFICANT VARIABLES AFFECTING NDT

The correlation matrix can perform an important function for the data analyst by giving an indication of those independent variables that by themselves have a linear relationship with the dependent variable. The correlation matrix, Table 7, showed that only three variables have a fairly high linear correlation with NDT temperature; they are:

1. V20 – Prior Austenitic Grain Size, $r = -0.78$
2. V36 – Percent Fibrous Fracture at –120 F, $r = -0.82$
3. V64 – Gamma Grain Size x *TYS*, $r = -0.77$

The next seven best variables have correlation values with NDT temperature ranging between 0.4 and 0.48; the rest of the variables were lower. These seven variables and their values were:

1. V33 – C_V Energy absorbed at the NDT Temperature, $r = 0.48$
2. V21 – Percent Bainite, $r = 0.47$
3. V24 – Percent Martensite, $r = -0.43$
4. V4 – Amount of Phosphorous, $r = 0.41$
5. V37 – C_V Energy Absorbed at +210 F, $r = 0.41$
6. V61 – Ti x N_2, $r = -0.41$
7. V45 – Cr x N_2, $r = 0.40$

The correlation of some of these factors with NDT temperature is understandable. V20 – Prior Gamma Grain Size has been reported in the literature to be a significant variable affecting the transition temperature of

tempered martensitic and bainitic steels,[11, 12, 29, 36, 37, 41, 44] as has strength.[27, 35, 38, 42, 44, 45] However, the correlation between NDT temperature and the interaction between austenitic grain size and tensile yield strength (*TYS*), V64, is more than likely due in this case to the dominating effect of changes in ASTM grain size number on a relatively constant 106 ± 10 ksi tensile yield strength and, as shown later, will not prove to be statistically or practically significant in the multiple variable analysis. The Charpy V-notch fibrous fracture appearance at −120 F, V36, has a strong correlation with NDT temperature. It is logical, since −120 F is close enough to the NDT temperature of most of these samples for the percent fibrous fracture appearance to give a good indication of the change in impact ductility. It is interesting to note that the Charpy V-notch energy absorbed at −120 F, V35, has only $r = -0.37$ in the correlation matrix, reflecting the fact that the producer's original mill rolling practice has introduced a large variability in the energy absorbed and markedly reduced its level of correlation with the NDT temperature.

The seven variables with correlation values between |0.40 and 0.48| are obviously not dominant factors affecting NDT temperature and require evaluation in terms of multiple regression to see if they still contribute significantly to the observed variation in NDT temperature when they are included with a more dominant factor such as prior gamma grain size. As will be subsequently shown, the inclusion of a singularly dominant variable in a multiple regression analysis will eliminate almost all of the variables that show a markedly lower singular correlation.

RESULTS OF REGRESSION ANALYSIS ON NDT

Almost 100 computer analyses were made using the regression analysis program XIRE and the statistical methods described in Reference 43 to evaluate the functional relationship between the NDT temperature, V32, and the other 82 variables listed in Table 7. In the initial computer analyses about 15 variables selected for their mutual independence were selected to determine their functional relationship to NDT temperature. The Charpy V-notch impact values were not included since they are just another aspect of the transition from ductile to brittle impact fracture characterized by the NDT temperature itself. One criterion for selection of significant independent variables was that the term coefficient, Bi in the computer output, consistently demonstrate that it was statistically significant, i.e., not likely to be zero in several regressions with a variety of other variables. As described in Reference 43, this requires that the term regression coefficient divided by the standard deviation of the coefficient, *T* in the output tables, be greater than some value of "*t*," Student "*t*," based on the degrees of freedom* (*DF*) for that particular run and a confidence level of at least 90 percent. Because of the large sample size (here 115 data sets) the usual value of acceptance was about $|T| > 1.70$ since small changes in a large value *DF* do not affect the value of "*t*" much. Another requirement for acceptance was that additional terms should significantly improve the functional relationship as evidenced by statistically significant improvements in the multiple correlation coefficient *R* and the standard deviation *Sx.y*, i.e., reduce the residual variance not accounted for by the terms in the regression equation. It was noted that if an additional term or terms significantly improved *R* it also significantly improved *Sx.y*; see examples 4–11 in Reference 43.

* DF = Sample size minus number of terms in regression, including the dependent variable.

Composition and Producer

The results of many regression analyses can be summarized by saying that most of the alloying additions and alloy interaction terms failed to indicate a consistent and statistically significant relationship to NDT temperature. This is not surprising since the range, minimum to maximum, of each element present is a result of commercial melting practice specifically aimed at trying to stay within procurement specification limits* as opposed to an artificially large range as would be the case in laboratory melts designed to explore the effect of a specific alloy addition.

The only element that displayed a measurable effect was hydrogen; Table 2 shows that it ranged from 0 to 12 ppm with a typical value of 0 to 2 ppm. As a result, even though hydrogen content is statistically significant, its total effect is small, about 2F/ppm H_2, resulting in a 0 to + 24 F change in NDT transition temperature.

The producer also turned out to be a statistically significant variable. The producer was coded as 1 for producer *X* and 2 for producer *Y* for the regression, and the results indicate that the NDT temperature of material made by producer *Y* is about 24 F less than that made by producer *X*, everything else being equal. In the sample of 115 data sets, 76 represent material made by producer *X* and 39 represent material made by producer *Y*. The reason underlying this observation is not simple chance and may be due to either some compositional difference, such as amount of P or Cu which by themselves were not consistently significant, or some difference in mill practice. In any case, the summation of differences is great enough to make the producer a significant variable that must be included in the regression analysis equation.

Prior Austenitic Grain Size

As indicated in Table 4, the prior gamma grain size represented in this sample ranged from ASTM 9.5 to ASTM 3, and was varied by changes in austenitizing temperature and holding time, in this study 1640 F for 1/2 hr and 2000 F for 1 hr, as well as by changes in composition from heat to heat. The regression analysis confirmed the importance of grain size reported in the literature and showed that adding a second order grain size term did not significantly improve the correlation.

It is interesting to note that these results indicate that the Petch linear relation between the 15 ft-lb Charpy V-notch transition temperature *T* and ferritic grain diameter *d*, i. e., $T = A_0 + A_1 \ln D^{-1/2}$, of ferritic steels has a linear corollary for martensitic steels and drop weight NDT temperature.[30, 46] As shown previously, the Petch relationship can be expressed as a linear function of ASTM grain size (*N*), $T = C + D(N)$. In terms of NDT temperature and prior austenitic grain size, it can be written NDTT = $B_0 + B_1 (\gamma GS)$; this is the form of the regression results given in Table 8. The correlation matrix and the regression analysis both indicate that this simple linear relationship will acount for about 80 percent of the observed variability in drop weight NDT temperature of the HY-80 steels studied.

An additional factor that must be considered when discussing prior austenitic grain size is that final gamma grain size prior to quenching reflects the interaction of a number of variables such as:

1. Austenitizing temperature. The higher the temperature above the upper critical, the coarser will be the gamma grain size with controlled grain size steels tending to retain finer grain sizes until their grain coarsening temperature is exceeded.

---

*HY-80 steel is melted to ASTM A 543-65 and MIL-S-16216G (SHIPS).

2. Compositional variations. If, as in the present case, the austenitizing time and temperature are fixed, composition changes will cause the difference between the upper critical temperature (A_{C3}) and the austenitizing temperature to vary slightly. Composition changes that increase this difference will result in a coarser gamma grain size. Increasing C, Mn, Ni, Cu, N_2, B, Cb, and Zn or decreasing Cr, Si, Mo, Ti, W, V, Sn, Al, P, and Zr will tend to increase the prior austenitic grain size if the austenitizing treatment is held constant for a hypoeutectoid steel.[48–54]

3. The longer the time at the austenitizing temperature, the coarser the gamma grain size, especially at temperatures above the grain coarsening temperature for controlled grain size steels.

4. Deoxidation practice or addition of grain refiners such as Al, Si, V, Ti, Mo, W, and rare earth additions will affect or inhibit gamma grain growth.

Such compositional variations would account for the range in gamma grain size resulting from the 1640 F for 1/2 hr austenitizing treatment; Table 4 indicates that gamma grain size ranged from 7 to 9.5 for this treatment. No attempt was made to pinpoint a specific compositional variation for this difference in grain size, but a quick review of the chemistry data in Table 2 indicates that the two heats that resulted in grain size 7 (*X*-3 and *Y*-11) had the lowest nitrogen contents, 0.003 and 0.002 percent, respectively versus an average value of 0.007 percent. Whether or not this is the underlying cause for the difference can not really be settled from these experiments. However, it has been reported in the literature that Al additions combine with nitrogen to form aluminum nitrides that inhibit grain growth.[52]

Microstructure

The previous studies reviewed herein showed that the tempered martensitic structure generally had the lowest transition temperature and that bainitic structures are intermediate to those of the same steel treated to produce martensite or ferrite. Hall indicates that grain size has an effect on transition temperature of the same order as that of degree of hardening.[51] The data in Table 5 show that the steels tested had been treated to produce from 0 to 69 percent bainite with the balance martensite and from 0 to 67 percent ferrite with the balance martensite, except in four cases where there was some pearlite formed during the final part of the 1200 F treatment. Up to 32 percent pearlite was found.

Table 9 gives the regression results for the effects of percent microconstituents on NDT temperature allowing for the effect of prior austenitic grain size, expressed as ASTM grain size number; 100 percent tempered martensite is the implicit baseline. Linear regression terms are used since higher order and interaction terms were not found to statistically improve the relationship. The results show that: (1) bainite raises the NDT transition temperature about one-half a degree per percent; (2) ferrite lowers the NDT transition temperature about three-fourths of a degree F per percent; (3) pearlite raises the NDT temperature about 5 F per percent; and (4) refining the prior austenitic grain size lowers the NDT transition temperature about 20.4 F per unit increase in ASTM grain size number. Thus, one sees that changes in prior austenitic grain size expressed in terms of ASTM grain size have an effect on the NDT temperature that is about an order of magnitude greater than the effect of percentage changes in microconstituents of the HY-80 steel studied here.

A question might arise as to whether there is a change in controlling effect on NDT temperature by the type of grain size, i. e., prior austenitic or ferritic, as the amount of isothermally produced ferrite increases. This question can be answered either by metallographic examination of the fracture path in the broken specimens

or by a graphical analysis of the difference between experimental and calculated values of the NDT temperature as a function of the ferrite content. The latter method has been selected to answer this question since such a graph can be quickly prepared from the back calculation data in the regression analysis computer output, whereas the former would require the laborious preparation of a series of metallographic specimens.

Figure 7 is a plot of the difference between the experimentally observed NDT temperature and the calculated value ($DF = Y - YC$) using the regression results of Table 10 for those specimens which contained a measurable amount up to 69 percent of ferrite. This shows that there is a slight tendency for the calculated value of the NDT temperature to be high, but this tendency is essentially confined to those very fine prior austenitic grain, 8.5 to 9.5, specimens containing only a trace of ferrite. Examining this figure shows that there does not appear to be a systematic difference between experimental and calculated value as the ferrite (and pearlite) is increased to large amounts, until as little as 8 percent martensite remains in a matrix of 69 percent ferrite and 23 percent pearlite. See Figures C1, C16 and C17 in Appendix C for the photomicrographs of the predominately ferrite and pearlite microstructures.

Judging by the results of regression analysis of these data, it is likely that prior austenitic grain size remains the dominant factor controlling NDT temperature of this steel, even as the amount of ferrite is increased to over 50 percent and significant amounts of pearlite are found. This is confirmed also by the relative magnitude of the term coefficients for prior austenitic grain size and percent ferrite in Table 10, which show that a change of one ASTM grain size number has about 100 times as much effect in determining the NDT temperature as a change of one percent ferrite, -19 F/ASTM G. S. number versus -0.2 F/Percent Ferrite.

No attempt was made in the present study either to deliberately vary ferritic grain size or to deliberately vary the prior austenitic grain size before the 1200 F transformation, even though the prior gamma grain size ranged from ASTM 7 to 9.5. While Geil et al.[4] have reported some data on the relative effects of ferrite and prior gamma grain size on the Charpy transition temperature of 0.3 C steels; they came to the conclusion that ferritic grain size is more important. It must be pointed out that they only changed the gamma grain size from 50 percent ASTM 4 plus 50 percent ASTM 6–7 to ASTM 7–8 with few 4–5 in three heats of an unkilled steel. Neither of these experiments has varied the prior gamma grain size enough to say with certainty that either predominantly controls transition temperature in ferritic steels. A definitive set of experiments remains to be done on the relative effects of prior austenitic grain size and ferrite grain size of the ferritic steels.

Inclusion Content

Examination of Table 3 and Figures 5 and 6 shows that the inclusions observed and measured in these samples were small and uniformly dispersed in a way that should not have affected the measured NDT temperature. This was confirmed by the regression analysis, which showed that the inclusion content of these samples did not correlate with the observed variations in NDT temperature of the HY-80 steel studied.

Strength

Reference 44 shows that the strength level of HY-80 steel, varied by tempering at various temperatures for one hour and then quenching, has a strong correlation with the NDT temperature of the steel. The NDT temperature increases as the strength is increased. The tensile yield strengths measured for the 115 data sets that mak up the sample being analyzed have an average value of 106 ksi and a standard deviation of 10.2 ksi. Over such a

restricted range a linear approximation should adequately describe the effect of strength on NDT temperature even though a higher order function would be required for a wider range.

Table 10 shows the results of linear regression analysis for the effects of producer, gamma grain size, percent microconstituents (bainite, ferrite and pearlite) and tensile yield strength in psi. These results show for these data, after accounting for the other variables, that tensile yield strength contributes to determining the NDT temperature only in a minor way, about 0.68 F per 1000 psi increase in tensile yield strength. This is slightly less than the 3 to 4 F per 1000 psi shown graphically in Reference 44 for the range in tensile yield strength (TYS) from 100 to 120 ksi for coarse and fine grained material respectively. The reason for this difference in $\Delta T/\Delta TYS$ between the two studies is that this study covers a slightly wider range in tensile yield strength, from about 86 to about 126 ksi, which includes the range from 80 to 100 ksi that Reference 46 shows has little or no effect on NDT temperature, as opposed to the 100 to 120 ksi range where tensile yield strength has about the maximum effect on NDT temperatures.

Analysis of other computer runs shows that higher order strength terms and terms expressing an interaction between austenitic grain size and either strength or microconstituents do not significantly improve the correlation for these sets of data Correlations based on ultimate tensile strength (UTS) show no statistical or practical improvement over those based on tensile yield strength.

The data in Reference 44 shows that strength level, as changed by variation in tempering temperature, has a larger effect on NDT temperature than is indicated in this study. This is due to the fact that in Reference 44 the strength was varied by tempering for one hour at temperatures ranging from 400 to 1330 F to produce a tensile yield strength ranging from 161 to 81 ksi in the tempered martensitic structure alone; in the present study the tensile yield strength ranged from only 107 to 122 ksi in the 100 percent martensitic structure tempered at 1150 F. Reference 44 also shows that the functional relationship between strength and NDT temperature cannot be represented over the full range of strength by a simple higher order polynomial and thus does not lend itself to regression; in fact, it would appear from Reference 46 that even higher order interaction terms are required to represent the interaction between strength and microstructure. Such a study is not warranted here since the graphs shown in Reference 44 clearly demonstrate the complexity of this interaction.

Summary of Factors Controlling NDT Temperature

Figure 8 gives a series of graphs showing various aspects of the function relationship between the significant variables and NDT temperature of HY-80 steel given in Table 10. The range of each variable shown in these plots is limited to approximately the range of the input data used to develop this relationship. These plots are intended to give the reader a visual understanding of the significance of the relationship and a feeling for the relative effect of small changes in each variable. Figure 8a shows the functional relationship between NDT temperature and prior austenitic grain size in terms of microconstituents and producer when the tensile yield strength is fixed at a typical value, 100 ksi. Figure 8b shows the functional relationship between NDT temperature and relative amounts of nonmartensitic microconstituents in terms of prior austenitic grain size for one producer and a fixed strength level, 100 ksi. In Figure 8c the relationship between tensile yield strength and NDT temperature is shown in terms of amount of nonmartensitic microconstituents and prior austenitic grain size; the range in tensile yield strength has been limited to the range observed experimentally in Table 6.

This study has shown that under carefully controlled conditions which eliminate the possibility of retained austenite and of temper embrittlement due to slow cooling after tempering, the dominant factor controlling the

NDT temperature of a low-carbon, Ni-Cr-Mo steels* such as HY-80 is the prior austenitic grain size. The results in Table 10 and Figure 8 show that prior austenitic grain size has from four to 100 times as much effect on NDT temperature as either the percent nonmartensitic isothermal products, percent bainite, ferrite and pearlite, in a tempered martensitic matrix or the tensile yield strength. The significant variables and the relative effect they had on the NDT temperature of the Ni-Cr-Mo steel used in this study are:

Variable	Range	Effect on NDT
Producer	(Coded 1 or 2)	−21.9 F
Prior Austenitic Grain Size	(3 to 9.5)	−19.2 F/ASTM Grain Size Number
Percent Bainite	(0 to 76 percent)	0.62 F/Percent B
Percent Ferrite	(0 to 69 percent)	− 0.23 F/Percent F
Percent Pearlite	(0 to 32 percent)	5.4 F/Percent P
Tensile Yield Strength	(61.5 to 124.7 ksi)	0.68 F/Ksi

The regression analysis equation is expressed mathematically under Table 10.

The standard deviation ($Sx.y$) of this correlation is 18.3 F and the multiple correlation coefficient (R) is 0.90 with an associated degrees of freedom of 108. Higher order terms and interaction terms did not significantly improve the correlation.

The value of the standard deviation for the correlation reported here, $Sx.y$ = 18.3 F is close to the theoretical limit of the best possible correlation based on the ±10 F repeatability of the drop weight test determination of the NDT temperature and the repeatability of measurement of the supposedly fixed valued independent variables.** For example, a repeatability of ±1/2 in the ASTM prior gamma grain size measurements would indicate that the best possible value of $Sx.y$ for the regression would be about ±15 F. Because of the small contribution of the other variables to NDT temperature variation, small errors in their measurement would not contribute as much to the magnitude of the standard deviation for the regression as would an error in the measurement of the prior austenitic grain size. However, the effect of the errors associated with each of the independent variables plus the variation in the experimental determination of the NDT temperature indicates that the value of the standard deviation associated with the final regression equation given in Table 10, $Sx.y$ = 18.3 F, is close to the theoretically best possible functional relationship between a set of variables and the NDT temperature; lower values can be attained but only by using a set of dummy variables that would have no true significance.

The producer who melted the steel and rolled out the plate is a significant variable when analyzing the variables affecting NDT temperature. This is attributed to basic differences in composition and mill practice that could not be quantified by themselves but are lumped together in this variable.

No chemical composition terms (other than amount of hydrogen) were found to consistently correlate with NDT temperatures, and the low level of hydrogen found in these tests, typically 0 to 2 ppm, results in

*ASTM A 543-65 and MIL-S-16216G (SHIPS).

**Regression analysis programs such as the one used to analyze these data[43] assume the error is associated with the dependent variable and that the independent variables are exact values. While this is not the true case, it is a commonly used assumption. The more rigorous technique has computational and analytical disadvantages that are discussed by Gross in Reference 21.

little practical effect on NDT temperature, 2 F per ppm H_2. The failure of other alloying and trace elements to significantly affect NDT temperature is attributed to the effect of these elements on the prior austenitic grain size which in itself is the dominant factor controlling NDT temperatures measured in these tests. In addition, the alloying and trace elements affect the microstructure and strength through their influence on quantity and type of transformation product produced by austenite decomposition, ferrite strength, temperability, secondary hardening and susceptibility to temper embrittlement, and through their effect on strength and microstructure exert an effect on the secondary factors that determine NDT temperature.

The steel used in these studies was relatively clean and free from inclusions. Inclusion content was not found to be a significant variable affecting the NDT temperature.

The range of tensile yield strength produced by this study was rather limited by the decision to use a single (1150 F) tempering treatment for all samples; the mean value was 106 ksi and ranged from 124.7 ksi for the highest strength tempered martensitic structure to 61.6 ksi for the lowest strength structure containing large amounts of tempered ferrite and pearlite and the least tempered martensite. Reference 44 indicates that the rather small effect of strength on NDT temperature (0.68 F/ksi) is related to the limited range of strengths obtained in this study. Reference 44 indicates that there should be an interaction between strength level and microstructure in their effect on the NDT temperature; this was not observed to be the case in the present study, again probably due to the limited strength range.

The order of magnitude of the effect of prior gamma grain size on the NDT temperature found in this study, -19 F/(γGS), is of the same order of magnitude as that reported in the literature for both ferritic, bainitic and martensitic steels, in terms of ferritic and prior austenitic grain sizes respectively. In plain carbon steels a unit increase in the ASTM ferritic grain size, $\Delta\alpha GS$, will reduce the transition temperature 22 F on the average with the change ranging from +9 to -39 F.[2, 6, 7, 13, 17, 18, 24, 28, 31] Drop weight NDT test of a ferritic steel gave -11 F/$\Delta\alpha GS$.[24] Pearlitic steels[8] (C1080 and C1095) and steels air cooled and tempered[3] (SAE 1045, 2340, and 3140) had $\Delta T/\Delta\gamma GS$ ranging from -17 to $\simeq -125$ F per unit change in prior austenitic grain size. In a study of the effect of impurity, P and Sn level, $\Delta T/\Delta\gamma GS$ ranged from -4 to -42 F per unit change in prior austenitic grain size in a 0.3 C, 2.0 Ni, 0.75 Cr steel with the value increasing with impurity level and embrittling treatment.[23]

The linear dependence of transition temperature of ferritic steels on ferrite grain size, $T = A_0 + A_1 \ln D^{-1/2}$, reported by Petch,[30, 46] and of pearlite, 0.84 and 0.95 C, steels on prior austenitic grain size reported by Gross and Stout[16] is in agreement with the linear dependence of NDT temperature on prior austenitic (ASTM) grain size observed for the martensite HY-80 steel used in this study. Irvine and Pickering[27] report that the transition temperature of low-carbon bainitic steels increases in an S shaped relationship, third order, with increasing prior gamma grain diameter as varied by reheating to various austenitizing temperatures. Replottting their data on semilog graph paper shows that the transition temperature of low-carbon bainitic steels also varies in an approximately linear manner with the logarithm of the grain diameter. The results of the present study indicate that a low-carbon tempered martensitic steel such as HY-80 also has a linear relation between NDT temperature and prior austenitic grain size as expressed in ASTM grain size numbers. This relationship is not affected by appreciable amounts of isothermally produced bainite and ferrite in a structure tempered at 1150 F.

CONCLUSIONS

The following conclusions are based on the results of a study on the effects on the NDT temperature of: (1) commercial variation in composition and inclusion content, (2) variation in microstructure, prior austenitic grain size and microconstituents produced by quenching and by partial isothermal transformation at 1200 and 875 F to produce ferrite and bainite prior to quenching, and (3) variation in strength level after an 1150 F temper for one hour followed by a water quench to prevent embrittlement while cooling from the tempering temperature.

The steel used in these studies is a high toughness, low impact transition temperature, quenched and tempered Ni-Cr-Mo steel of the type made to ASTM Standard A 543-65 and Military Specification MIL-S-16216G (SHIPS). Sixteen coupons were obtained from one producer and eleven coupons from another. The average composition of the steels used in this study are given below:

0.18 Percent C	0.10 Percent Cu
0.36 Percent Mn	0.032 Percent Acid Soluble Al
0.016 Percent P	0.040 Percent Total Al
0.019 Percent S	0.002 Percent Ti
0.30 Percent Si	0.014 Percent O_2
2.75 Percent Ni	0.007 Percent N_2
1.51 Percent Cr	1 ppm H_2
0.38 Percent Mo	

FACTORS AFFECTING THE NDT TEMPERATURE

The results of this study show that the NDT temperature of the low-carbon Ni-Cr-Mo steel tested is primarily determined by a single variable and that the other significant variables act in a secondary way. The conclusions drawn from this study are as follows:

1. Using a tempered 100 percent martensitic microstructure as the baseline, the significant variables acting to determine the NDT temperature measured in this study and their relative (from Table 10) effects are:

Variable	Range	Effect on NDT
Producer	(Coded 1 or 2)	−21.9 F
Prior Austenitic Grain Size	(3 to 9.5)	−19.2 F/ASTM Grain Size Number
Percent Bainite	(0 to 76 percent)	0.62 F/Percent B
Percent Ferrite	(0 to 69 percent)	− 0.23 F/Percent F
Percent Pearlite	(0 to 32 percent)	5.4 F/Percent P
Tensile Yield Strength	(61.5 to 124.7 ksi)	0.68 F/Ksi

The effect of a unit change in prior austenitic grain size on NDT temperature is one and one-half to two orders of magnitude greater than the effect of either a percentage change in the amount of isothermally produced bainite and ferrite or a 1000 psi change in tensile yield strength.

$$\text{NDT Temperature (F)} = -77 - 22\,(\text{Producer 1 or 2}) - 19.2\,(\gamma GS) + 0.62\,(\text{Percent B}) - 0.23\,(\text{Percent F}) + 5.4\,(\text{Percent P}) + 0.68\,(TYS \text{ in ksi})$$

2. A linear function of the significant terms gives the best expression of the functional relationship between these variables and the NDT temperature since it was found that higher order and interaction terms did not significantly improve the correlation.

3. No chemical composition terms were found to consistently correlate with measured NDT temperatures in a statistically significant manner, except for the amount of hydrogen in the steel, and the low level of hydrogen found in these steels, typically 0 to 2 ppm, results in little practical effect on NDT temperature, 2 F per ppm H_2. The failure of alloying and trace elements to significantly affect NDT temperature is attributed primarily to the fact that these elements interact with: (a) the austenitizing treatment to control prior austenitic grain size; (b) the transformation product; (c) temperability and final strength of the steel; and (d) basic susceptibility to embrittlement during normal tempering, as well as the fact that ranges in the amount of each element were so restricted by the specifications and commercial melting practice as to make it impossible to detect their relatively weak effect on a sound statistical basis.

4. The inclusion content was not found to be a significant factor affecting the NDT temperatures measured in these studies.

5. The weak correlation between tensile yield strength and NDT temperatures observed in this study, as opposed to the strong effect reported in References 44 and 45 is attributed to the limited range of strengths produced by the 1150 F temper used on all material in the present study.

6. The linear relationship between ASTM prior austenitic grain size and NDT temperature of the low-carbon Ni-Cr-Mo steel used in this study is similar to the linear dependence between: (a) prior austenitic grain diameter and the transition temperature of low-carbon bainitic steels reported by Irvine and Pickering;[27] (b) prior austenitic grain size and the transition temperature of pearlitic 0.84 and 0.95 C steels reported by Gross and Stout;[16] and (c) the logarithm of the ferritic grain diameter and the transition temperature of ferritic steels reported by Petch.[30]

7. The results of these studies indicate that the steel producer is a statistically significant variable that can account for about 22 F of the observed variation in NDT temperature, depending upon which producer made the steel; this is attributed to a combination of small compositional differences, such as amount of P or Cu which by themselves were not consistently significant, and to differences in mill practice. In any case, these results indicate that the producer is a significant variable that should be considered in any analysis of variables affecting the NDT temperature of low-carbon Ni-Cr-Mo steels.

ACKNOWLEDGMENT

This report is based on work carried out by the author in the course of his employment with the Naval Ship Research and Development Center, Bethesda, Maryland. Use of the data as a basis for a thesis was approved by the University of Michigan and NSRDC.

The author gratefully acknowledges the advice and guidance given by Professor M. J. Sinnott and members of his doctoral committee from the University of Michigan and by Mr. A. R. Willner of the Center whose encouragement and support made this work possible. Thanks are given to Mr. Daniel Embody of the Biometrical Service, U. S. Department of Agriculture, Beltsville, Maryland, for his advice and guidance on the use of regression analysis programs. The contributions of J. Hogben, R. J. Langley and R. Martin and other members of the Center staff are especially appreciated.

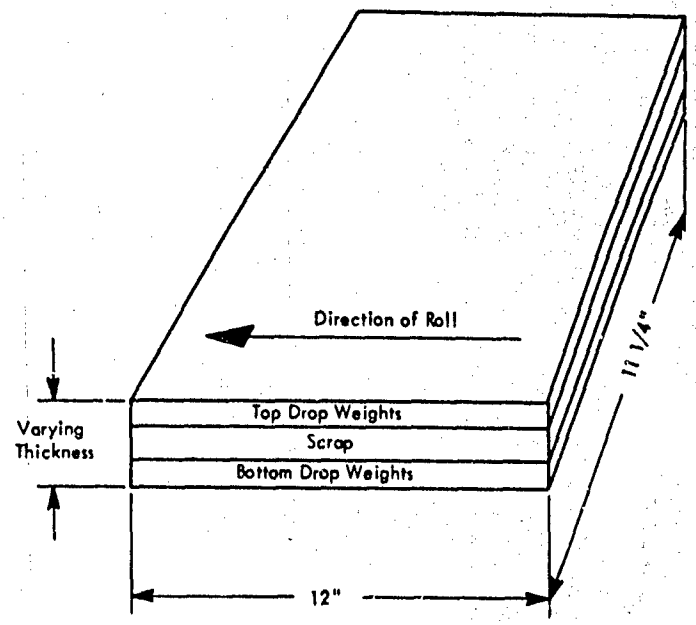

Figure 1 – Location of Material Used in This Study

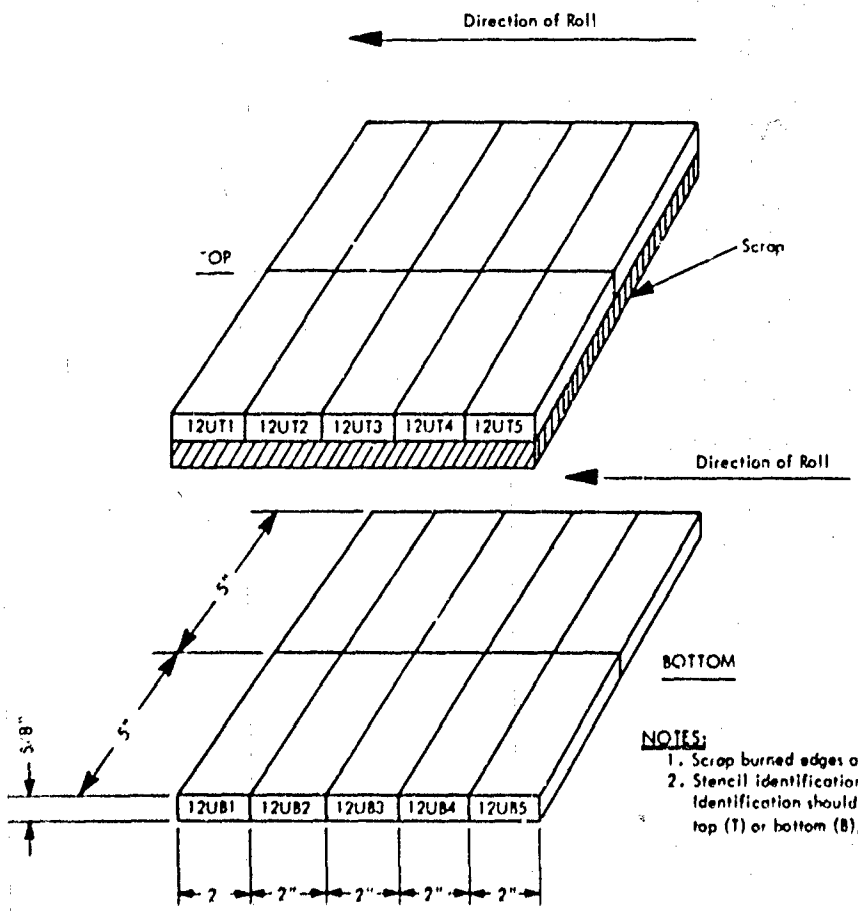

NOTES:
1. Scrap burned edges of coupon for at least 1/2 inch all around.
2. Stencil identification on 5/8" x 2 inch face shown on sketch. Identification should include: coupon number (12U, 13U, etc.), top (T) or bottom (B), and specimen number (1-10).

Figure 2 -- Layout of Drop Weight Test Specimens

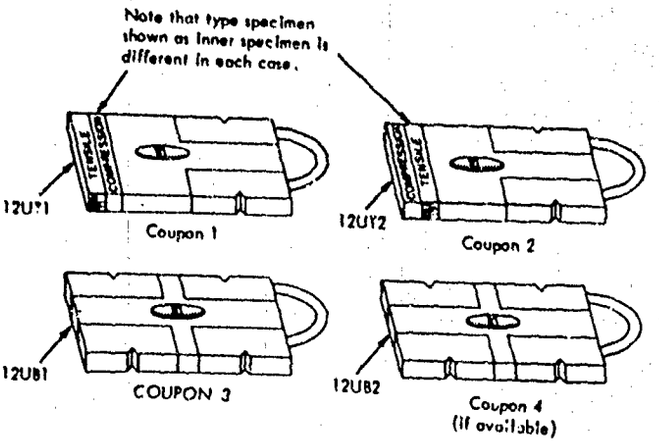

NOTE:

1. Take the following specimens at the locations shown from each group of coupons:
   (A.) 2 longitudinal modified S-914 tensile specimens.
   (B.) 2 longitudinal S-12914 compression specimens.
   (C.) 10 transverse B-328-4 Charpy V-notch speciments. (See sheet No. 2 for additional instructions regarding the Charpy specimens.)
2. Identify each specimen with the following:
   (A.) Coupon No. (12UT4 for example)
   (B.) Direction (L or T)
   (C.) Specimen No. 1→4 (or 6 if necessary)
3. Identify tensile and Charpy specimens on both ends by stamping.
4. Identify compression specimens by scribing on the side only.
5. If any Charpy specimens have to come from under weld bead they should come from coupons 1 and 2.

Figure 3a – Location of Test Specimens

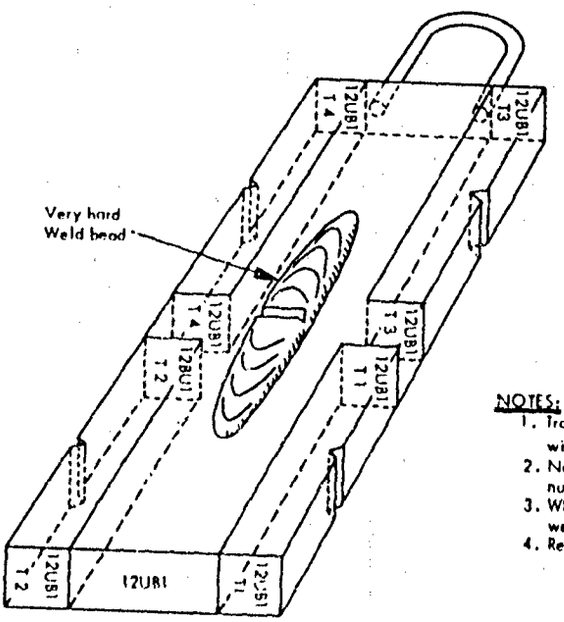

NOTES:

1. Transverse Charpy V-Notch Impact Specimens in accordance with NSRDC drawing B-328-4.
2. Note direction of notch and specimen identification numbers, see drawing B-328-4 for details.
3. When sawing specimens out of coupon stay away from the weld deposit; it is very hard.
4. Reidentify coupon after sawing specimens.

Figure 3b – Details of Layout of Charpy V-Notch Specimens

Figure 3 – Location of Mechanical Property and Transverse Charpy V-Notch Impact Specimens Made from Tested Drop Weight Specimens

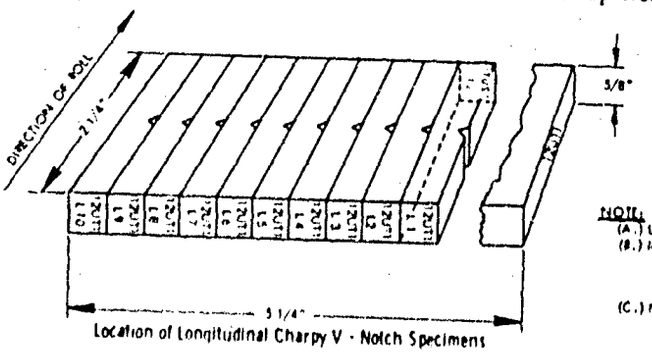

NOTE:

(A.) Longitudinal Specimens in accordance with DTMB Drawing B-328-5.
(B.) Identify each Specimen as shown in B-328-5 with the following:
   1. Coupon number.
   2. Direction L (longitudinal for parallel to direction of roll).
   3. Specimen sequence 1 through 10.
(C.) Notch through the plate thickness as shown in B-328-5.

Figure 4 – Location of Longitudinal Charpy V-Notch Impact Specimens Made from Special Specimen Blocks

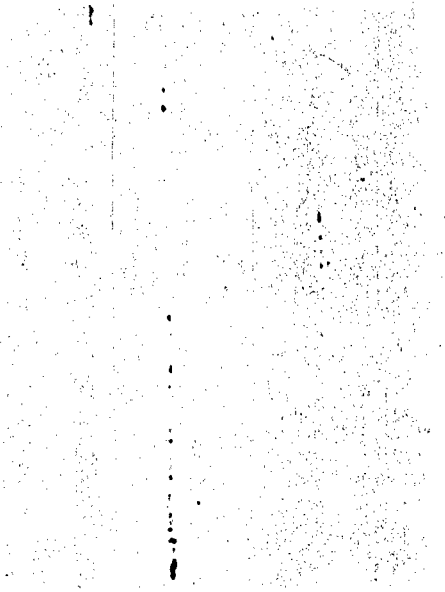

Figure 5a – Mid-Thickness, Longitudinal

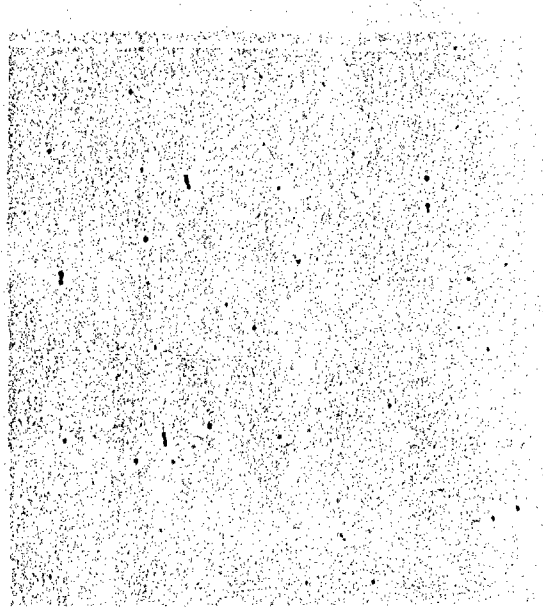

Figure 5b – Mid-Thickness, Transverse

Figure 5c -- Adjacent to Surface, Longitudinal

Figure 5d – Adjacent te Surface, Transverse

Figure 5 -- Photomicrographs of the Inclusion Content of Coupon *X*-18

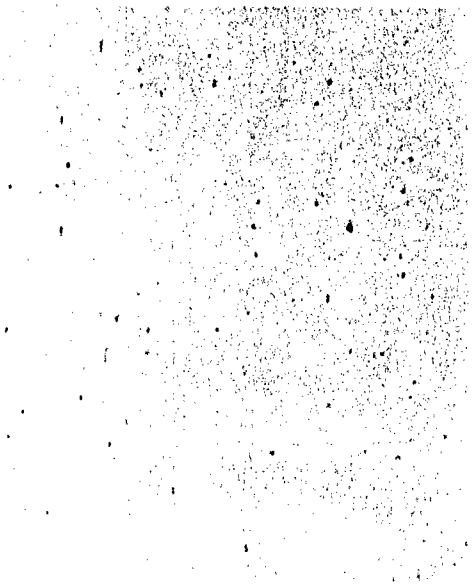

Figure 6a – Mid-Thickness, Longitudinal

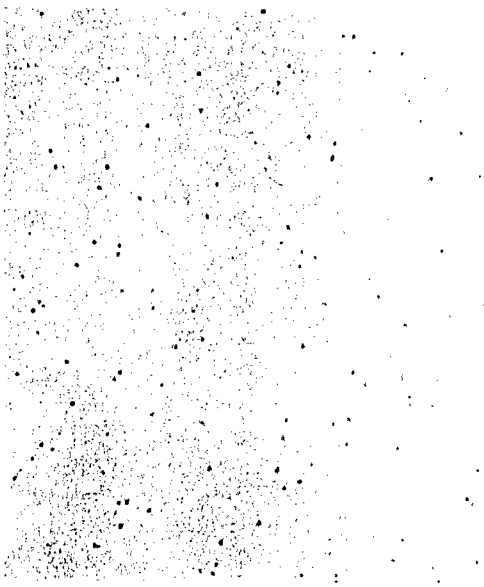

Figure 6b – Mid-Thickness, Transverse

Figure 6c – Adjacent to Surface, Longitudinal

Figure 6d – Adjacent to Surface, Transverse

Figure 6 – Photomicrographs of the Inclusion Content of Coupon Y-1

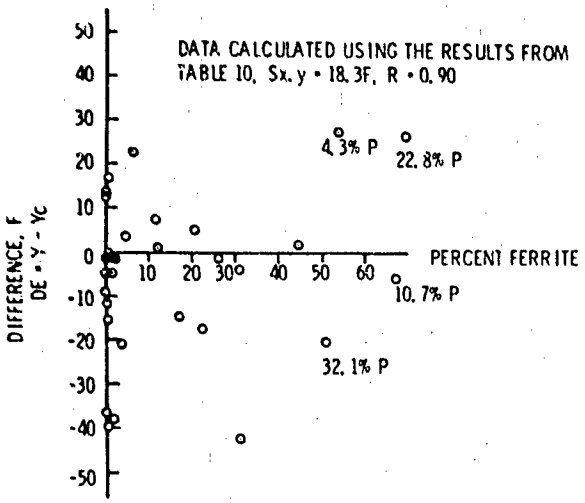

Figure 7 -- A Plot of the Difference between Calculated and Experimental NDT Temperature of Material Containing from a Trace to 69 Percent Ferrite versus Ferrite Content

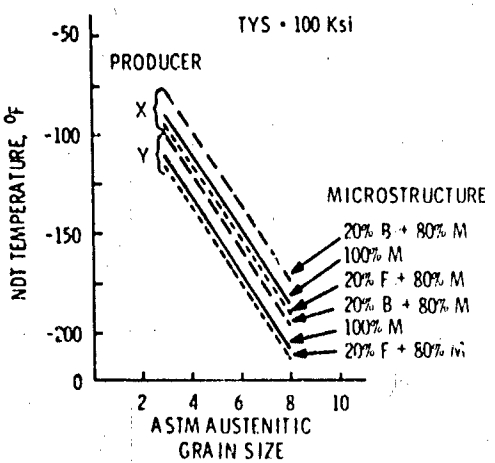

Figure 8a -- Functional Relationship between NDT Temperature and Prior Austenitic Grain Size in Terms of Microconstituents and Producer

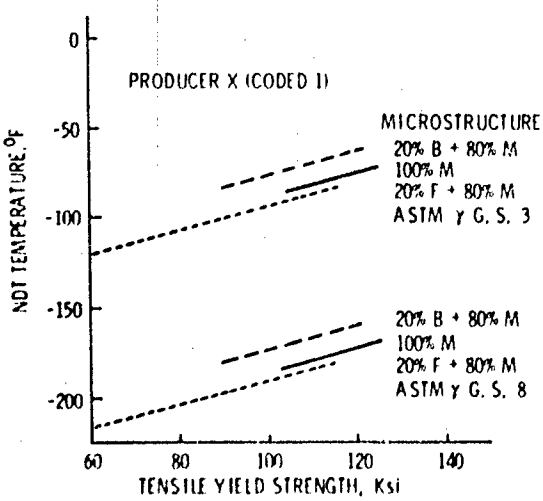

Figure 8c -- Functional Relationship between NDT Temperature and Tensile Yield Strength in Terms of Microconstituents and Prior Austenitic Grain Size

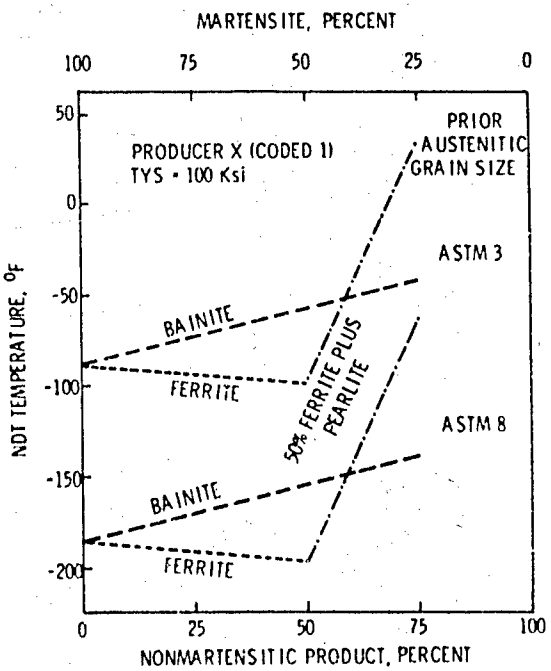

Figure 8b -- Functional Relationship between NDT Temperature and Microconstituents in Terms of Prior Austenitic Grain Size

Figure 8 -- Plots Showing the Relative Effect of Prior Austenitic Grain Size, Producer Percent Nonmartensitic Isothermal Transformation Produce (Bainite, Ferrite and Pearlite), and Tensile Yield Strength on the NDT Temperature of a Low-Carbon Ni-Cr-Mo Alloy Steel Tempered at 1150 F

TABLE I

Producer's Reported Chemical Composition and Mechanical Properties

IDENT. NO.	HEAT NO.	LOC.	CHEMICAL COMPOSITION, PCT C	MN	P	S	CU	SI	NI	CR	MO	COUPON SIZE TXWXL, IN.	SPEC. DIR.	MECHANICAL PROPERTIES STRENGTH, KSI YIELD	TENSILE	ELONG. IN 2 IN., PCT	RED. IN AREA, PCT	LONGITUDINAL CHARPY V-NOTCH ENERGY, FT-LB
X- 1	655399	L	.16	.26	.011	.020		.23	2.60	1.35	.47	2X21X90	TRANS	88.1	108.0	24.0	63.8	101-108-108
		F	.16	.25	.014	.020		.22	2.59	1.40	.44		LONG.	84.2	102.8	24.0	73.0	90- 89- 92
		R	.16	.28	.014	.019		.24	2.61	1.40	.36							
X- 2	725686	L	.14	.30	.013	.016		.24	2.85	1.53	.41	6X18X126	TRANS	80.8	100.7	26.0	70.1	
		F	.15	.30	.015	.017		.22	2.83	1.58	.38		LONG.	80.7	100.8	24.0	71.9	96- 96-104
		R	.15	.28	.020	.017		.18	2.80	1.50	.39							
X- 3	725686	L	.14	.30	.013	.016		.24	2.85	1.53	.41	1.62X18X118	TRANS	88.8	106.2	22.5	68.7	99- 97-97
		F	.15	.30	.015	.017		.22	2.83	1.58	.38		LONG.	86.3	102.0	25.0	75.0	110- 85- 85
		R	.15	.28	.020	.017		.18	2.80	1.50	.39							
X- 4	665411	L	.16	.34	.016	.019		.28	2.84	1.66	.46	2X21X140	TRANS	93.7	113.7	23.0	57.2	84- 87- 86
		F	.19	.34	.016	.019		.27	2.85	1.72	.41		LONG.	96.3	114.5	25.0	68.8	82- 92-102
		R	.18	.34	.027	.020		.24	2.85	1.74	.40							
X- 5	665357	L	.17	.30	.011	.018		.28	2.80	1.69	.45	2.13X17X133	TRANS	91.3	112.0	22.0	63.9	110-106-112
		F	.16	.32	.015	.019		.24	2.82	1.71	.42		LONG.	89.1	110.4	24.0	71.5	110-110-124
		R	.16	.30	.022	.018		.22	2.83	1.71	.42							
X- 6	655799	L	.16	.32	.013	.015		.27	2.82	1.70	.46	3.75X18X76	TRANS	86.0	104.0	22.0	69.1	
		F	.15	.30	.013	.015		.27	2.80	1.75	.45		LONG.	80.1	101.2	22.0	74.3	124-130-120
		R	.14	.32	.012	.016		.25	2.85	1.75	.44							
X- 8	660040	L	.15	.25	.013	.017		.23	2.76	1.52	.35	2X23X140	TRANS	92.0	107.6	24.0	69.6	113-117-114
		F	.15	.26	.015	.016		.24	2.76	1.50	.27		LONG.	87.5	105.7	24.0	63.9	121-125-113
		R	.14	.27	.021	.016		.18	2.74	1.38	.32							
X- 9	700032	L	.14	.29	.013	.016		.28	2.85	1.78	.38	1.5X24X100	TRANS	84.0	108.2	23.0	64.0	120-132-133
		F	.16	.28	.017	.017		.26	2.88	1.76	.36		LONG.	80.1	102.1	24.0	75.2	127-117-124
		R	.14	.28	.012	.017		.25	2.81	1.77	.34							
X-10	650178	L	.16	.35	.018	.017		.27	3.00	1.62	.36	1.75X42X130	TRANS	90.8	111.2	22.0	64.4	123-125-122
		F	.16	.35	.012	.014		.24	2.91	1.68	.42		LONG.	88.2	108.8	22.0	73.2	99- 91- 85
		R	.17	.38	.013	.015		.24	2.90	1.58	.36							
X-11	X51294	L	.15	.26	.009	.011		.23	2.95	1.50	.50	2.13X36X139	TRANS	83.1	102.0	26.0	66.6	85- 82- 89
		F	.16	.28	.009	.012		.23	2.90	1.50	.48		LONG.	80.1	104.9	26.0	71.6	99- 99- 94
		R	.17	.28	.010	.012		.23	2.89	1.49	.48							
X-12	68U369	L	.16	.27	.012	.018		.27	3.00	1.58	.40	1.5X28X96	TRANS	91.6	109.2	23.0	66.8	127-135-131
		F	.17	.29	.011	.018		.22	2.99	1.50	.38		LONG.	90.7	108.5	24.0	72.7	122-125-130
		R	.16	.29	.017	.017		.18	3.03	1.52	.37							
X-13	68U369	L	.16	.27	.012	.018		.27	3.00	1.58	.40	4.5X23X96	TRANS	86.3	110.5	24.0	68.5	
		F	.17	.29	.011	.018		.22	2.99	1.50	.38		LONG.	82.6	103.6	24.0	73.8	115-102-119
		R	.16	.29	.017	.017		.18	3.03	1.52	.37							

TABLE 1 (Continued)

X-14	66U397	L	.19	.27	.010	.017		.25	2.90	1.75	.41	2X20X135	TRANS	85.7	110.2	24.0	59.7	91- 68- 97
		F	.19	.29	.011	.016		.27	2.87	1.73	.39		LONG.	85.6	108.6	22.0	68.9	102-100- 70
			.16	.25	.016	.017		.22	2.87	1.75	.40							
X-15	66U397	L	.19	.27	.010	.017		.25	2.90	1.75	.41	4.5X26X114	TRANS	92.8	110.8	20.0	67.9	
		F	.19	.29	.011	.016		.27	2.87	1.73	.39		LONG.	89.7	109.1	24.0	62.9	94- 96- 97
		R	.16	.25	.016	.017		.22	2.87	1.75	.40							
X-16	N51533	L	.16	.30	.014	.015		.22	2.92	1.63	.53	1.8X74X97	TRANS	91.1	109.3	22.0	63.5	
		F	.16	.31	.013	.014		.21	2.89	1.65	.51		LONG.	89.8	108.9	24.0	68.3	95- 97- 97
		R	.16	.33	.012	.015		.22	2.87	1.65	.52							
X-17	N51533	L	.16	.30	.014	.015		.22	2.92	1.63	.53	6X22X67	TRANS	91.2	108.5	25.0	68.3	
		F	.16	.31	.013	.014		.21	2.89	1.65	.51		LONG.	88.2	106.8	26.0	71.4	86- 60- 65
		R	.16	.33	.012	.015		.22	2.87	1.65	.52							
Y- 1	A2171-9A		.15	.22	.021	.024		.22	2.15	1.28	.27	.69X15X148	TRANS	87.4	104.5	26.0		
													LONG.	90.5	106.5	25.0		90- 92- 97
Y- 2	A2345-4			.26	.010	.017				1.28		2X15X161	TRANS	88.4	107.9	27.0		
													LONG.	91.9	110.8	26.0		89- 96- 90
Y- 3	A2472-10		.14	.19	.010	.026		.22	2.11	1.10	.26	.75X15X103	TRANS	86.2	103.4	23.0		
													LONG.	82.8	101.0	25.0		96- 92- 95
Y- 4	A2480-4C		.17	.35	.011	.022		.28	2.77	1.55	.37	2.62X15X75	TRANS	84.8	106.9	25.0		
													LONG.	86.6	107.4	26.0		64- 71- 73
Y- 5	A2848-2		.17	.31	.010	.023	.19	.26	2.81	1.49	.39	2.25X15X155	TRANS	88.5	109.0	24.0		
													LONG.	87.1	107.9	26.0		87- 88- 86
Y- 6	20730-5		.17	.32	.010	.024	.17	.25	2.75	1.54	.42	2X15X121	TRANS	90.0	109.5	24.0		
													LONG.	88.9	107.6	25.0		89- 90- 88
Y- 7	19540-6		.16	.35	.010	.025	.16	.30	2.74	1.67	.40	1.5X15X96	TRANS	85.1	104.1	25.0		
													LONG.	82.1	102.5	26.0		86- 90- 90
Y- 8	19540-1		.16	.35	.010	.025	.16	.30	2.74	1.67	.40	2X15X161	TRANS	85.1	105.0	25.0		
													LONG.	90.6	108.9	26.0		83- 81- 83
Y- 9	20844-2		.16	.29	.010	.025	.15	.25	2.76	1.47	.43	2X8.5X109	TRANS	88.6	108.4	25.0		
													LONG.	88.4	108.1	28.0		109-109-108
Y-10	21222-2		.16	.34	.013	.023	.23	.27	2.80	1.53	.42	2.5X15X168	TRANS	85.1	105.0	25.0		
													LONG.	90.6	108.9	26.0		78- 72- 75
Y-11	22616-1		.15	.25	.010	.025	.17	.20	2.85	1.42	.23	3.62X15X158	TRANS	81.6	103.5	25.0		
													LONG.	80.1	99.0	27.0		45- 55- 53

* L IS LADLE, F IS FRONT AND R IS REAR

TABLE 2

Actual Chemical Composition of Coupons

CHEMISTRY DATA

SPEC. NO.	AMT. C	AMT. MN	AMT. P	AMT. S	AMT. SI	AMT. NI	AMT. CR	AMT. MO	AMT. CU	ACID SOL AL	TOTAL AL	AMT. TI	AMT. V	AMT. CO	AMT. O(2)	AMT. N(2)	AMT H(2) PPM	D(I) 50M	GRAIN SIZE
X- 1	0.15	.280	.015	.018	0.210	2.590	1.450	0.360	0.076	.0280	.0400	.0040	.0010	.	.0110	.0050	1	5.78	8.50
X- 2	0.16	.380	.016	.021	0.300	2.750	1.490	0.350	0.048	.0320	.0360	.0010	.0020	.	.0050	.0060	0	7.83	8.00
X- 3	0.14	.390	.023	.020	0.270	2.760	1.470	0.350	0.049	.0230	.0260	.0010	.0020	.	.0150	.0030	1	7.95	7.00
X- 4	0.18	.360	.017	.018	0.260	2.930	1.800	0.310	0.075	.0240	.0420	.0050	.0010	.	.0490	.0080	7	9.33	9.50
X- 5	0.17	.300	.019	.017	0.230	2.780	1.740	0.320	0.044	.0230	.0470	.0050	.	.	.0480	.0060	3	8.96	8.50
X- 6	0.14	.290	.016	.011	0.210	2.710	1.730	0.290	0.040	.0230	.0330	.0040	.	.	.0200	.0070	1	5.71	8.00
X- 8	0.20	.370	.014	.023	0.320	2.750	1.400	0.300	0.047	.0410	.0460	.0010	.0020	.	.0150	.0090	1	8.41	8.50
X- 9	0.17	.420	.020	.015	0.300	2.810	1.620	0.310	0.048	.0320	.0360	.0010	.0030	.	.0060	.0080	0	8.85	8.50
X-10	0.22	.440	.015	.017	0.300	2.780	1.460	0.310	0.041	.0470	.0530	.0010	.0020	.	.0060	.0080	0	13.83	9.50
X-11	0.18	.390	.013	.015	0.310	2.890	1.420	0.470	0.074	.0400	.0480	.0020	.0030	.	.0130	.0110	0	10.27	8.50
X-12	0.18	.360	.021	.018	0.360	2.930	1.450	0.350	0.069	.0260	.0300	.0020	.0050	.0210	.0130	.0050	0	7.62	8.50
X-13	0.16	.340	.020	.017	0.320	2.850	1.420	0.350	0.054	.0360	.0410	.0010	.0040	.0190	.0110	.0060	0	7.58	8.00
X-14	0.22	.360	.017	.018	0.360	2.750	1.600	0.370	0.049	.0350	.0410	.0010	.0020	.0100	.0120	.0060	1	8.00	9.50
X-15	0.16	.370	.019	.018	0.300	2.700	1.610	0.350	0.060	.0360	.0410	.0010	.0040	.0110	.0100	.0050	0	7.53	8.50
X-16	0.18	.400	.017	.018	0.300	2.830	1.550	0.500	0.088	.0580	.0650	.0020	.0060	.0100	.0100	.0070	0	12.10	9.50
X-17	0.17	.390	.019	.022	0.310	2.780	1.540	0.500	0.101	.0640	.0710	.0020	.0060	.0100	.0080	.0070	1	10.50	8.50

SPEC. NO.	AMT. C	AMT. MN	AMT. P	AMT. S	AMT. SI	AMT. NI	AMT. CR	AMT. MO	AMT. CU	ACID SOL AL	TOTAL AL	AMT. TI	AMT. V	AMT. CO	AMT. O(2)	AMT. N(2)	AMT H(2) PPM	D(I) 50M	GRAIN SIZE
Y- 1	0.21	.320	.013	.023	0.310	2.150	1.200	0.270	0.160	.0220	.0250	.0010	.0020	.	.0040	.0090	2	4.68	8.50
Y- 2	0.19	.260	.008	.017	0.260	2.690	1.560	0.420	0.170	.0060	.0280	.0040	.	.	.0090	.0090	1	7.17	9.50
Y- 3	0.18	.290	.015	.021	0.320	2.100	1.100	0.270	0.170	.0320	.0360	.0010	.0010	.	.0160	.0090	1	3.87	8.50
Y- 4	0.21	.370	.010	.017	0.290	2.910	1.580	0.510	0.190	.0030	.0250	.0050	.	.	.0240	.0090	12	13.29	9.50
Y- 5	0.19	.320	.007	.019	0.280	2.890	1.520	0.340	0.260	.0150	.0360	.0040	.	.	.0310	.0100	1	8.14	8.50
Y- 6	0.18	.340	.011	.021	0.240	2.770	1.570	0.350	0.250	.0270	.0370	.0040	.	.	.0240	.0070	7	8.61	9.50
Y- 7	0.20	.380	.009	.025	0.300	2.750	1.670	0.550	0.190	.0270	.0470	.0050	.0010	.	.0250	.0090	1	13.47	8.50
Y- 8	0.17	.490	.015	.028	0.330	2.650	1.520	0.370	0.150	.0380	.0430	.0020	.0030	.	.0040	.0090	1	8.28	8.50
Y- 9	0.19	.420	.015	.018	0.300	2.730	1.400	0.400	0.150	.0320	.0360	.0010	.0020	.	.0040	.0070	0	10.02	8.50
Y-10	0.20	.490	.021	.018	0.330	2.700	1.450	0.380	0.190	.0380	.0420	.0110	.0020	.	.0110	.0070	2	9.69	8.50
Y-11	0.17	.380	.020	.022	0.290	2.790	1.400	0.390	0.160	.0100	.0130	.0010	.0030	.	.0080	.0020	0	9.89	7.00

TABLE 3

Inclusion Content

INCLUSION RATING AT THE SURFACE AND MID-THICKNESS
(ASTM E45-63, METHOD B)

SPECIMEN NUMBER	MID-THICKNESS LONGITUDINAL INCLUSIONS LONGEST	MID-THICKNESS LONGITUDINAL INCLUSIONS OTHERS	MID-THICKNESS LONGITUDINAL BACK-GROUND	MID-THICKNESS TRANSVERSE INCLUSIONS LONGEST	MID-THICKNESS TRANSVERSE INCLUSIONS OTHERS	MID-THICKNESS TRANSVERSE BACK-GROUND	BOTTOM SURFACE LONGITUDINAL INCLUSIONS LONGEST	BOTTOM SURFACE LONGITUDINAL INCLUSIONS OTHERS	BOTTOM SURFACE LONGITUDINAL BACK-GROUND	BOTTOM SURFACE TRANSVERSE INCLUSIONS LONGEST	BOTTOM SURFACE TRANSVERSE INCLUSIONS OTHERS	BOTTOM SURFACE TRANSVERSE BACK-GROUND
X- 1	3.5^{6}	1.2^{2}	A	1.0^{vd}	1.2^{1}	A	3.0^{vd}	1.6^{3}	B	3.7^{d}	1.1^{4}	A
X- 2	3.5^{vd}	.0	D	2.5^{d}	1.0^{1}	C	1.5^{vd}	1.4^{1}	A	2.0^{d}	1.0^{1}	B
X- 3	5.0^{d}	2.1^{5}	A	3.5^{vd}	1.5^{1}	A	3.5^{8}	1.5^{4}	C	5.7^{vd}	1.7^{1}	B
X- 4	3.0^{d}	1.8^{2}	A	1.5^{d}	1.3^{3}	C	1.9^{vd}	1.2^{3}	B	2.0^{vd}	.0	B
X- 5	8.0^{vd}	1.6^{2}	A	1.3^{vd}	.0	B	1.0^{d}	.0	A	6.0^{d}	3.6^{2}	C
X- 6	6.1^{8}	1.9^{2}	A	6.0^{8}	1.9^{6}	B	2.8^{d}	2.0^{1}	A	1.5^{vd}	1.0^{1}	A
X- 8	3.5^{vd}	2.1^{7}	B	2.7^{d}	1.5^{4}	A	3.5^{d}	1.7	D	4.2^{vd}	1.5^{3}	D
X- 9	2.5^{8}	1.3^{7}	B	3.5^{8}	1.0^{2}	D	3.7^{8}	1.7^{4}	C	$.6^{d}$	.0	A
X-10	2.3^{d}	1.7^{6}	D	2.0^{d}	1.5^{3}	B	1.5^{d}	1.1^{5}	C	$.7^{vd}$	.0	A
X-11	2.8^{d}	1.4^{13}	C	5.0^{vd}	1.5^{9}	C	1.6^{d}	1.3^{10}	D	1.3^{d}	.0	B
X-12	2.5^{vd}	1.6^{13}	C	1.0^{vd}	.0	A	4.3^{vd}	1.6^{21}	C	2.7^{vd}	1.1	B
X-13	1.7^{vd}	1.4^{11}	B	1.3^{d}	1.1^{2}	A	1.1^{d}	1.0^{1}	D	2.2^{8}	1.2^{2}	A
X-18	4.3^{vd}	2.0^{24}	C	1.9^{8}	1.0^{3}	C	3.2^{vd}	1.6^{16}	C	1.2^{d}	.0	A
X-15	2.1^{d}	1.2^{8}	D	1.5^{8}	.0	B	2.7^{vd}	1.36	C	3.2^{d}	1.4^{1}	B
X-16	5.6^{d}	2.1^{63}	C	2.2^{vd}	1.5^{3}	B	6.0^{d}	2.1^{39}	C	2.6^{8}	1.2^{3}	D
X-17	4.3^{8}	1.6^{5}	B	1.2^{8}	1.1^{3}	A	2.1^{d}	1.36	A	$.6^{d}$	.0	A
Y- 1	2.9^{vd}	2.1^{5}	C	7.4^{d}	2.7^{8}	D	3.0^{vd}	.0	A	6.0^{vd}	.0	D
Y- 2	1.2^{d}	.0	A	4.0^{d}	1.1^{1}	A	1.9^{d}	1.2^{5}	A	2.6^{8}	1.5^{1}	A
Y- 3	4.1^{vd}	1.5^{7}	A	7.0^{8}	.0	A	4.2^{vd}	2.6^{2}	A	1.5^{8}	.0	A
Y- 4	2.4^{vd}	1.2^{2}	A	1.5^{8}	1.3^{1}	B	4.0^{d}	1.0^{1}	A	5.4^{d}	1.3^{3}	A
Y- 5	4.2^{d}	1.3^{1}	A	5.5^{vd}	2.2^{4}	C	4.0^{vd}	1.3^{4}	A	2.5^{vd}	1.3^{2}	C
Y- 6	2.5^{d}	1.1^{3}	B	3.2^{8}	1.4^{4}	C	2.0^{vd}	1.2^{4}	B	1.1^{vd}	1.1^{1}	B
Y- 7	3.0^{vd}	1.6^{13}	C	1.0^{d}	.0	A	2.1^{d}	1.2^{1}	B	1.8	1.1^{2}	A
Y- 8	2.0^{d}	1.0^{1}	B	1.2^{d}	1.1^{5}	A	1.9^{d}	.0	A	2.0^{d}	1.0^{1}	D
Y- 9	2.1^{d}	1.4^{4}	A	1.2^{d}	1.1^{1}	C	5.0^{8}	2.9^{3}	A	2.0^{vd}	.0	B
Y-10	3.0^{8}	1.6^{14}	C	3.0^{d}	1.3^{8}	B	1.5^{d}	1.3^{1}	C	3.1^{d}	1.7^{2}	A
Y-11	2.5^{d}	1.7^{4}	A	3.0^{vd}	1.0^{1}	A	2.5^{d}	.0	B	$.7^{d}$	.0	A

TABLE 4

Prior Austenitic Grain Size

SPECIMEN NUMBER	AS RECEIVED MATERIAL MID-THICKNESS	AUSTENITIZING TREATMENT * 1640 F-1/2 HR-W.Q.	2000 F-1 HR-W.Q.
X- 1	6	8.5	
X- 2	6	8	
X- 3	5	7	
X- 4	6	9.5	
X- 5	4	8.5	
X- 6	7	8.	
X- 8	5	8.5	
X- 9	6	8.5	
X-10	4	9.5	
X-11	6	8.5	
X-12	8	8.5	3
X-13	6	8	3
X-18	5	9.5	5
X-15	7	8.5	5
X-16	5	9.5	6
X-17	6	8.5	6
Y- 1	7	8.5	
Y- 2	7	9.5	
Y- 3	7	8.5	
Y- 4	5	9.5	
Y- 5	6	8.5	
Y- 6	5	9.5	
Y- 7	5	8.5	
Y- 8	7	8.5	
Y- 9	5	8.5	
Y-10	7	8.5	
Y-11	4	7	

* AFTER AUSTENITIZING AND QUENCHING, -120 F 1 HR, TEMPERED AT 1150 F 1 HR THEN WATER QUENCHED.

TABLE 5

Percent Microconstituents Produced by Various Isothermal Treatments

AUSTENITIZING TEMPERATURE / TIME	1640 F 1/2 HR	1640 F 1/2 HR	1640 F 1/2 HR		1640 F 1/2 HR		2000 F 1 HR
ISOTHERMAL TEMPERATURE / TIME	875 F 152 SEC	875 F 1600 SEC	1200 F 3350 SEC		1200 F 8500 SEC		875 F 1600 SEC
MICRO-CONSTITUENTS	BAINITE	BAINITE	FERRITE	PEARLITE	FERRITE	PEARLITE	BAINITE
COUPON NUMBER							
X- 1	29	54	31	0	67	11	
X- 2	14	54	TRACE	0	2	0	
X- 3	21		31	0			
X- 4	2		11	0			
X- 5	1		0	0			
X- 6	0		1	0			
X- 8	14		5	0			
X- 9	7		26	0			
X-10	1		TRACE	0			
X-11	0		0	0			
X-12	1	50	TRACE	0	1	0	63
X-13	14	60	TRACE	0	TRACE	0	67
X-14	TRACE	21	0	0	0	0	56
X-15	1	27	0	0	0	0	58
X-16	0	16	TRACE	0	TRACE	0	58
X-17	0	32	0	0	TRACE	0	30
Y- 1	53		50	32			
Y- 2	9	41	22	0	53	4	
Y- 3	76		69	23			
Y- 4	1	39	7	0	21	0	
Y- 5	3		17	0			
Y- 6	1		12	0			
Y- 7	1		3	0			
Y- 8	1		1	0			
Y- 9	6		2	0			
Y-10	4		1	0			
Y-11	27	63	3	0	44	0	

TABLE 6

Results of Mechanical Property Tests

Table 6a – Specimens Austenitized at 1640 F for 1/2 Hour, Water Quenched and Tempered at 1150 F for 1 Hour

TRANSVERSE

SPEC. NO.	PCT. BAINITE	PCT. FERRITE	PCT. PEARLITE	MARTEN-SITE	ISO-THERMAL HOLDING TEMP. (F)	ISO-THERMAL HOLDING TIME (SEC)	ULT. TEN. STH. (PSI)	TEN. YIELD STH. (PSI)	PCT. EL. IN 2 IN.	PCT. RED. IN AREA	COMP. YIELD STH. (PSI)	NDT TEMP (F)	CHARPY V-NOTCH IMPACT PROPERTIES NDT ENERGY (FT-LBS)	NDT PCT. FIBER	-120F ENERGY (FT-LBS)	-120F PCT. FIBER	+210F ENERGY (FT-LBS)	+210F PCT. FIBER
X- 1	0.	0.	0.	100.0	0	0	125907	113820	22.0	73.9	123334	-190	31.0	24.5	49.5	100.0	66.0	100.0
X- 2	0.	0.	0.	100.0	0	0	122392	107343	24.0	73.5	118860	-170	48.0	37.0	62.0	72.0	90.0	100.0
X- 3	0.	0.	0.	100.0	0	0	124850	114128	22.0	72.7	121686	-120	39.0	43.5	39.0	43.5	61.0	100.0
X- 4	0.	0.	0.	100.0	0	0	128526	113023	23.0	72.6	123578	-190	28.0	57.8	46.0	92.8	56.0	100.0
X- 5	0.	0.	0.	100.0	0	0	128115	113043	22.0	72.5	119830	-190	30.0	57.8	69.2	92.8	69.0	100.0
X- 6	0.	0.	0.	100.0	0	0	121792	107759	23.0	74.5	114383	-170	38.0	57.8	64.0	92.8	73.0	100.0
X- 8	0.	0.	0.	100.0	0	0	121756	109280	23.0	74.7	118068	-190	37.0	34.0	62.5	93.5	77.0	100.0
X- 9	0.	0.	0.	100.0	0	0	117448	104138	23.0	76.5	111430	-190	35.5	35.0	60.0	77.0	79.0	100.0
X-10	0.	0.	0.	100.0	0	0	125926	111561	23.0	74.2	119220	-190	44.0	59.0	68.5	100.0	74.0	100.0
X-11	0.	0.	0.	100.0	0	0	128527	118118	22.0	69.6	126668	-190	30.5	35.0	45.5	82.5	61.5	100.0
X-12	0.	0.	0.	100.0	0	0	127346	114571	22.5	74.7	124813	-180	42.5	41.5	58.0	85.5	66.5	100.0
X-13	0.	0.	0.	100.0	0	0	126275	112988	23.0	72.7	123228	-180	48.0	38.5	83.0	99.0	93.0	100.0
X-18	0.	0.	0.	100.0	0	0	130601	116000	23.0	72.8	126265	-190	44.0	71.0	60.5	100.0	62.5	100.0
X-15	0.	0.	0.	100.0	0	0	128074	112289	23.0	73.4	124506	-190	44.0	47.0	70.0	94.0	74.5	100.0
X-16	0.	0.	0.	100.0	0	0	130870	116883	23.0	74.5	132264	-210	40.0	36.5	56.0	100.0	62.0	100.0
X-17	0.	0.	0.	100.0	0	0	129743	116617	22.0	71.9	124533	-180	47.0	71.0	63.0	100.0	69.0	100.0
Y- 1	0.	0.	0.	100.0	0	0	125874	113686	21.0	70.2	122785	-210	34.0	39.0	50.5	86.5	68.5	100.0
Y- 2	0.	0.	0.	100.0	0	0	135325	122294	22.0	70.3	138652	-190	28.5	33.0	44.0	90.0	58.0	100.0
Y- 3	0.	0.	0.	100.0	0	0	123600	114600	22.0	72.0	125312	-230	32.5	70.5	53.5	97.0	61.0	100.0
Y- 4	0.	0.	0.	100.0	0	0	138777	124698	22.0	68.7	134012	-210	27.5	26.0	42.0	86.5	48.0	100.0
Y- 5	0.	0.	0.	100.0	0	0	131421	115871	22.0	69.1	129079	-230	27.0	57.8	46.0	92.8	52.0	100.0
Y- 6	0.	0.	0.	100.0	0	0	130814	115277	23.0	71.7	123819	-190	31.0	57.8	51.0	92.8	56.0	100.0
Y- 7	0.	0.	0.	100.0	0	0	133000	117150	21.0	66.5	126756	-220	27.0	31.0	41.0	99.0	42.5	100.0
Y- 8	0.	0.	0.	100.0	0	0	127600	112100	22.0	71.8	120685	-210	26.5	51.5	34.5	99.5	38.5	100.0
Y- 9	0.	0.	0.	100.0	0	0	126527	111611	22.0	74.2	120598	-190	35.5	35.5	55.0	100.0	62.5	100.0
Y-10	0.	0.	0.	100.0	0	0	128001	112000	23.0	71.1	121602	-230	26.5	12.0	54.0	100.0	58.5	100.0
Y-11	0.	0.	0.	100.0	0	0	122955	109532	22.5	71.3	117168	-150	35.0	54.0	40.5	72.5	64.0	100.0

LONGITUDINAL

SPEC. NO.	PCT. BAINITE	PCT. FERRITE	PCT. PEARLITE	MARTEN-SITE	ISO-THERMAL HOLDING TEMP. (F)	ISO-THERMAL HOLDING TIME (SEC)	ULT. TEN. STH. (PSI)	TEN. YIELD STH. (PSI)	PCT. EL. IN 2 IN.	PCT. RED. IN AREA	COMP. YIELD STH. (PSI)	NDT TEMP (F)	CHARPY V-NOTCH IMPACT PROPERTIES NDT ENERGY (FT-LBS)	NDT PCT. FIBER	-120F ENERGY (FT-LBS)	-120F PCT. FIBER	+210F ENERGY (FT-LBS)	+210F PCT. FIBER
X- 3	0.	0.	0.	100.0	0	0	124850	114128	22.0	72.7	121686	-120	102.0	100.0	102.0	100.0	103.5	100.0
X-12	0.	0.	0.	100.0	0	0	127346	114571	22.5	74.7	124813	-180	94.0	92.5	101.0	99.5	114.0	100.0
X-13	0.	0.	0.	100.0	0	0	126275	112988	23.0	72.7	123228	-180	83.0	91.5	100.0	100.0	103.0	100.0
X-18	0.	0.	0.	100.0	0	0	130601	116000	23.0	72.8	126265	-190	84.5	100.0	93.0	100.0	103.0	100.0
X-15	0.	0.	0.	100.0	0	0	128074	112289	23.0	73.4	124506	-190	64.0	75.5	87.0	100.0	100.0	100.0
X-16	0.	0.	0.	100.0	0	0	130870	116883	23.0	74.5	132264	-210	70.5	72.0	97.5	100.0	102.5	100.0
X-17	0.	0.	0.	100.0	0	0	129743	116617	22.0	71.9	124533	-180	56.0	56.0	75.0	98.0	87.0	100.0
Y- 1	0.	0.	0.	100.0	0	0	125874	113686	21.0	70.2	122785	-210	77.0	100.0	82.0	100.0	92.5	100.0
Y- 3	0.	0.	0.	100.0	0	0	123600	114600	22.0	72.0	125312	-230	67.5	49.5	104.5	100.0	107.0	100.0
Y- 7	0.	0.	0.	100.0	0	0	133000	117150	21.0	66.5	126756	-220	37.0	48.5	60.0	99.0	68.5	100.0

Table 6b – Specimens Austenitized at 1640 F for 1/2 Hour, Isothermally Treated at 875 F for 152 Seconds, Water Quenched and Tempered at 1150 F for 1 Hour

TRANSVERSE

SPEC. NO.	PCT. BAINITE	PCT. FERRITE	PCT. PEARLITE	MARTEN-SITE	ISO-THERMAL HOLDING TEMP. (F)	ISO-THERMAL HOLDING TIME (SEC)	ULT. TEN. STH. (PSI)	TEN. YIELD STH. (PSI)	PCT. EL. IN 2 IN.	PCT. RED. IN AREA	COMP. YIELD STH. (PSI)	NDT TEMP (F)	CHARPY V-NOTCH IMPACT PROPERTIES NDT ENERGY (FT-LBS)	NDT PCT. FIBER	-120F ENERGY (FT-LBS)	-120F PCT. FIBER	+210F ENERGY (FT-LBS)	+210F PCT. FIBER
X- 1	29.0	0.	0.	71.0	875	152	120984	105422	24.0	75.3	111571	-210	30.0	16.5	42.0	69.0	66.0	100.0
X- 2	14.2	0.	0.	85.8	875	152	119382	103331	24.0	74.3	121926	-150	54.0	50.5	63.5	68.0	90.0	100.0
X- 3	21.2	0.	0.	78.8	875	152	118500	105099	22.0	73.1	111957	-110	38.0	23.5	36.0	19.0	68.0	100.0
X- 4	1.5	0.	0.	98.5	875	152	127008	109036	23.0	72.9	118620	-191	26.0	36.3	46.0	80.6	52.0	100.0
X- 5	0.6	0.	0.	99.4	875	152	127204	109175	23.0	72.9	119614	-191	30.0	36.3	55.0	80.6	68.0	100.0
X- 6	0.3	0.	0.	99.7	875	152	121291	105253	24.0	75.8	115366	-191	50.0	36.3	51.0	80.6	81.0	100.0
X- 8	13.5	0.	0.	86.5	875	152	116[illegible]	101897	23.0	73.9	110132	-190	37.5	34.5	64.0	81.0	81.0	100.0
X- 9	6.8	0.	0.	93.2	875	152	1[illegible]	104594	23.0	76.1	113073	-180	41.0	37.5	60.0	76.0	81.5	100.0
X-10	1.1	0.	0.	98.9	875	152	1[illegible]	126784	23.0	76.0	118691	-210	41.0	45.0	66.0	94.5	74.0	100.0
X-11	0.	0.	0.	100.0	875	152	120[illegible]	103550	23.0	72.0	124016	-190	36.0	41.0	47.1	75.0	65.0	100.0
X-12	1.1	0.	0.	98.9	875	152	120[illegible]	105399	23.0	75.1	115540	-170	49.0	43.5	67.0	86.0	78.5	100.0
X-13	14.1	0.	0.	85.9	875	152	1183[illegible]	102789	23.0	73.7	109078	-170	52.0	50.0	70.5	81.5	95.5	100.0
X-18	0.7	0.	0.	99.3	875	152	124799	107999	23.0	74.7	120065	-220	32.5	26.0	54.0	86.5	69.0	100.0
X-15	0.7	0.	0.	99.3	875	152	123352	106389	23.0	73.1	115127	-210	33.0	34.0	66.0	89.0	79.0	100.0
X-16	0.	0.	0.	100.0	875	152	123755	109473	23.0	74.3	119487	-210	35.0	32.0	59.0	91.0	64.0	100.0
X-17	0.	0.	0.	100.0	875	152	123307	108168	23.0	72.9	120074	-190	39.0	43.0	55.0	88.0	65.5	100.0
Y- 1	53.0	0.	0.	47.0	875	152	114885	98902	23.0	70.9	106646	-170	33.0	57.0	44.5	96.5	65.0	100.0
Y- 2	9.0	0.	0.	91.0	875	152	130814	116780	23.0	72.1	125320	-240	25.5	18.5	52.5	87.0	60.0	100.0
Y- 3	76.0	0.	0.	24.0	875	152	107480	92724	24.0	73.1	103014	-170	36.0	34.5	52.5	68.0	67.0	100.0
Y- 4	0.7	0.	0.	99.3	875	152	134932	119382	22.0	69.9	132787	-210	28.0	41.0	45.0	100.0	54.0	100.0
Y- 5	2.2	0.	0.	97.8	875	152	131526	116466	22.0	71.3	129051	-210	32.0	36.3	48.0	80.6	72.0	100.0
Y- 6	0.9	0.	0.	99.1	875	152	126906	109350	23.0	73.3	124078	-210	28.0	36.3	52.0	80.6	56.0	100.0
Y- 7	1.4	0.	0.	98.6	875	152	132600	116201	21.0	67.9	123508	-220	23.5	29.0	39.5	98.5	43.0	100.0
Y- 8	1.1	0.	0.	98.9	875	152	128614	113709	22.5	71.1	124195	-220	22.0	38.0	36.0	97.5	38.5	100.0
Y- 9	6.3	0.	0.	93.7	875	152	125896	109761	22.5	74.3	121646	-210	31.0	33.0	48.0	84.5	61.5	100.0
Y-10	4.0	0.	0.	96.0	875	152	129155	114828	22.0	71.6	123200	-210	33.0	42.5	46.0	95.0	56.0	100.0
Y-11	27.0	0.	0.	73.0	875	152	119841	106182	22.0	71.9	112789	-150	30.5	22.5	33.0	41.0	56.5	100.0

LONGITUDINAL

SPEC. NO.	PCT. BAINITE	PCT. FERRITE	PCT. PEARLITE	MARTEN-SITE	ISO-THERMAL HOLDING TEMP. (F)	ISO-THERMAL HOLDING TIME (SEC)	ULT. TEN. STH. (PSI)	TEN. YIELD STH. (PSI)	PCT. EL. IN 2 IN.	PCT. RED. IN AREA	COMP. YIELD STH. (PSI)	NDT TEMP (F)	CHARPY V-NOTCH IMPACT PROPERTIES NDT ENERGY (FT-LBS)	NDT PCT. FIBER	-120F ENERGY (FT-LBS)	-120F PCT. FIBER	+210F ENERGY (FT-LBS)	+210F PCT. FIBER
X- 1	54.0	0.	0.	46.0	875	1600	112337	92530	24.0	73.4	104176	-130	96.0	79.0	101.0	84.0	115.0	100.0
X- 2	53.7	0.	0.	46.3	875	1600	109457	93914	25.0	74.2	104142	-170	78.0	64.0	106.5	94.5	118.5	100.0
Y- 2	40.8	0.	0.	59.2	575	1600	123818	107536	23.0	71.3	116268	-180	60.5	55.0	73.0	90.0	89.5	100.0
Y- 4	38.6	0.	0.	61.4	875	1600	124374	109128	23.0	70.5	118196	-190	29.5	54.0	79.0	100.0	91.0	100.0

b. Bainites will exhibit ragged grain boundaries, with this becoming more pronounced at the lower transformation temperatures. In general, it may also be said that the bainites will not exhibit the large flat blocky areas of the ferrite but will be smaller and peppered with darker areas of martensite or precipitated carbides; this becomes more pronounced as the transformation temperature is lowered.

3. A smeared structure or an oxidized surface will make proper evaluation of the results of this technique impossible.

APPENDIX C

PHOTOMICROGRAPHS

OF

MICROSTRUCTURES

Figure C1a – 29 Percent Bainite – 71 Percent Martensite
875 F – 152 Sec

Figure C1b – 31 Percent Ferrite – 69 Percent Martensite
1200 F – 3350 Sec

Figure C1c – 54 Percent Bainite – 46 Percent Martensite
875 F – 1600 Sec

Figure C1d – 67 Percent Ferrite – 11 Percent Pearlite
22 Percent Martensite
1200 F – 8500 Sec

Cropped End Number X-1

Figure C1 – Microstructure (1000X) of Specimens from Cropped End Number X-1 Austenitized at 1640 F, Isothermally Treated at 875 F and 1200 F, and Then Tempered at 1150 F

Figure C2a – 14 Percent Bainite – 86 Percent Martensite
875 F – 152 Sec

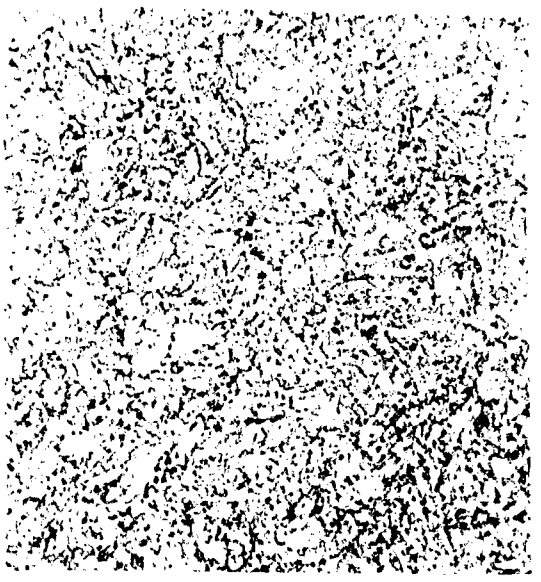

Figure C2b – Trace Ferrite – 100 Percent Martensite
1200 F – 3350 Sec

Figure C2c – 54 Percent Bainite – 46 Percent Martensite
875 F – 1600 Sec

Figure C2d – 2 Percent – 98 Percent Martensite
1200 F – 8500 Sec

Cropped End Number X-2

Figure C2 – Microstructure (1000X) of Specimens from Cropped End Number X-2 Austenitized at [illegible] Isothermally Treated at 875 F and 1200 F, and Then Tempered at 1150 F

Figure C3a – 21 Percent Bainite – 79 Percent Martensite
875 F – 152 Sec

Figure C3b – 31 Percent Ferrite – 60 Percent Martensite
1200 F – 3350 Sec

Cropped End Number X-3

Figure C3c – 2 Percent Bainite – 98 Percent Martensite
875 F – 152 Sec

Figure C3d – 11 Percent Ferrite – 89 Percent Martensite
1200 F – 3350 Sec

Cropped End Number X-4

Figure C3 – Microstructure (1000X) of Specimens from Cropped Ends X-3 and X-4 Austenitized at 1640 F, Isothermally Treated at 875 F and 1200 F, and Then Tempered at 1150 F

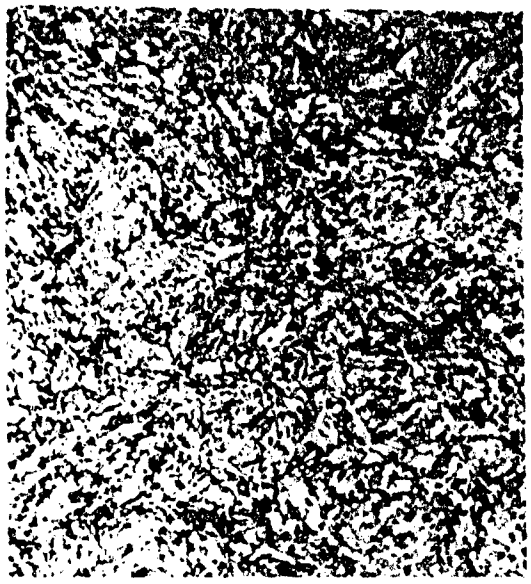

Figure C4a – 1 Percent Bainite – 99 Percent Martensite
875 F – 152 Sec

Figure C4b – 100 Percent Martensite
1220 F – 3350 Sec

Cropped End Number X-5

Figure C4c – Trace Bainite – 100 Percent Martensite
875 F – 152 Sec

Figure C4d – 1 Percent Ferrite – 99 Percent Martensite
1220 F – 3350 Sec

Cropped End Number X-6

Figure C4 – Microstructure (1000X) of Specimens from Cropped Ends X-5 and X-6 Austenitized at 1640 F, Isothermally Treated at 875 F and 1200 F, and Then Tempered at 1150 F

Figure C5a – 14 Percent Bainite – 86 Percent Martensite
875 F – 152 Sec

Figure C5b – 5 Percent Ferrite – 95 Percent Martensite
1200 F – 3350 Sec

Cropped End Number X-8

Figure C5c – 7 Percent Bainite – 93 Percent Martensite
875 F – 152 Sec

Figure C5d – 26 Percent Ferrite – 74 Percent Martensite
1200 F – 3350 Sec

Cropped End Number X-9

Figure C5 – Microstructure (1000X) of Specimens from Cropped Ends X-8 and X-9 Austenitized at 1640 F, Isothermally Treated at 875 F and 1200 F, and Then Tempered at 1150 F

Figure C6a – 1 Percent Bainite – 99 Percent Martensite
875 F – 152 Sec

Figure C6b – Trace Ferrite – 100 Percent Martensite
1200 F – 3350 Sec

Cropped End Number X-10

Figure C6c – 100 Percent Martensite
875 F – 152 Sec

Figure C6d – 100 Percent Martensite
1200 F – 3350 F

Cropped End Number X-11

Figure C6 – Microstructure (1000X) of Specimens from Cropped Ends X-10 and X-11 Austenitized at 1640 F, Isothermally Treated at 875 F and 1200 F, and Then Tempered at 1150 F

Figure C7a -- 1 Percent Bainite -- 99 Percent Martensite
875 F -- 152 Sec

Figure C7b -- Trace Ferrite -- 100 Percent Martensite
1200 F -- 3550 Sec

Figure C7c -- 50 Percent Bainite -- 50 Percent Martensite
875 F -- 1690 Sec

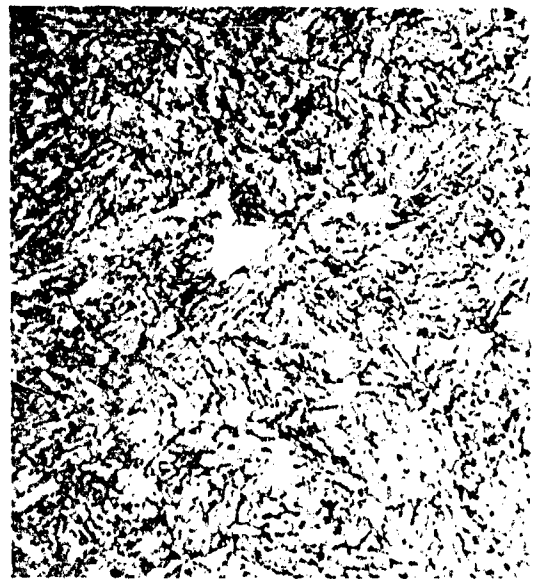

Figure C7d -- 1 Percent Ferrite -- 99 Percent Martensite
1200 F -- 8500 Sec

Cropped End Number X-12

Figure C7 -- Microstructure (1000X) of Specimens from Cropped End Number X-12 Austenitized at 1640 F, Isothermally Treated at 875 F and 1200 F, and Then Tempered at 1150 F

Figure C8a – 50 Percent Bainite – 50 Percent Martensite
875 F – 1600 Sec

Figure C8b – 63 Percent Bainite – 37 Percent Martensite
875 F – 1600 Sec

Cropped End Number X-12

Figure C8c – 60 Percent Bainite – 40 Percent Martensite
875 F – 1600 Sec

Figure C8d – 67 Percent Bainite – 33 Percent Martensite
875 F – 1600 Sec

Cropped End Number X-13

Figure C8 – Effects of Prior Austenitic Grain Size on the Microstructure (1000X) of Cropped Ends X-12 and X-13

Figure C9a — 14 Percent Bainite – 86 Percent Martensite
875 F – 152 Sec

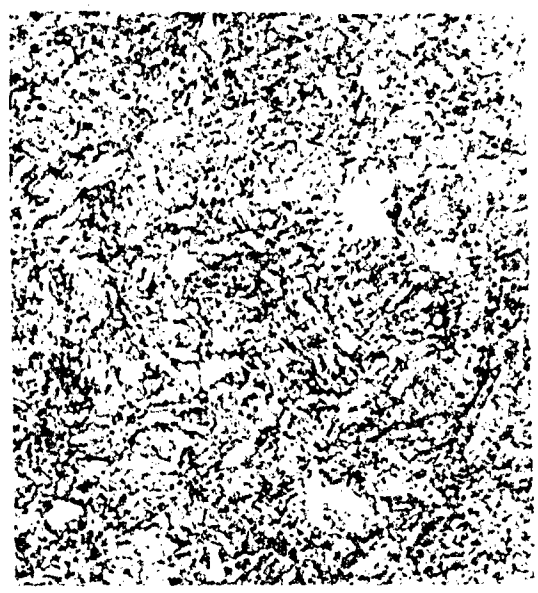

Figure C9b – Trace Ferrite – 100 Percent Martensite
1200 F – 3350 Sec

Figure C9c — 60 Percent Bainite – 40 Percent Martensite
875 F – 1600 Sec

Figure C9d — Trace Ferrite – 100 Percent Martensite
1200 F – 8500 Sec

Cropped End Number X-13

Figure C9 — Microstructure (1000X) of Specimens from Cropped End Number X-13 Austenitized at 1630 F, Isothermally Treated at 875 F and 1200 F, and Then Tempered at 1150 F

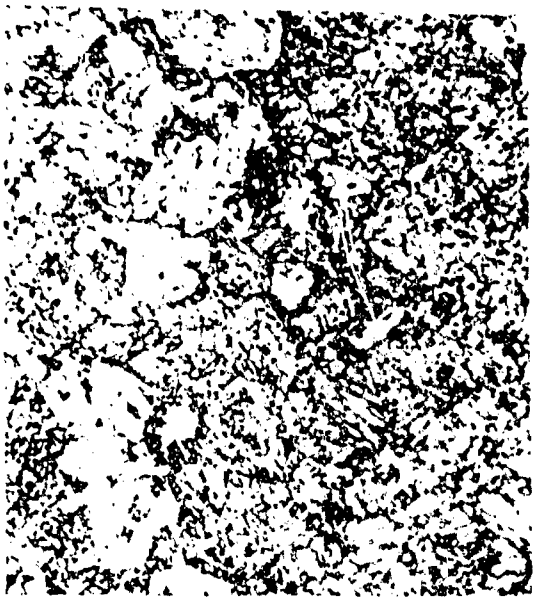

Figure C10a – 21 Percent Bainite – 79 Percent Martensite
875 F – 1600 Sec

Figure C10b – 56 Percent Bainite – 44 Percent Martensite
875 F – 1600 Sec

Cropped End Number X-18

Figure C10c – 27 Percent Bainite – 73 Percent Martensite
875 F – 1600 Sec

Figure C10d – 58 Percent Bainite – 42 Percent Martensite
875 F – 1600 Sec

Cropped End Number X-15

Figure C10 – Effects of Prior Austenitic Grain Size on the Microstructure (1000X) of Cropped Ends X-15 and X-18

Figure C11a – 1 Percent Bainite – 99 Percent Martensite
875 F – 152 Sec

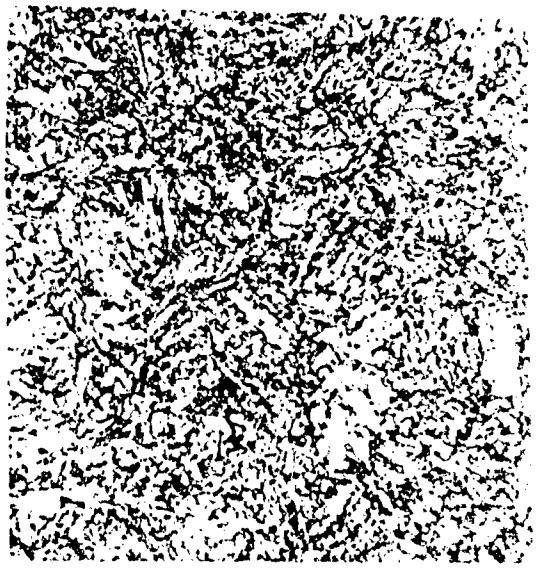

Figure C11b – 100 Percent Martensite
1200 F – 3350 Sec

Figure C11c – 27 Percent Bainite – 73 Percent Martensite
875 F – 1600 Sec

Figure C11d – 100 Percent Martensite
1200 F – 8500 Sec

Cropped End Number X-15

Figure C11 – Microstructure (1000X) of Specimens from Cropped End Number X-15 Austenitized at 1640 F, Isothermally Treated at 875 F and 1200 F, and Then Tempered at 1100 F

Figure C12a – 100 Percent Martensite
875 F – 152 Sec

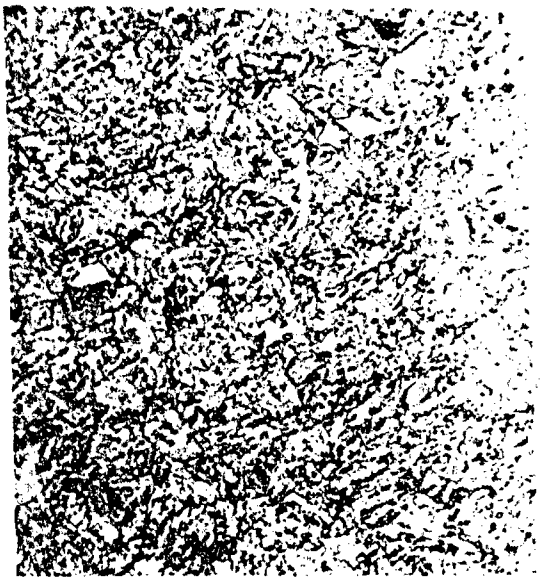

Figure C12b – Trace Ferrite – 160 Percent Martensite
1200 F – 3350 Sec

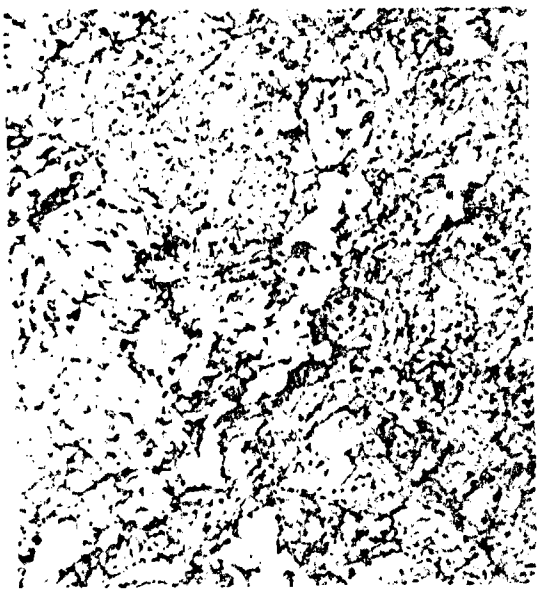

Figure C12c – 16 Percent Bainite – 84 Percent Martensite
875 F – 1600 Sec

Figure C12d – Trace Ferrite – 100 Percent Martensite
1200 F – 8500 Sec

Cropped End Number X-16

Figure C12 – Microstructure (1000X) of Specimens from Cropped End Number X-16 Austenitized at 1640 F, Isothermally Treated at 875 F and 1200 F, and Then Tempered at 1150 F

Figure C13a – 16 Percent Bainite – 84 Percent Martensite
875 F – 1600 Sec

Figure C13b – 58 Percent Bainite – 42 Percent Martensite
875 F – 1600 Sec

Cropped End Number X-16

Figure C13c – 32 Percent Bainite – 68 Percent Martensite
875 F – 1600 Sec

Figure C13d – 30 Percent Bainite – 70 Percent Martensite
875 F – 1600 Sec

Cropped End Number X-17

Figure C13 – Effects of Prior Austenite Grain Size on the Microstructure (1000X) of Cropped Ends X-16 and X-17

Figure C14a – 100 Percent Martensite
875 F – 152 Sec

Figure C14b – 100 Percent Martensite
1200 F – 3350 Sec

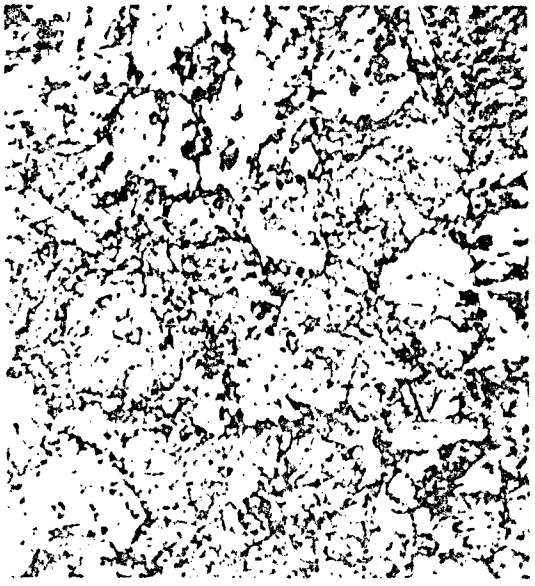

Figure C14c – 32 Percent Bainite – 68 Percent Martensite
875 F – 1600 Sec

Figure C14d – Trace Ferrite – 100 Percent Martensite
1200 F – 8500 Sec

Cropped End Number X-17

Figure C14 – Microstructure (1000X) of Specimens from Cropped End Number X-17 Austenitized at 1640 F, Isothermally Treated at 875 F and 1200 F, and Then Tempered at 1150 F

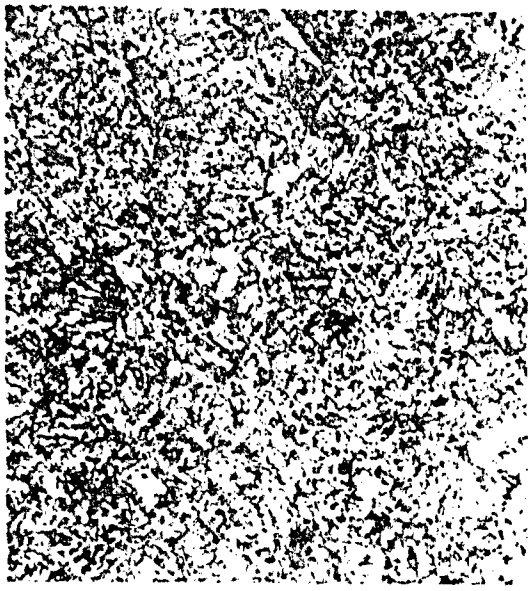

Figure C15a – Trace Bainite – 100 Percent Martensite
875 F – 152 Sec

Figure C15b – 100 Percent Martensite
1200 F – 3350 Sec

Figure C15c – 21 Percent Bainite – 79 Percent Martensite
875 F – 1600 Sec

Figure C15d – 100 Percent Martensite
1200 F – 8500 Sec

Cropped End Number X-18

Figure C15 – Microstructure (1000X) of Specimens from Cropped End Number X-18 Austenitized at 1640 F, Isothermally Treated at 875 F and 1200 F, and Then Tempered at 1150 F

Figure C16a – 53 Percent Bainite – 47 Percent Martensite
875 F – 152 Sec

Figure C16b – 50 Percent Ferrite – 32 Percent Pearlite
18 Percent Martensite
1200 F – 3350 Sec

Cropped End Number Y-1

Figure C16c – 76 Percent Bainite – 24 Percent Martensite
875 F – 152 Sec

Figure C16d – 69 Percent Ferrite – 23 Percent Pearlite
8 Percent Martensite
1200 F – 3350 Sec

Cropped End Number Y-3

Figure C16 – Microstructure (1000X) of Specimens from Cropped Ends Y-1 and Y-3 Austenitized at 1640 F, Isothermally Treated at 875 F and 1200 F, and Then Tempered at 1150 F

Figure C17a – 9 Percent Bainite – 91 Percent Martensite
875 F – 152 Sec

Figure C17b – 22 Percent Ferrite – 78 Percent Martensite
1200 F – 3350 Sec

Figure C17c – 41 Percent Bainite – 59 Percent Martensite
875 F – 1600 Sec

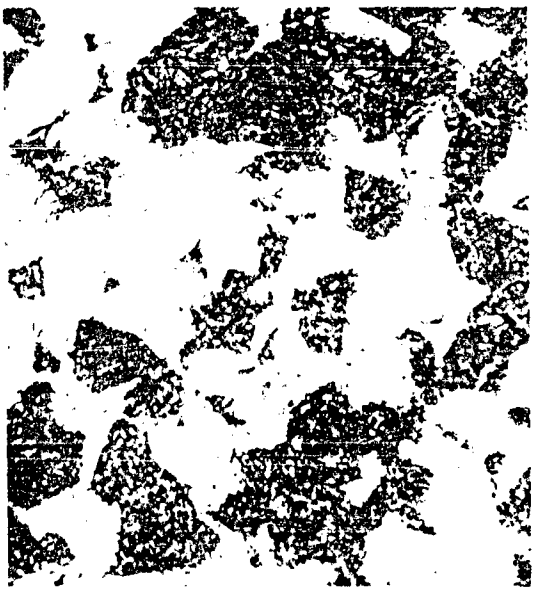

Figure C17d – 53 Percent Ferrite – 4 Percent Pearlite
43 Percent Martensite
1200 F – 8500 Sec

Cropped End Number Y-2

Figure C17 – Microstructure (1000X) of Specimens from Cropped End Number Y-2 Austenitized at 1646 F, Isothermally Treated at 875 F and 1200 F, and Then Tempered at 1150 F

Figure C18a – 1 Percent Bainite – 99 Percent Martensite
875 F – 152 Sec

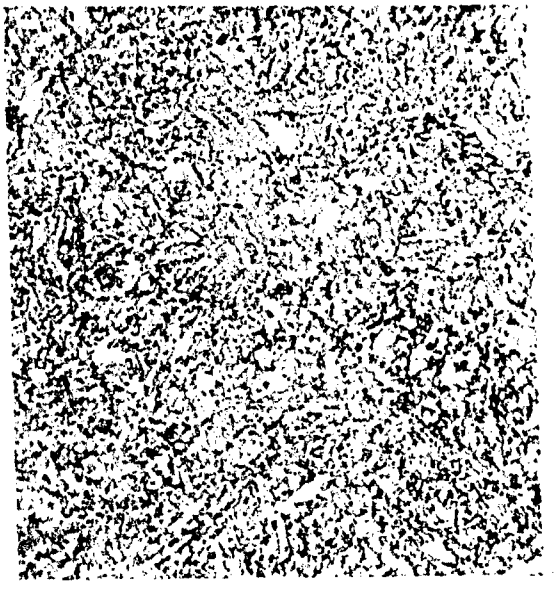

Figure C18b – 7 Percent Ferrite – 93 Percent Martensite
1200 F – 3350 Sec

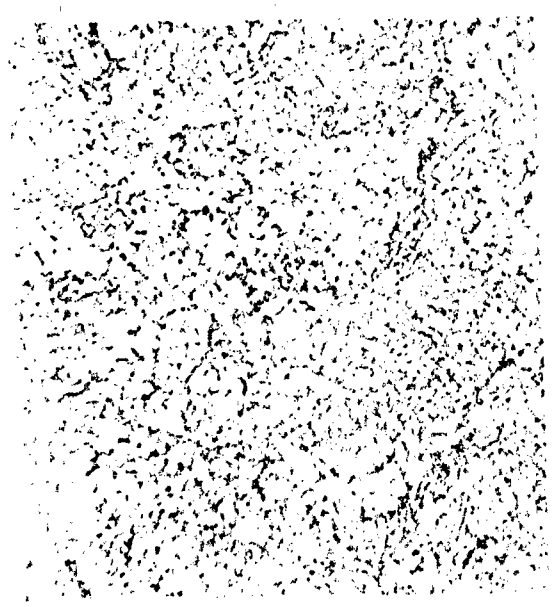

Figure C18c – 39 Percent Bainite – 61 Percent Martensite
875 F – 1600 Sec

Figure C18d – 21 Percent Ferrite – 79 Percent Martensite
1200 F – 8500 Sec

Cropped End Number Y-4

Figure C[illegible] – M[illegible] Case (1000X) of Specimens from Cropped End Number Y-4 Austenitized at 1650 F [illegible] ally Treated at 875 F and 1200 F and Then Tempered at 1150 F

Figure C19a — 3 Percent Bainite — 97 Percent Martensite
875 F — 1½2 Sec

Figure C19b — 17 Percent Ferrite — 83 Percent Martensite
1200 F — 3350 Sec

Cropped End Number Y-5

Figure C19c — 1 Percent Bainite — 99 Percent Martensite
875 F — 1½2 Sec

Figure C19d — 12 Percent Ferrite — 88 Percent Martensite
1200 F — 3350 Sec

Cropped End Number Y-6

Figure C19 — Microstructure (1000X) of Specimens from Cropped Ends Y-5 and Y-6 Austenitized at 1650 F, Isothermally Treated at 875 F and 1200 F, and Then Tempered at 1150 F

Figure C20a – 1 Percent Bainite – 99 Percent Martensite
875 F – 152 Sec

Figure C20b – 3 Percent Ferrite – 97 Percent Martensite
1200 F – 3350 Sec

Cropped End Number Y-7

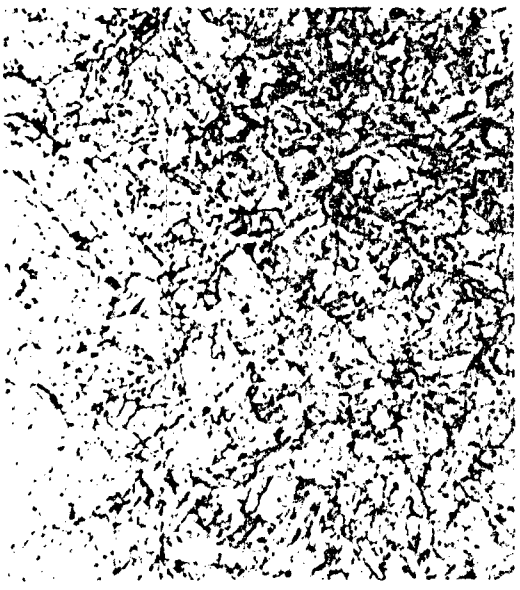

Figure C20c – 1 Percent Bainite – 99 Percent Martensite
875 F – 152 Sec

Figure C20d – 1 Percent Ferrite – 99 Percent Martensite
1200 F – 3350 Sec

Cropped End Number Y-8

Figure C20 – Microstructure (1000X) of Specimens from Cropped Ends Y-7 and Y-8 Austenitized at 1650 F Isothermally Treated at 875 F and 1200 F, and Then Tempered at 1150 F

Figure C21a – 6 Percent Bainite – 94 Percent Martensite
875 F – 152 Sec

Figure C21b – 2 Percent Ferrite – 98 Percent Martensite
1200 F – 3350 Sec

Cropped End Number Y-9

Figure C21c – 4 Percent Bainite – 96 Percent Martensite
875 F – 152 Sec

Figure C21d – 1 Percent Ferrite – 99 Percent Martensite
1200 F – 3350 Sec

Cropped End Number Y-10

Figure C21 – Microstructure (1000X) of Specimens from Cropped Ends Y-9 and Y-10 Austenitized at 1640 F, Isothermally Treated at 875 F and 1200 F, and Then Tempered at 1150 F

Figure C22a -- 27 Percent Bainite -- 73 Percent Martensite
875 F -- 152 Sec

Figure C22b -- 3 Percent Ferrite -- 97 Percent Martensite
1200 F -- 3350 Sec

Figure C22c -- 63 Percent Bainite -- 37 Percent Martensite
875 F -- 1600 Sec

Figure C22d -- 44 Percent Ferrite -- 56 Percent Martensite
1200 F -- 8500 Sec

Cropped End Number Y-11

Figure C22 -- Microstructure (1000X) of Specimens from Cropped End Number Y-11 Austenitized at 1640 F, Isothermally Treated at 875 F and 1200 F, and Then Tempered at 1150 F

APPENDIX D

CHARPY V-NOTCH IMPACT PROPERTY CURVES

Preceding page blank

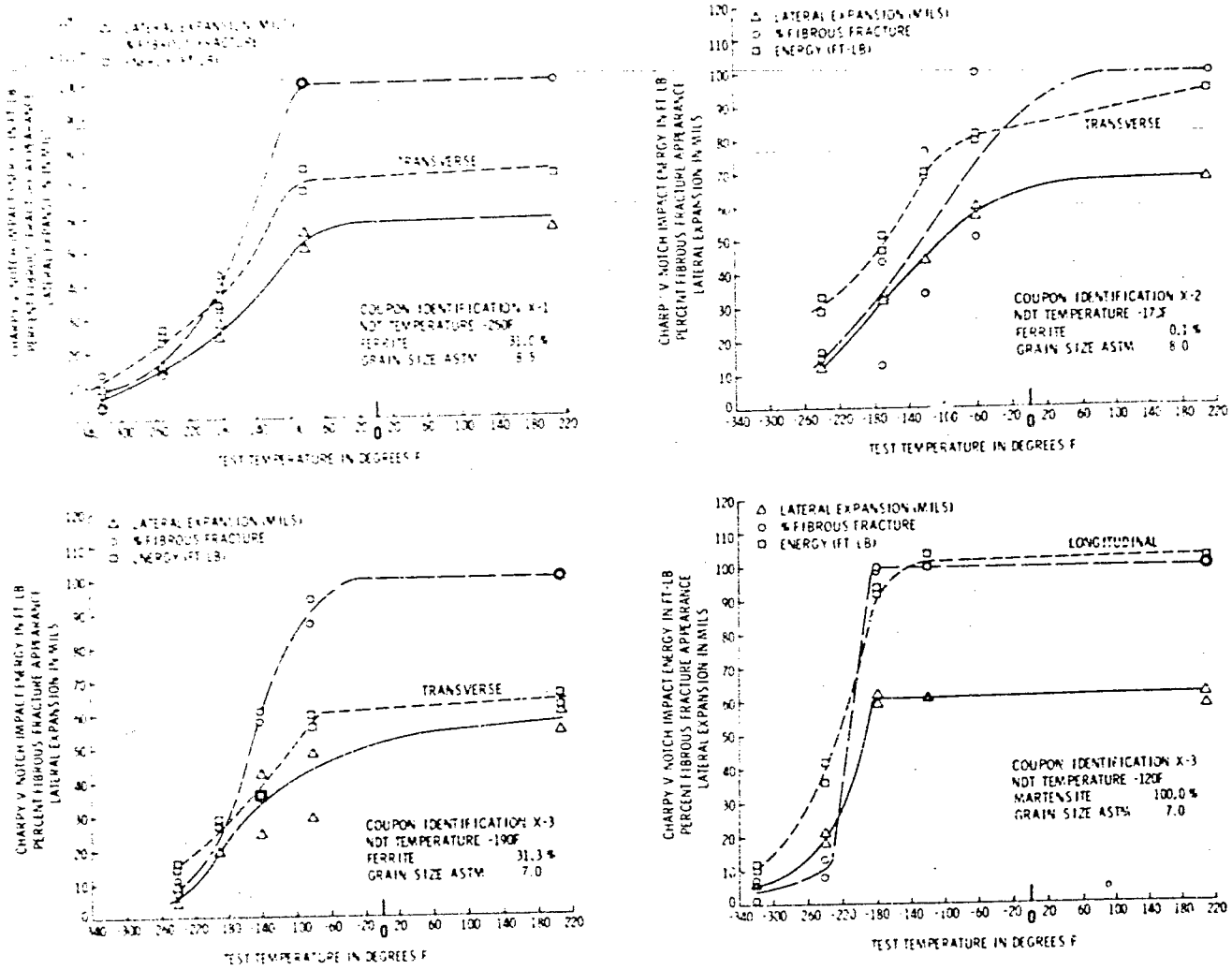

Figure D1 – Transverse and Longitudinal Charpy V-Notch Impact Data for Specimens Austenitized at 1640 F for 1/2 Hour, *Water Quenched* and Tempered at 1150 F for 1 Hour

Figure D1 (Continued)

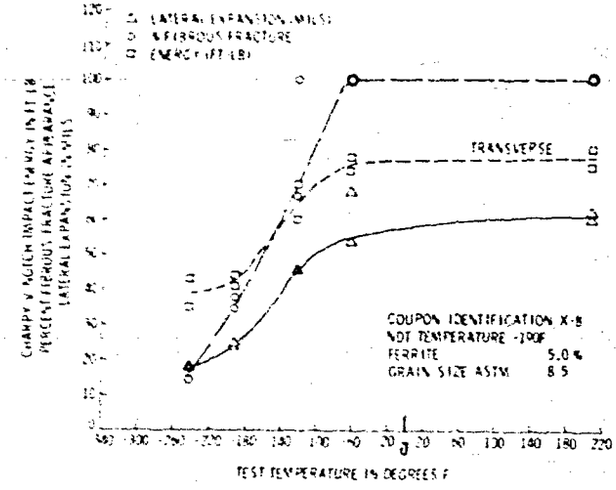

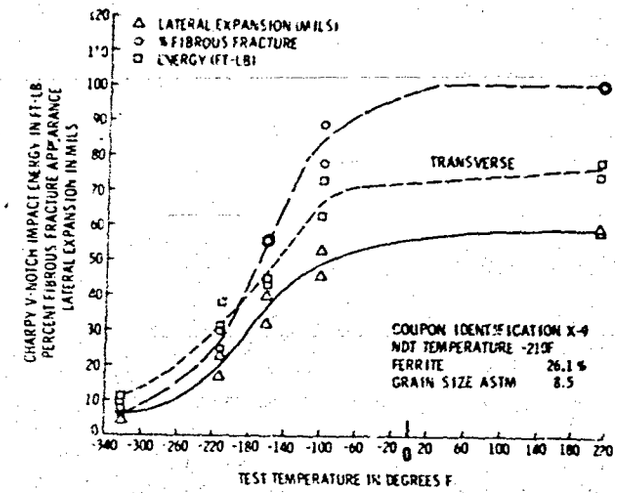

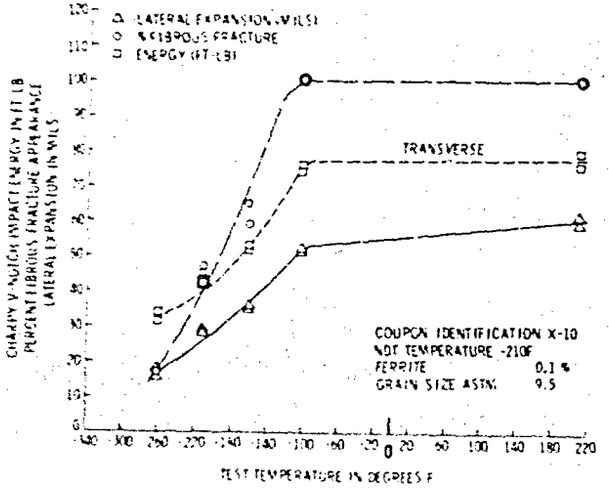

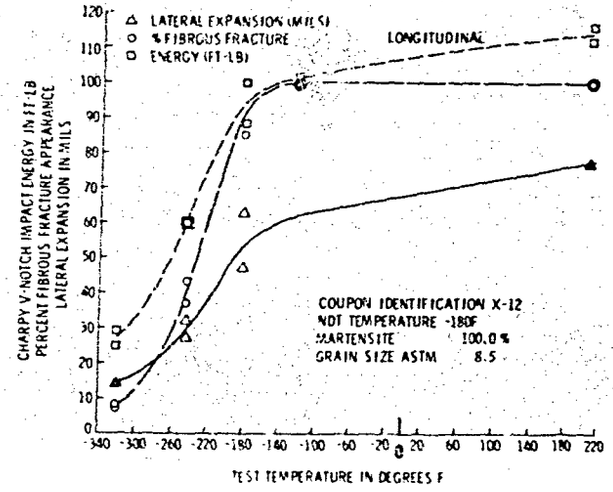

Figure D1 (Continued)

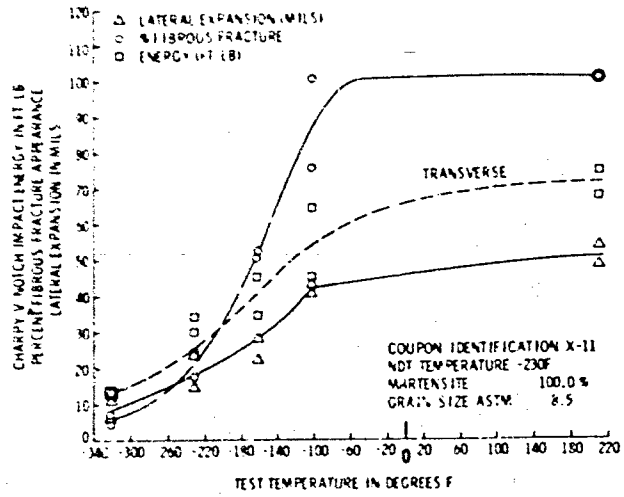

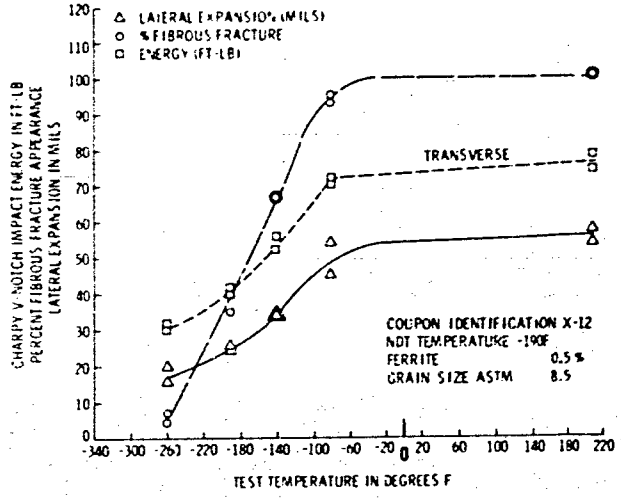

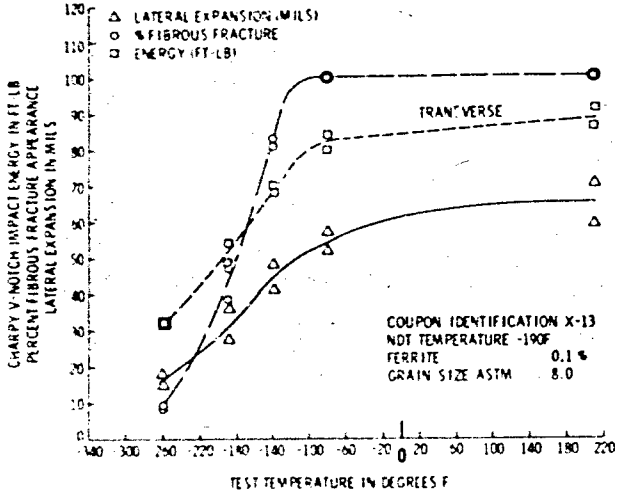

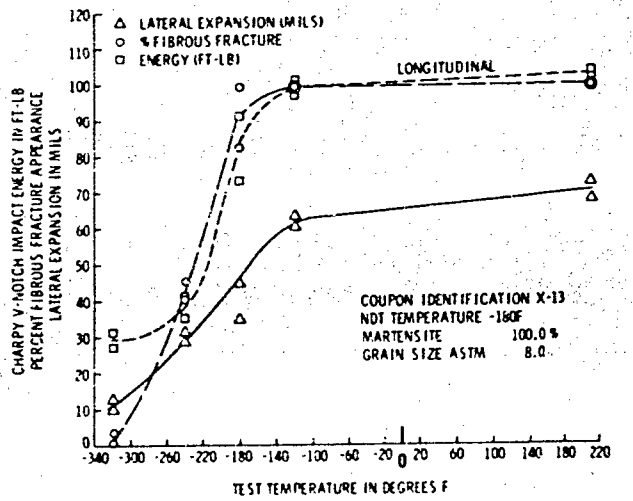

Figure D1 (Continued)

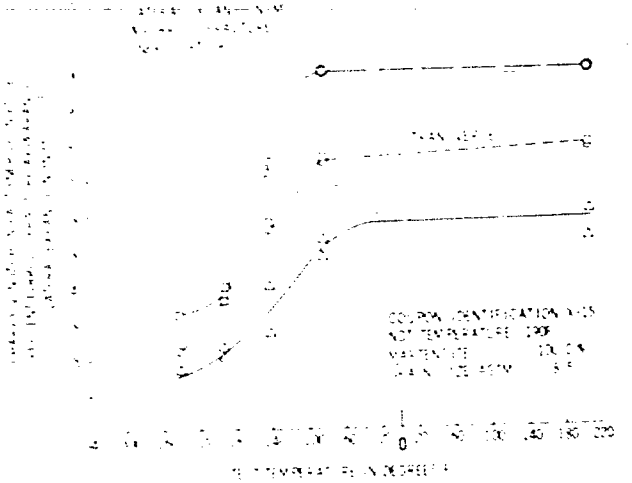

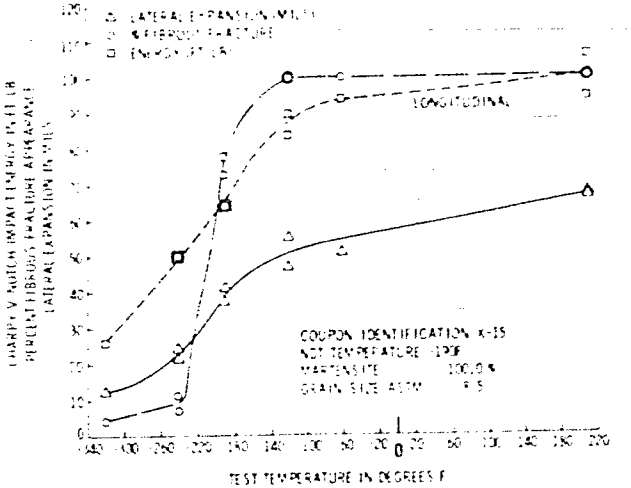

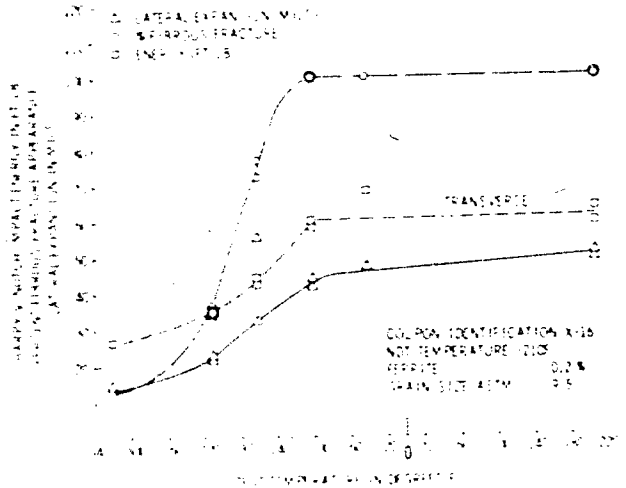

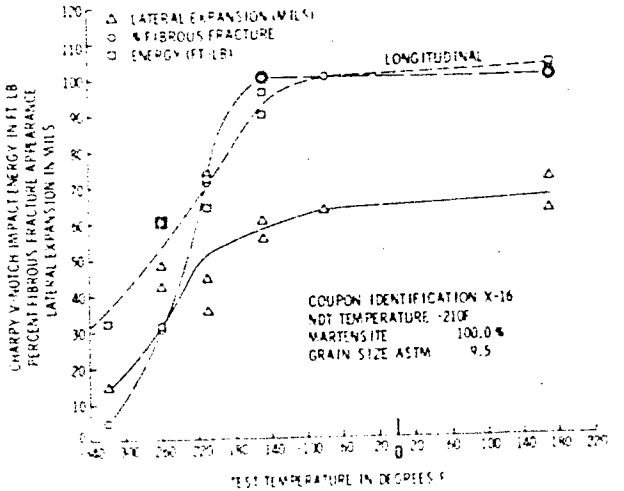

Figure D1 (Continued)

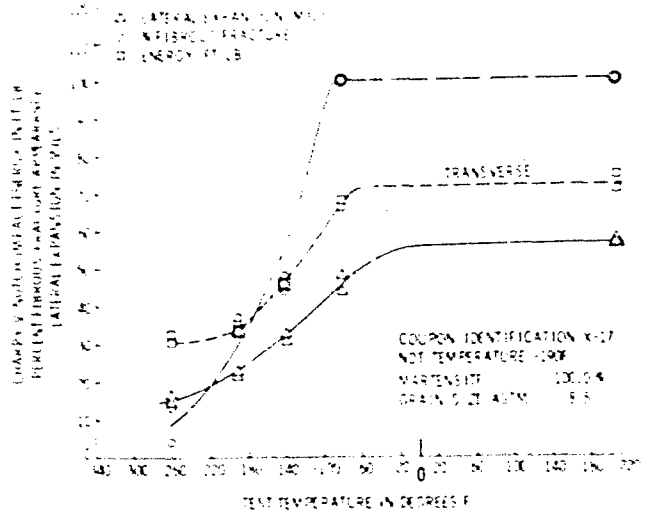

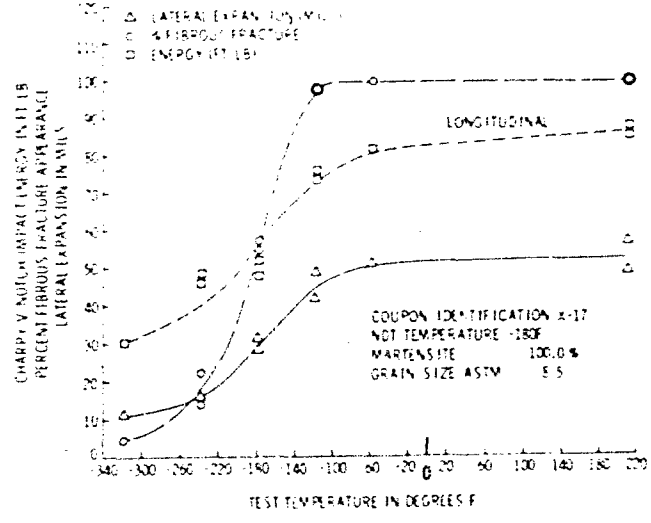

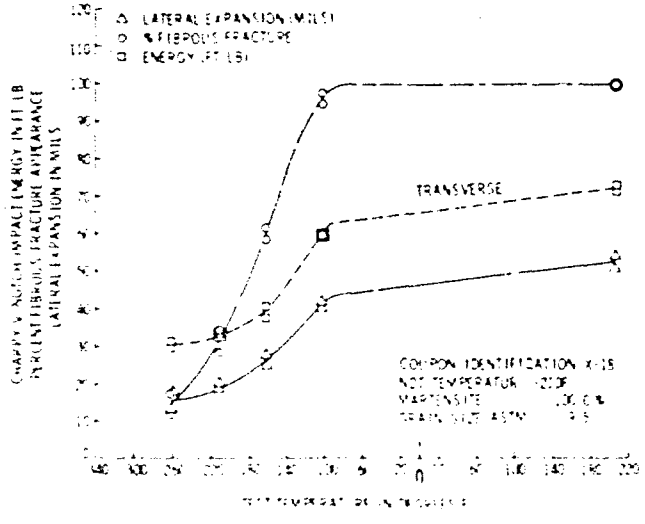

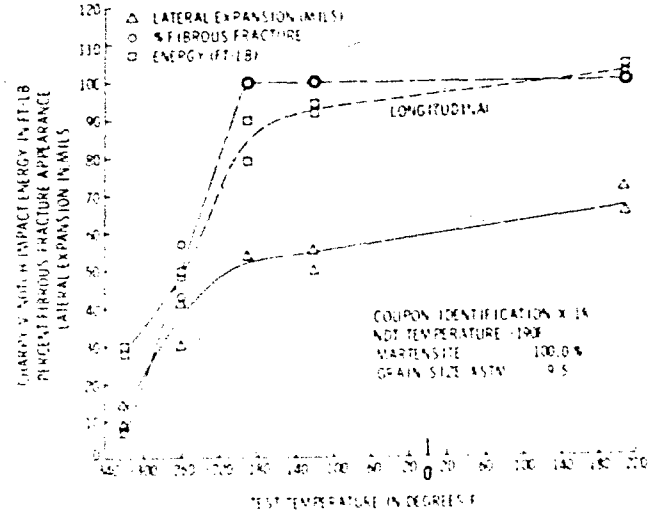

Figure D1 (Continued)

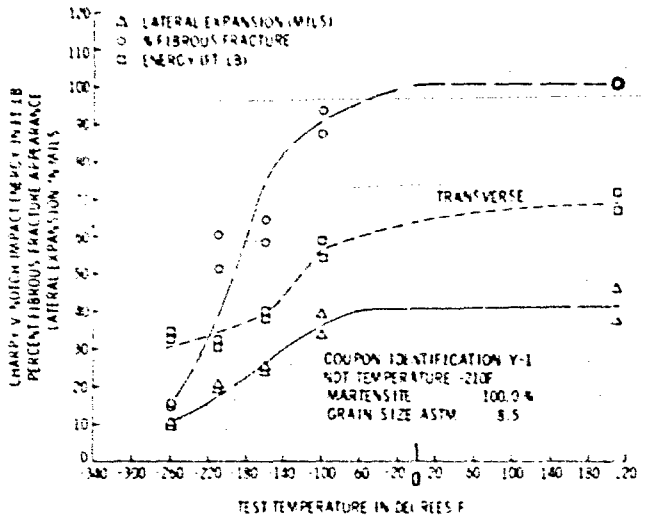

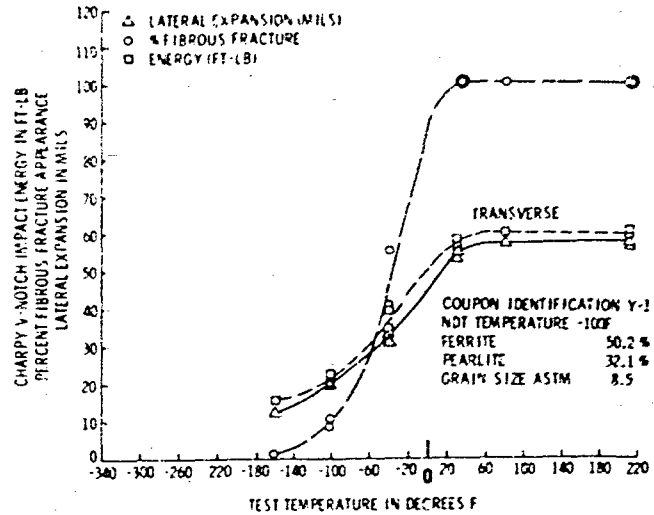

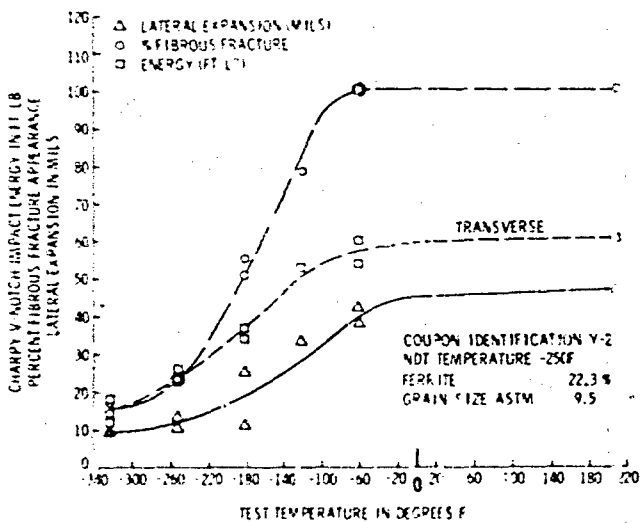

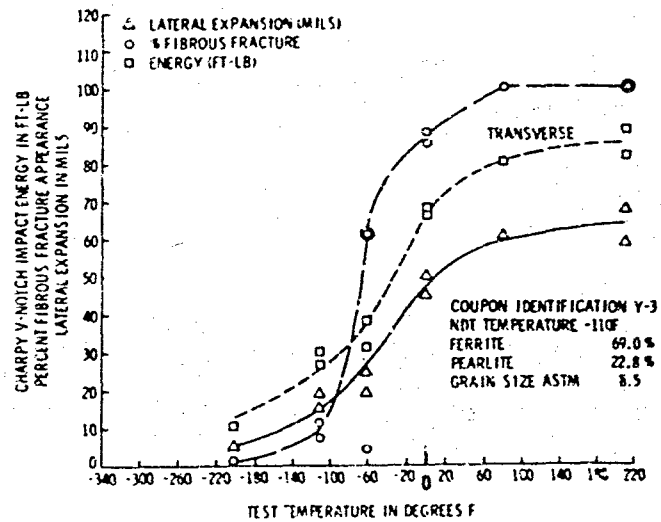

Figure D1 (Continued)

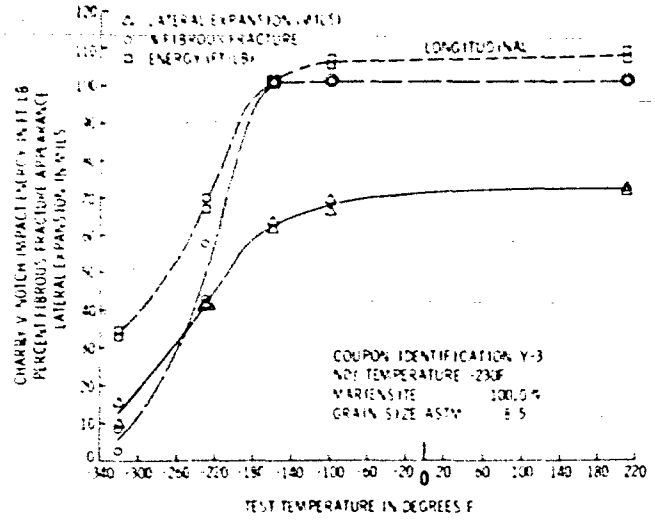

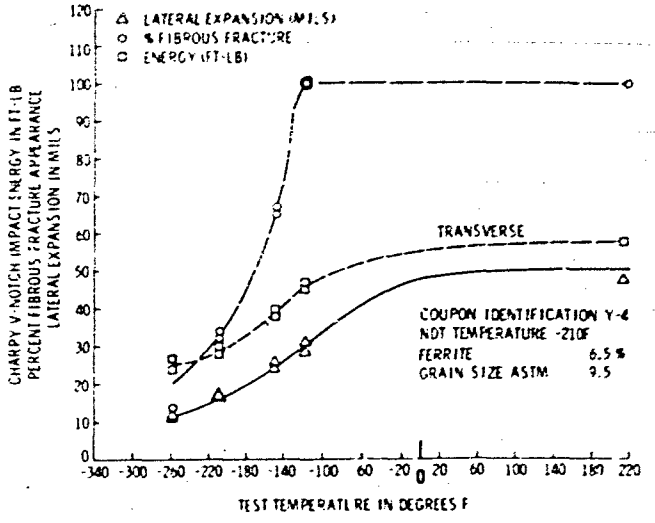

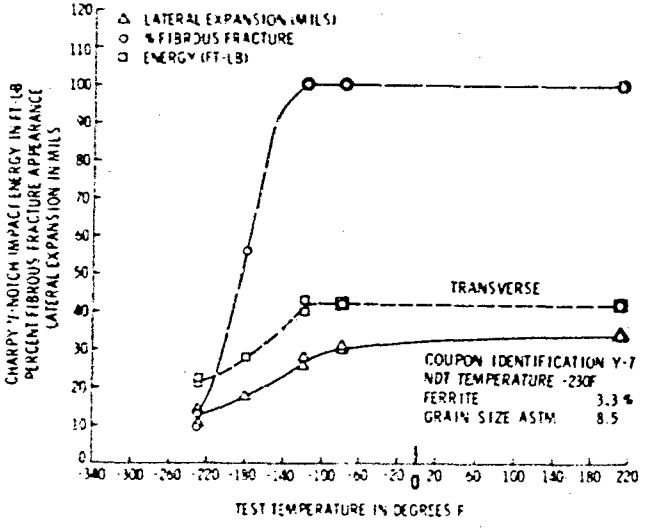

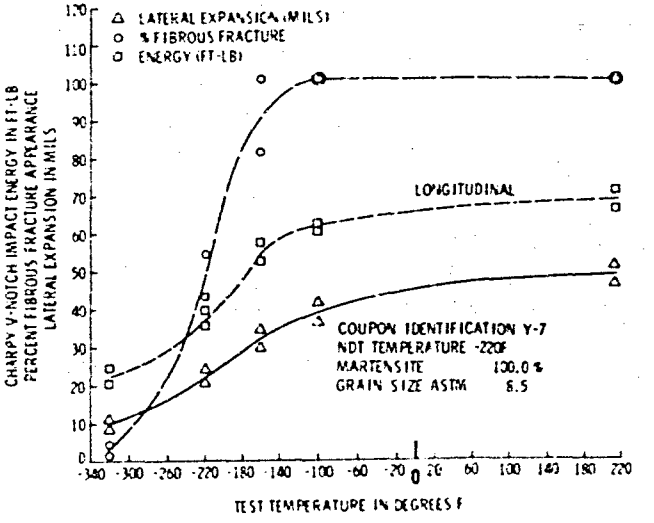

Figure D1 (Continued)

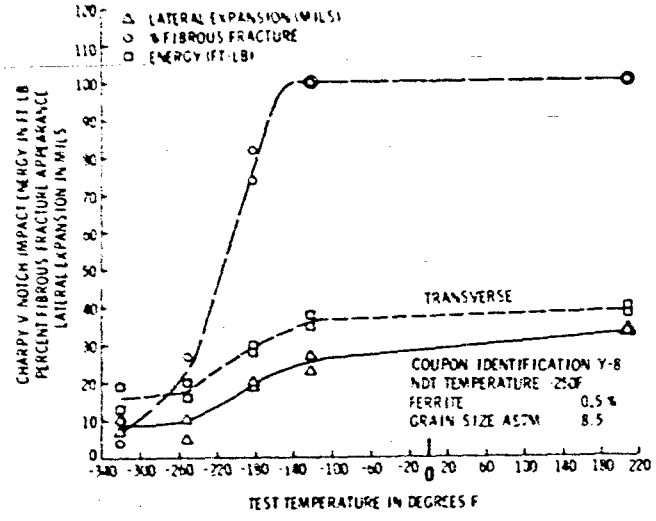

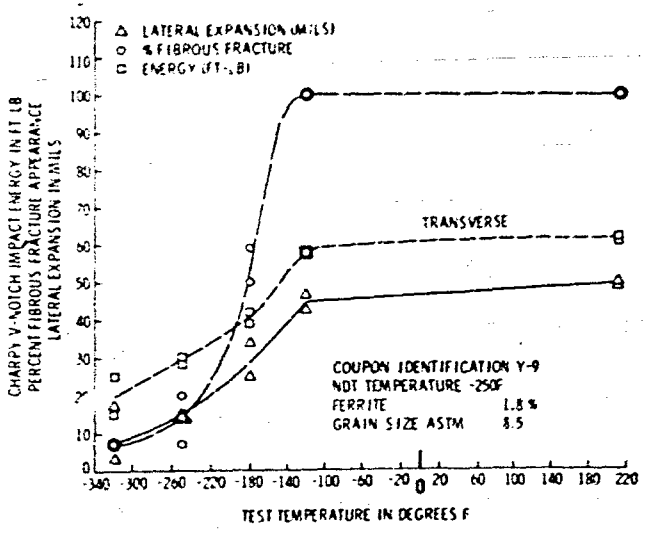

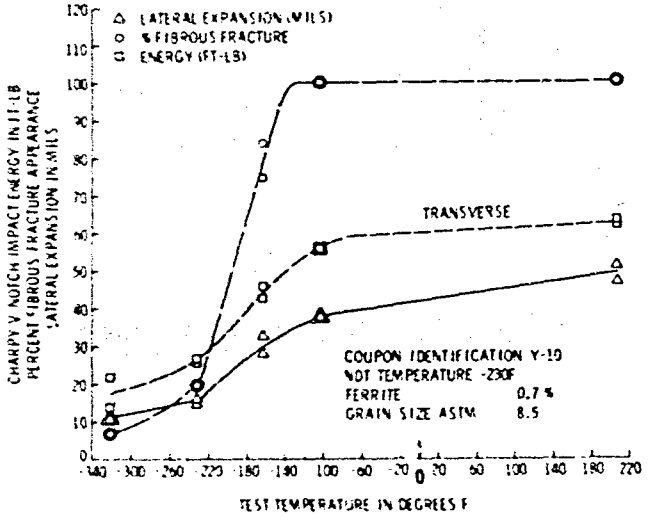

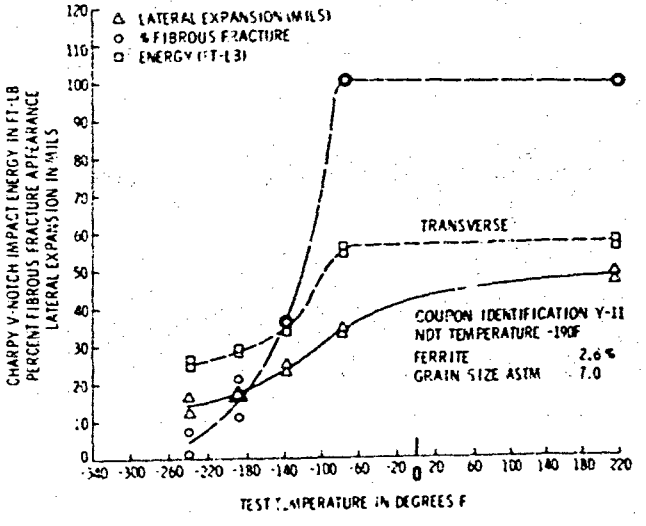

Figure D2 – Transverse Charpy V-Notch Impact Data for Specimens Austenitized at 1640 F for 1/2 Hour, *Isothermally Treated at 875 F for 152 Seconds*, Water Quenched and Tempered at 1150 F for 1 Hour

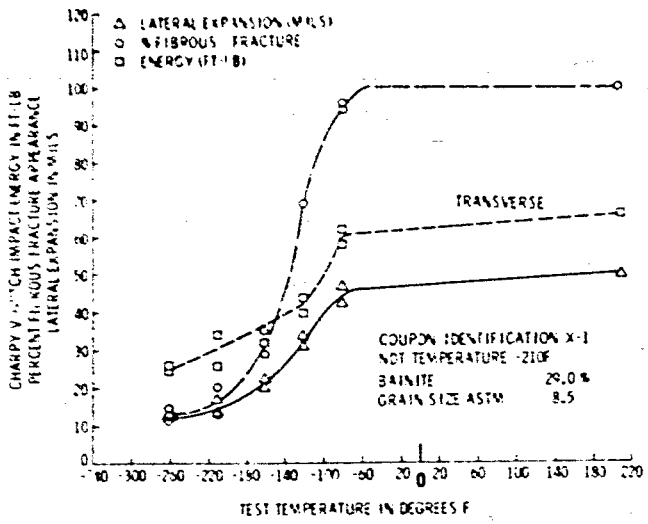

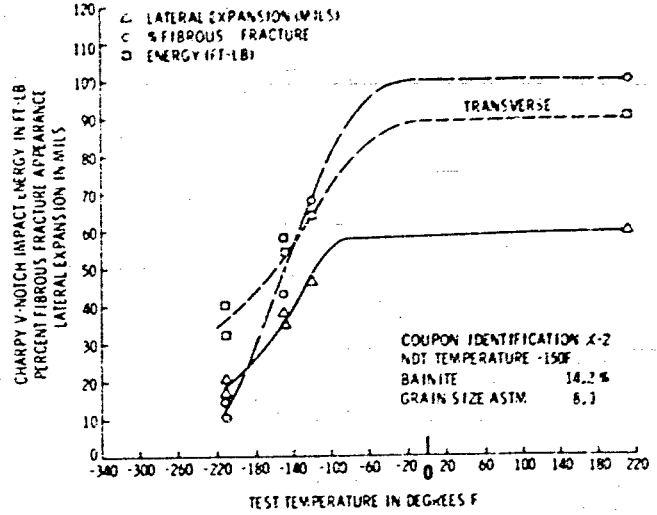

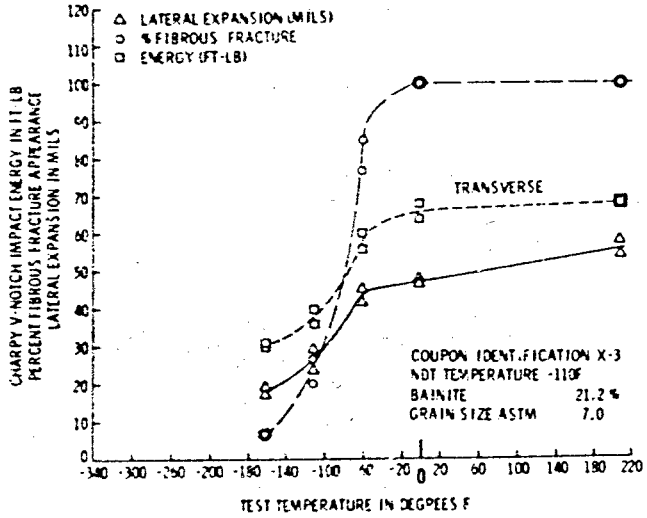

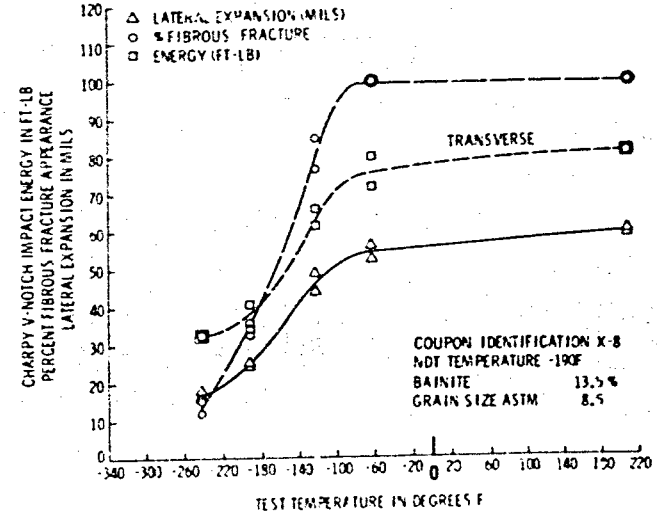

Figure D2 (Continued)

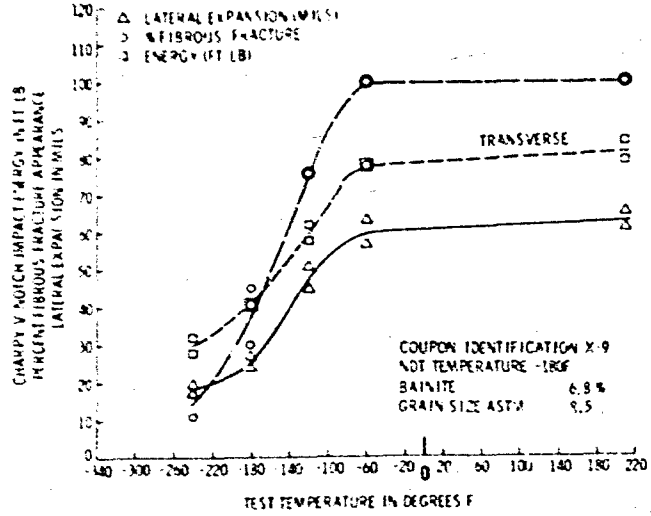

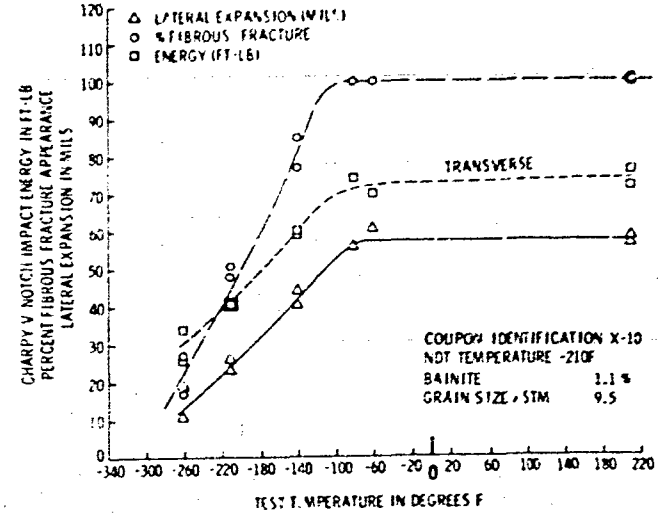

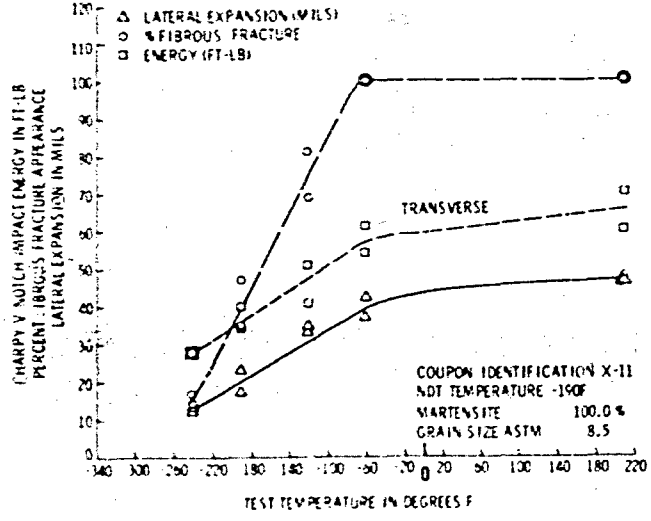

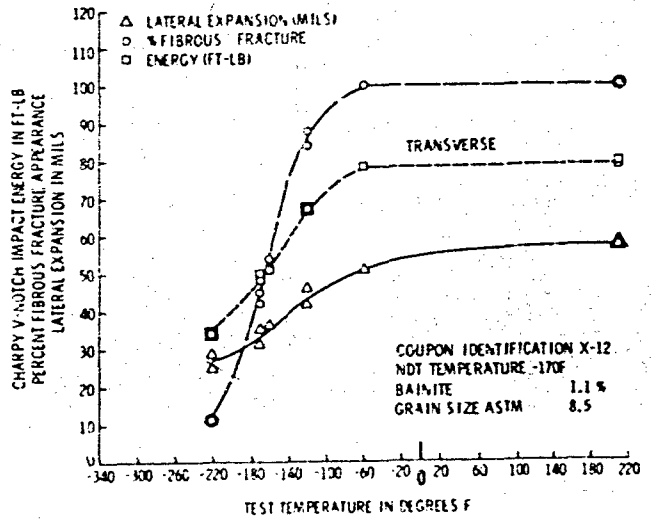

Figure D2 (Continued)

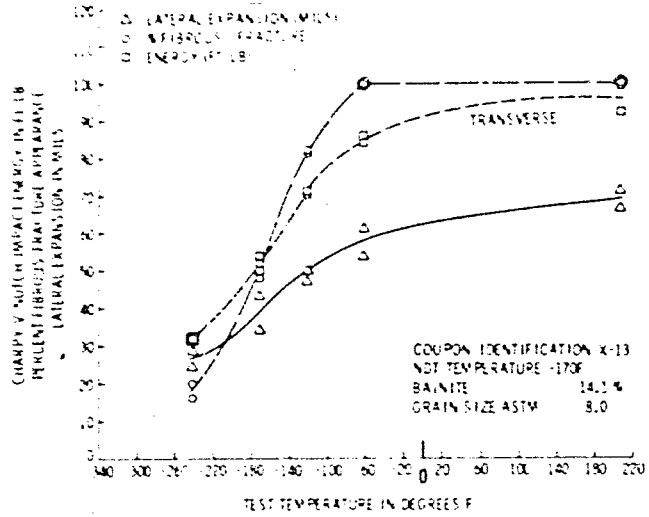

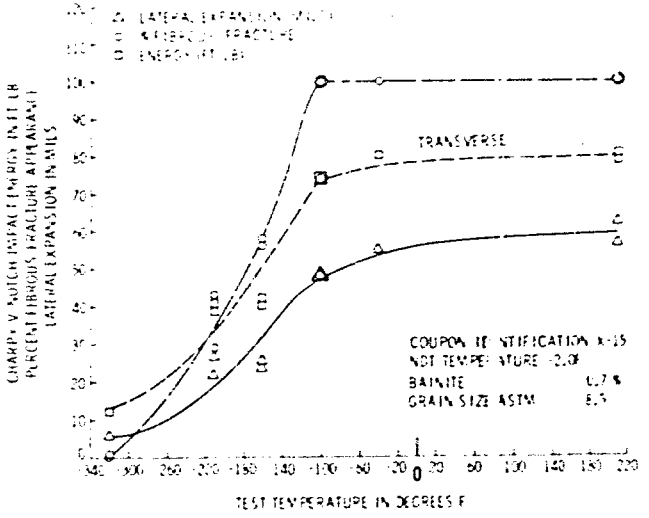

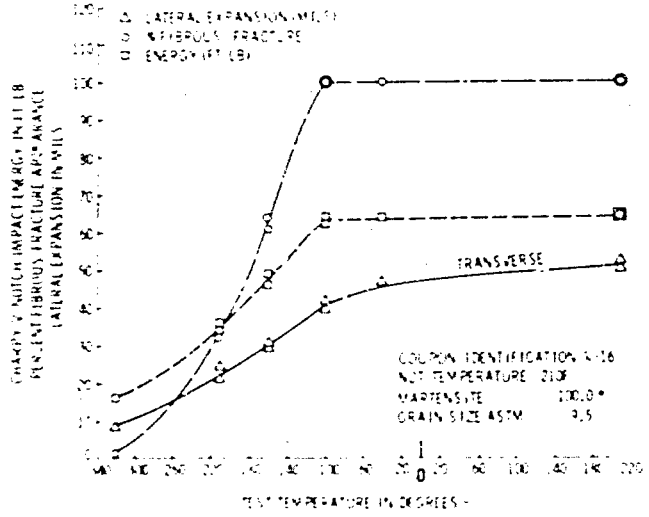

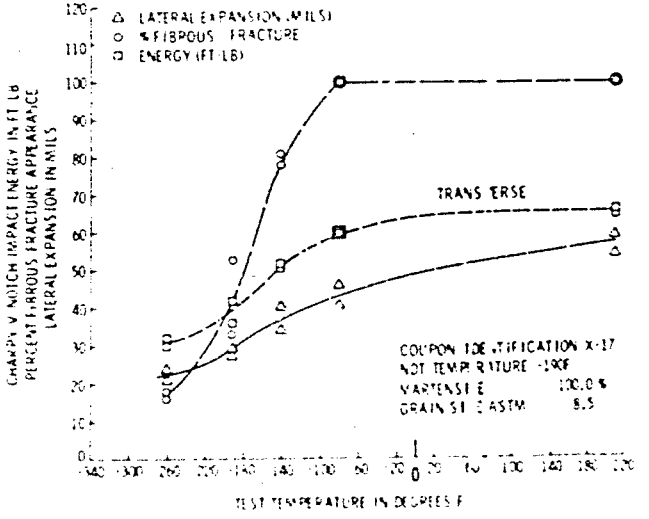

Figure D2 (Continued)

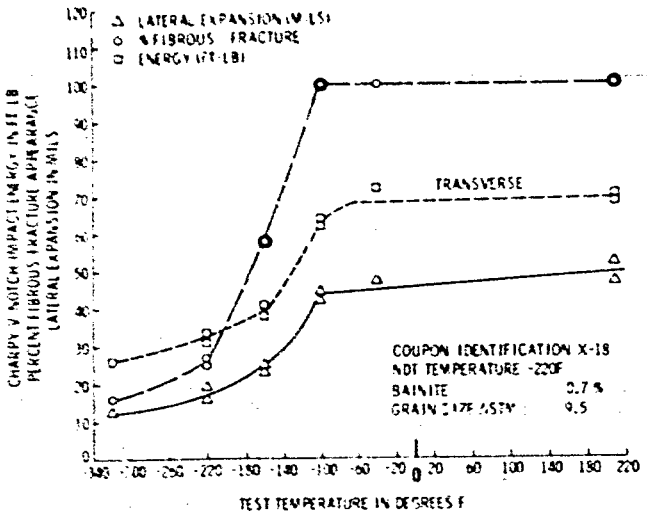

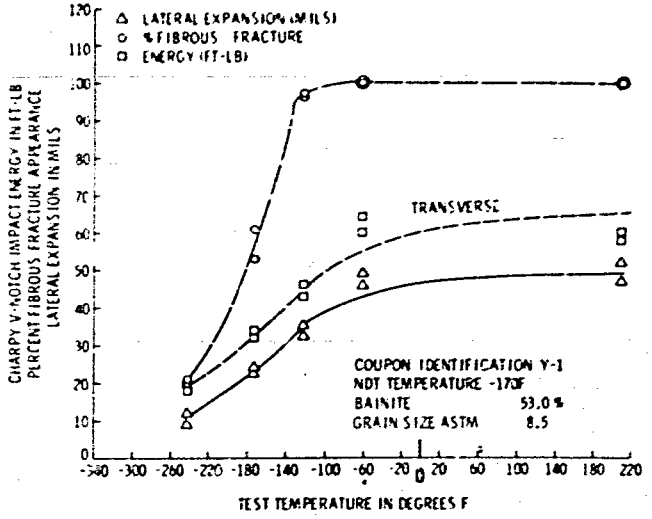

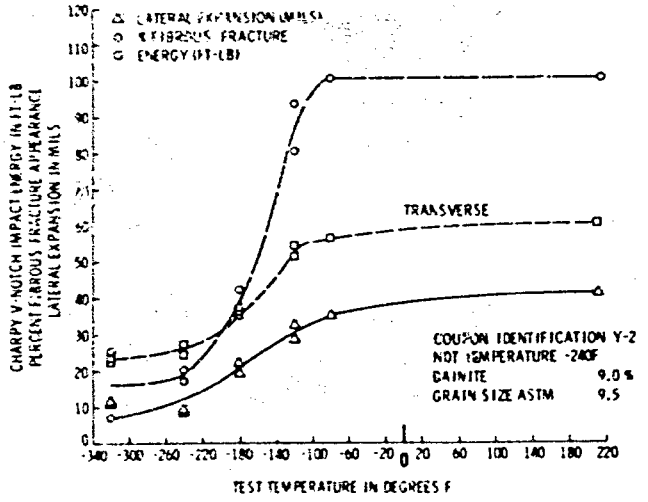

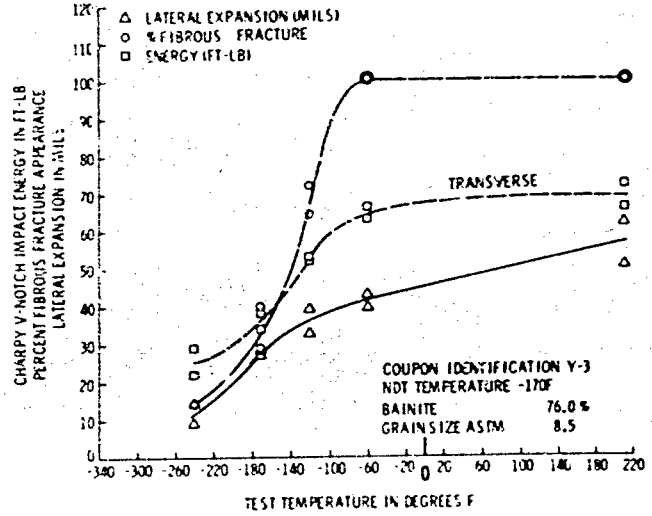

Figure D2 (Continued)

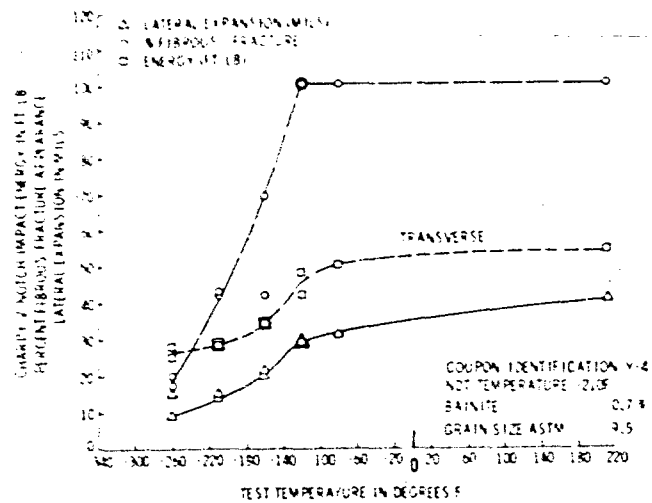

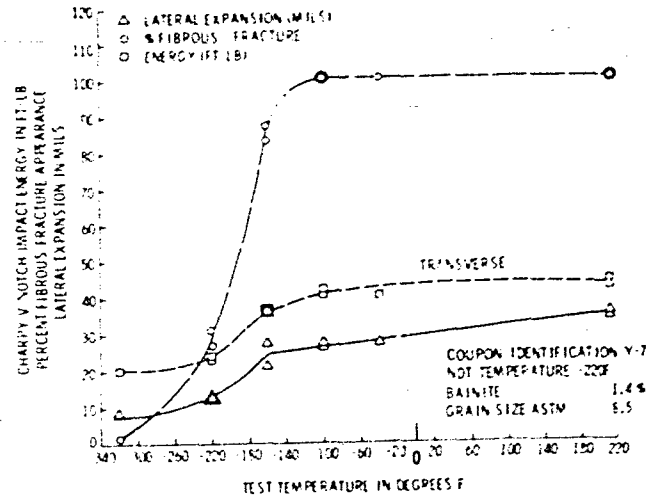

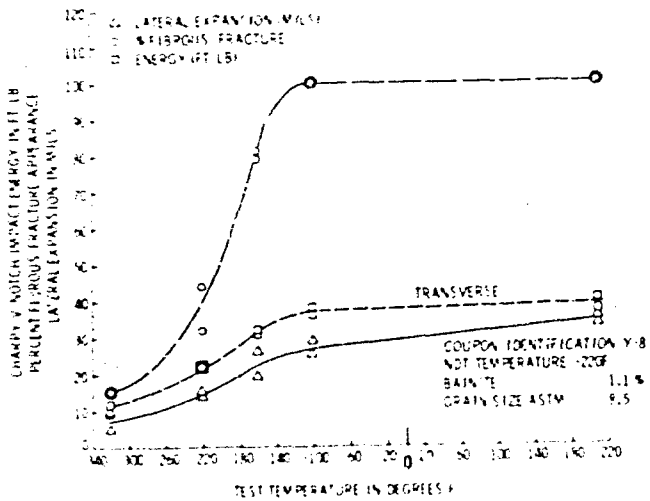

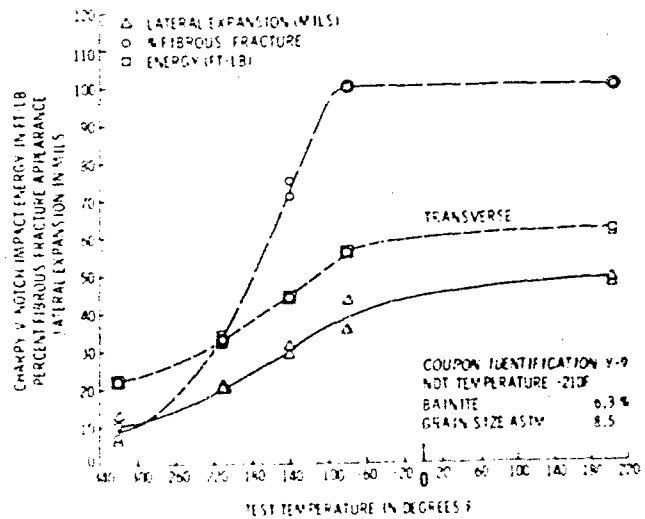

Figure D2 (Continued)

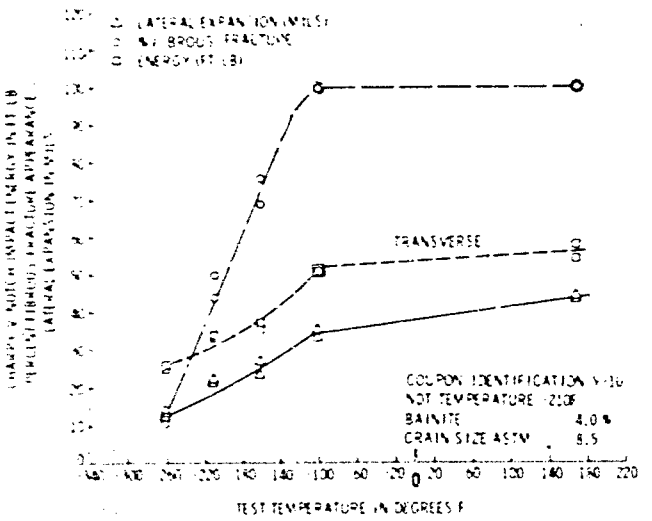

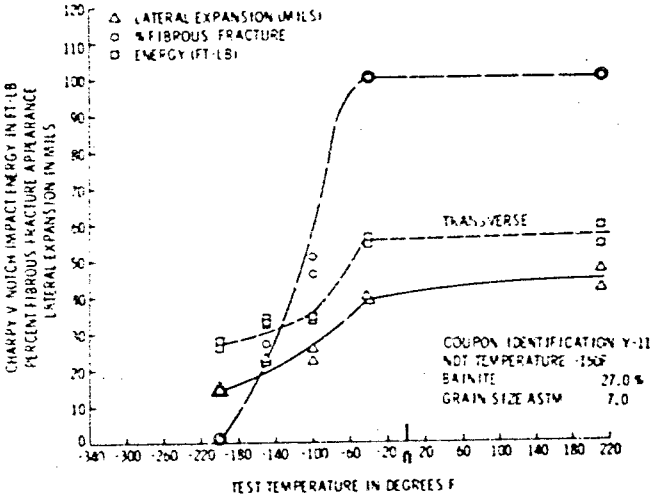

Figure D3 Transverse and Longitudinal Charpy V-Notch Impact Data for Specimens Austenitized at 1640 F for 1/2 Hour, *Isothermally Treated at 875 F for 1600 Seconds*, Water Quenched and Tempered at 1150 F for 1 Hour

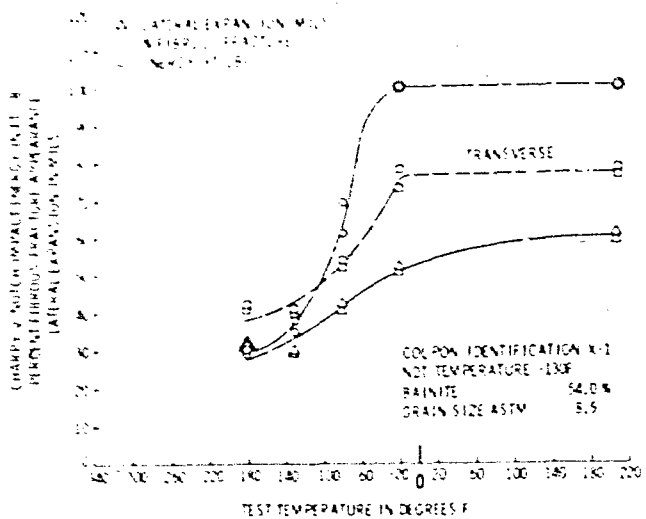

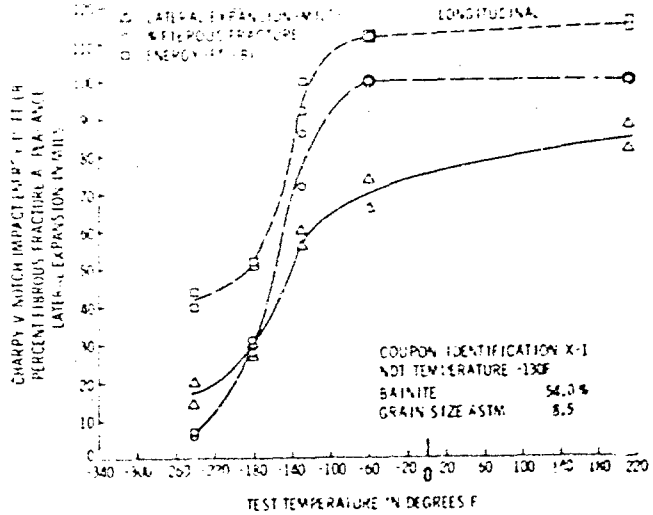

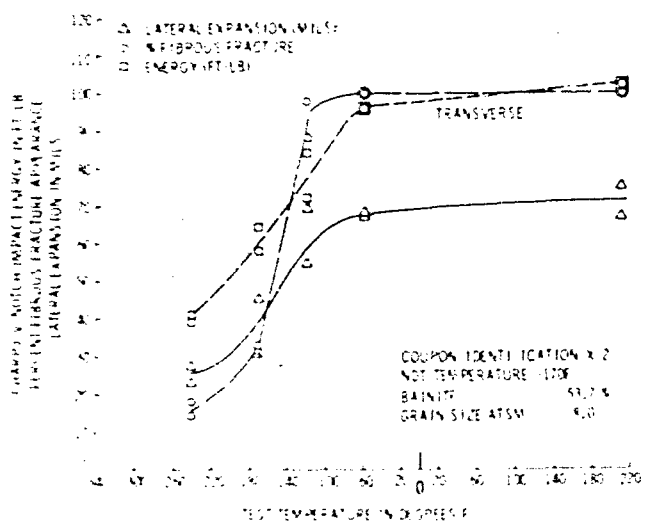

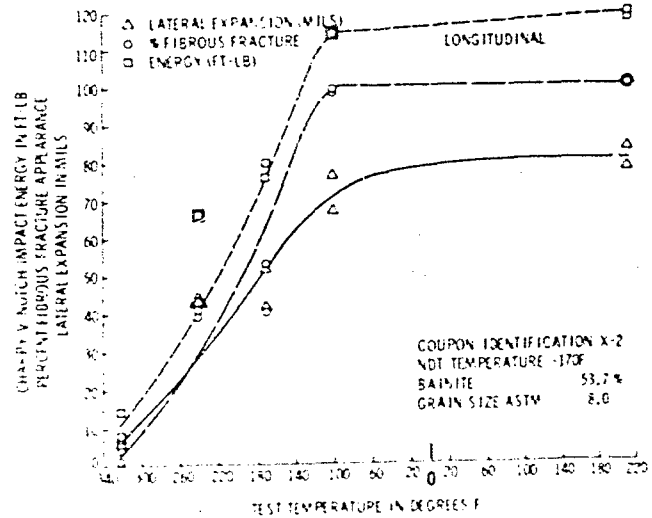

Figure D3 (Continued)

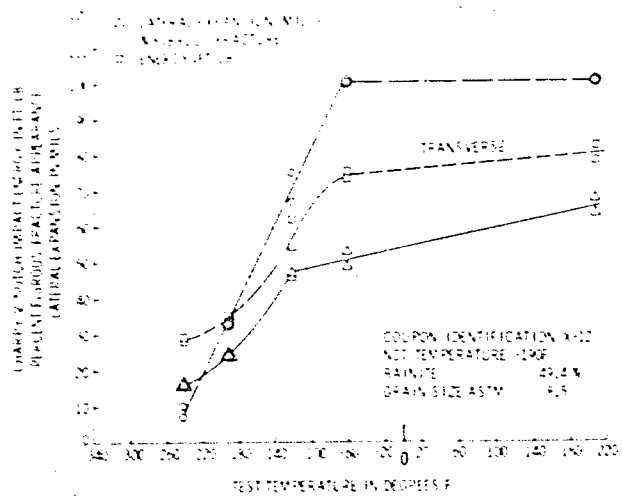

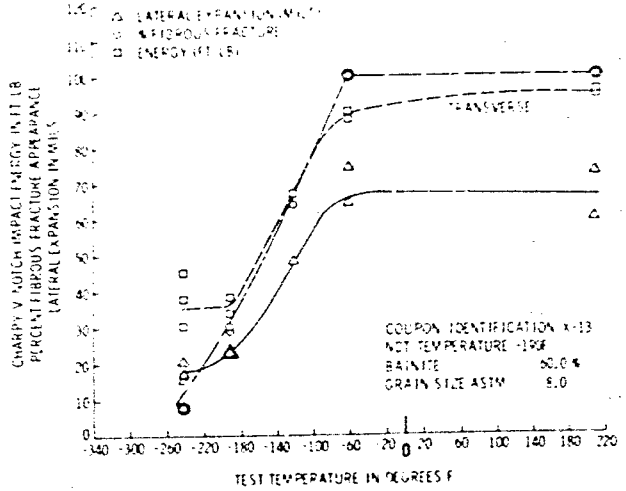

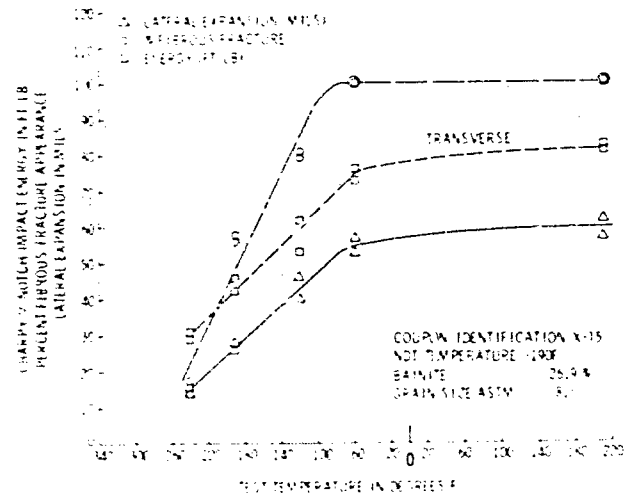

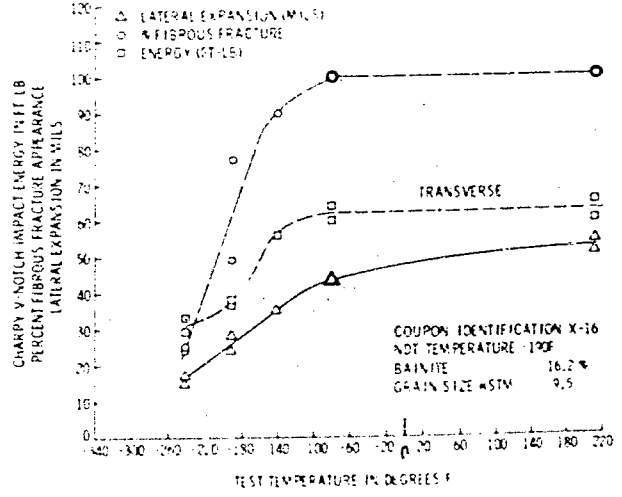

Figure D3 (Continued)

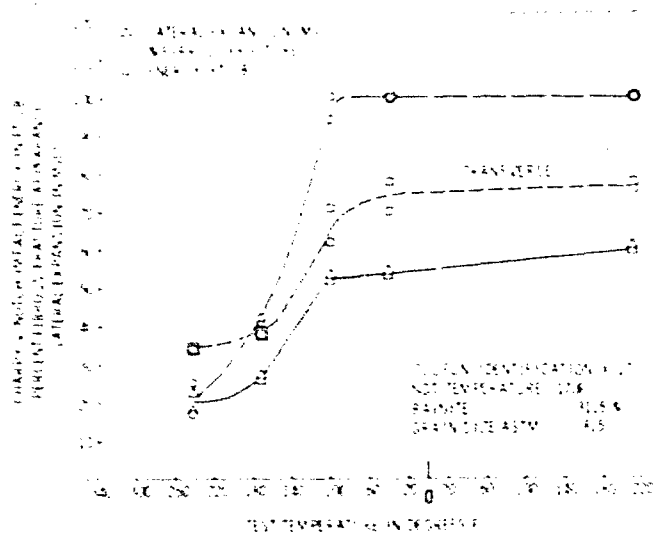

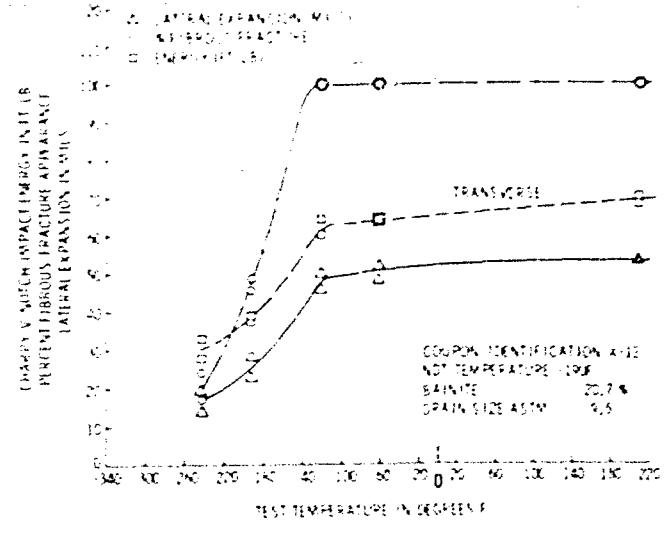

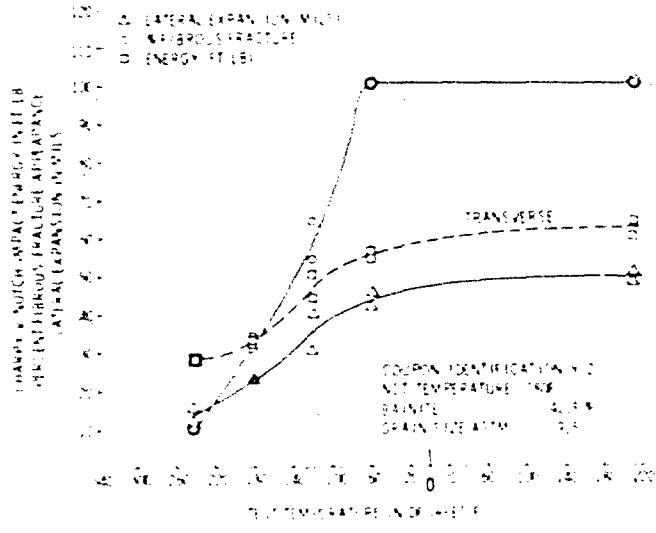

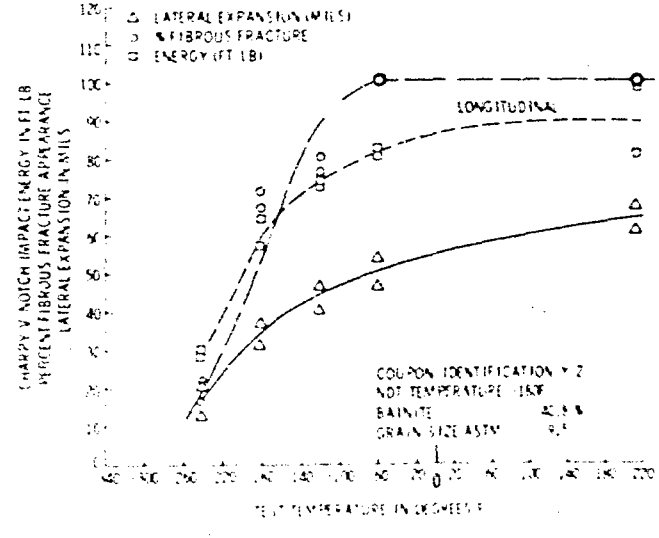

Figure D3 (Continued)

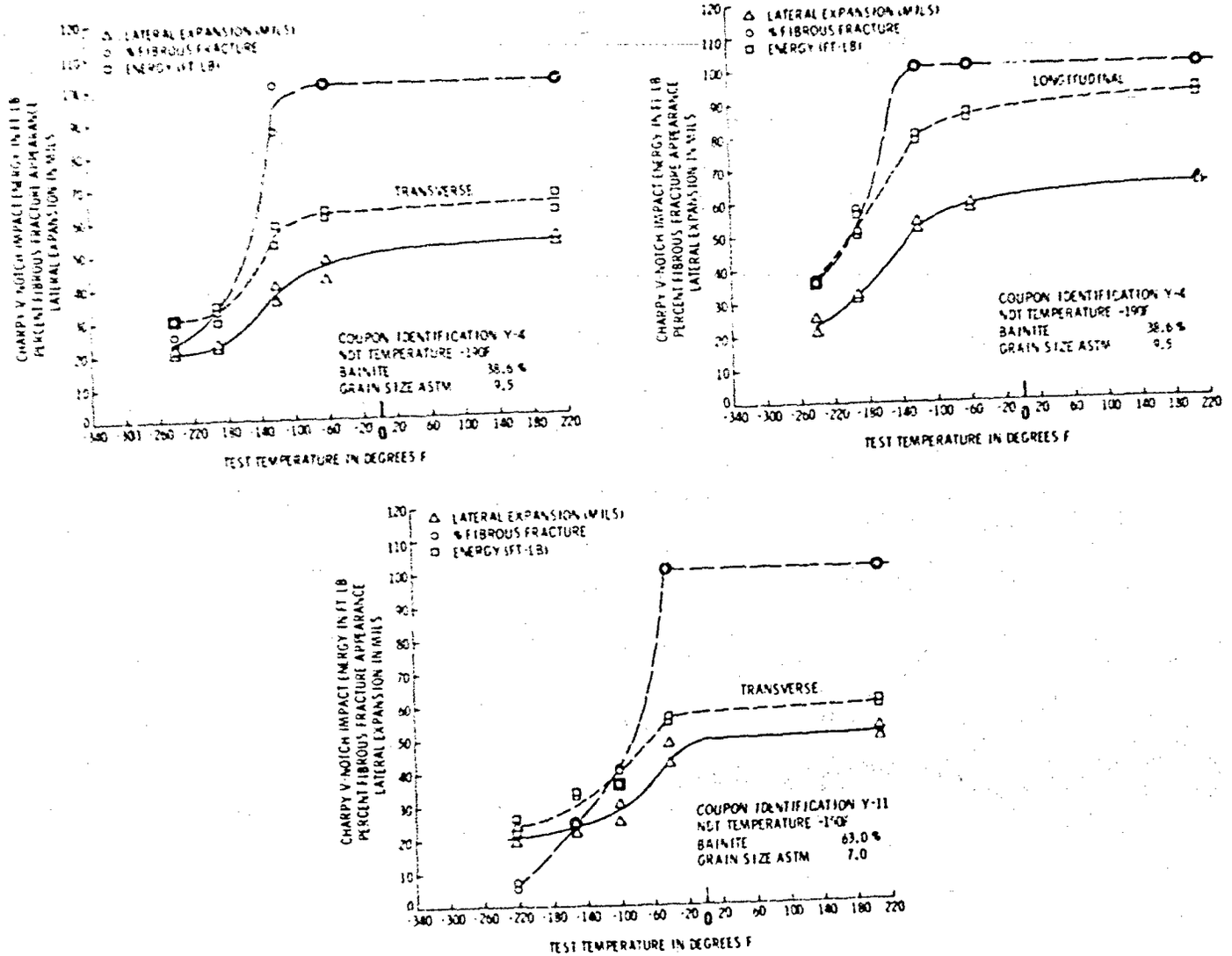

Figure D4 — Transverse Charpy V-Notch Impact Data for Specimens Austenitized at 1640 F for 1/2 Hour, *Isothermally Treated at 1200 F for 3350 Seconds*, Water Quenched and Tempered at 1150 F for 1 Hour

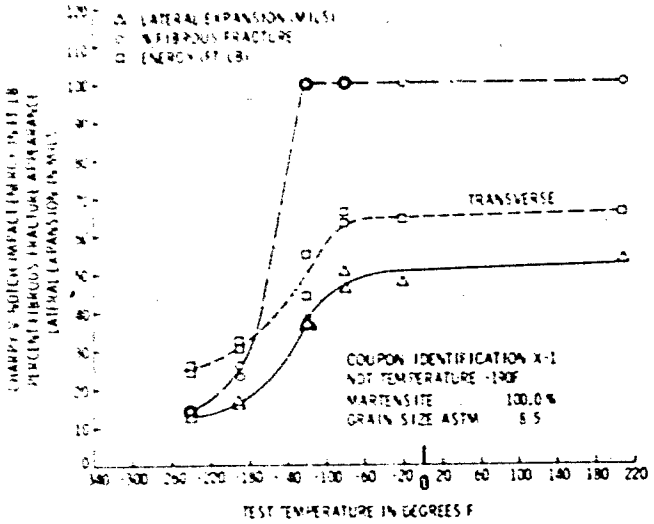

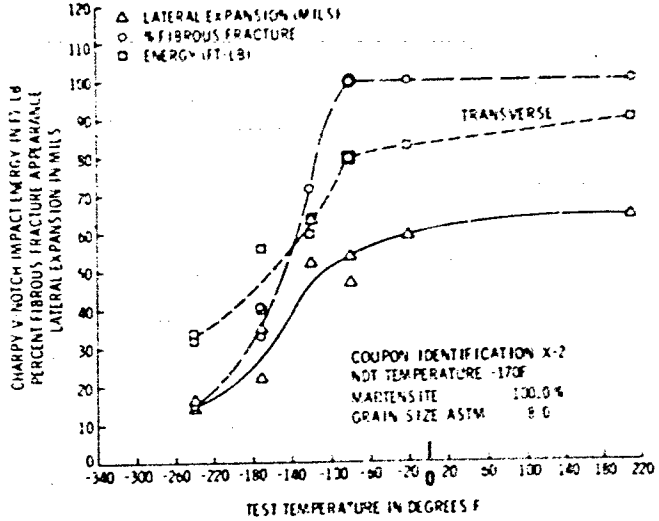

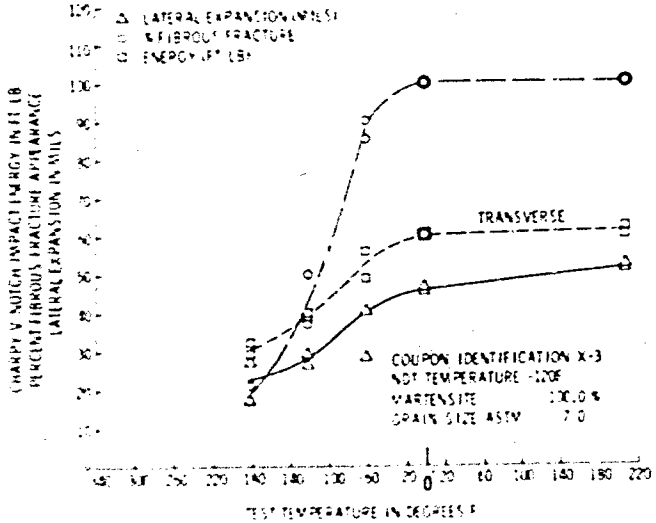

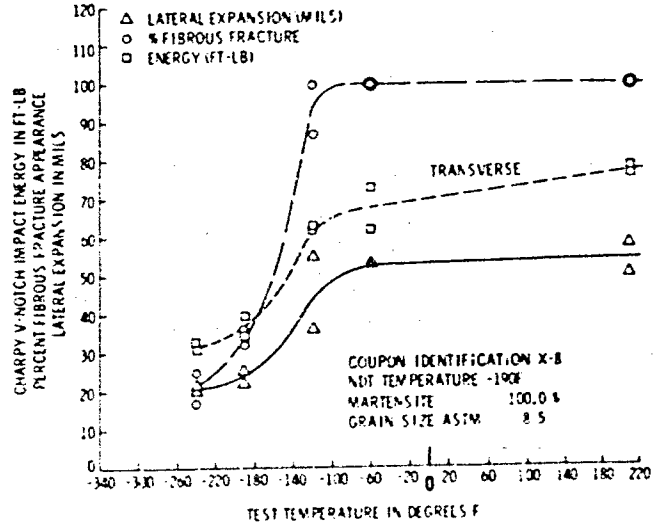

Figure D4 (Continued)

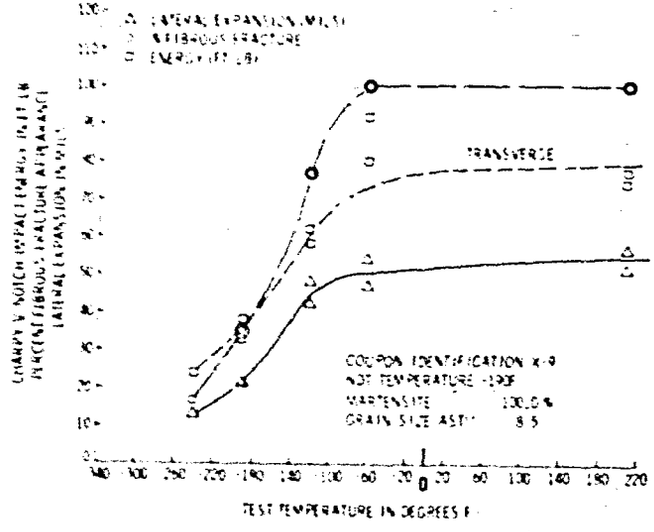

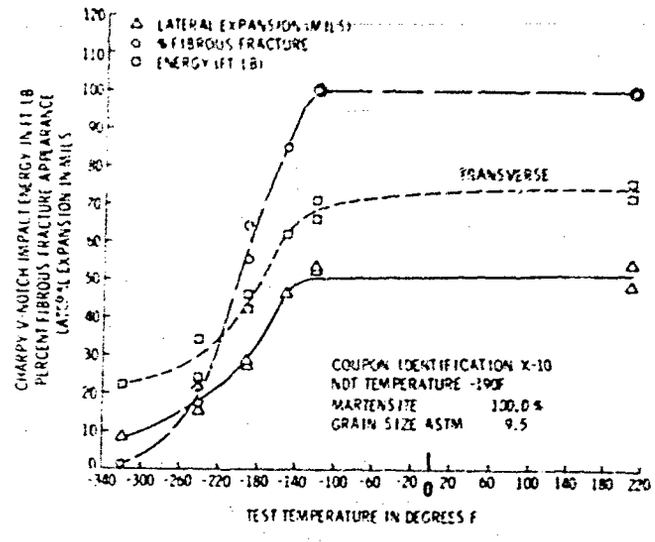

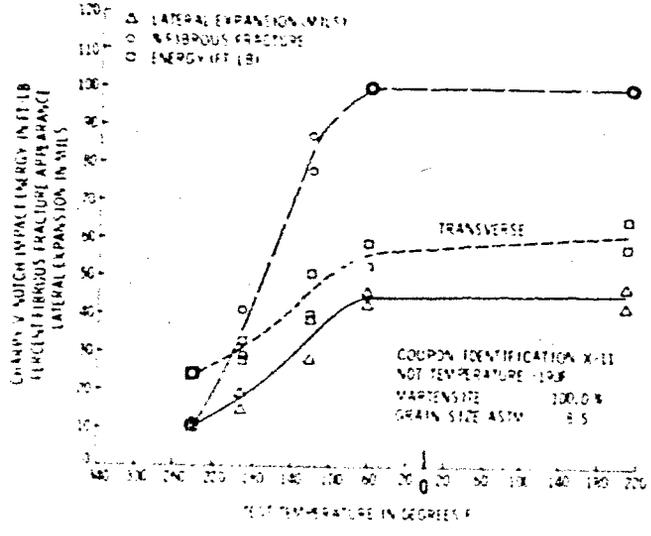

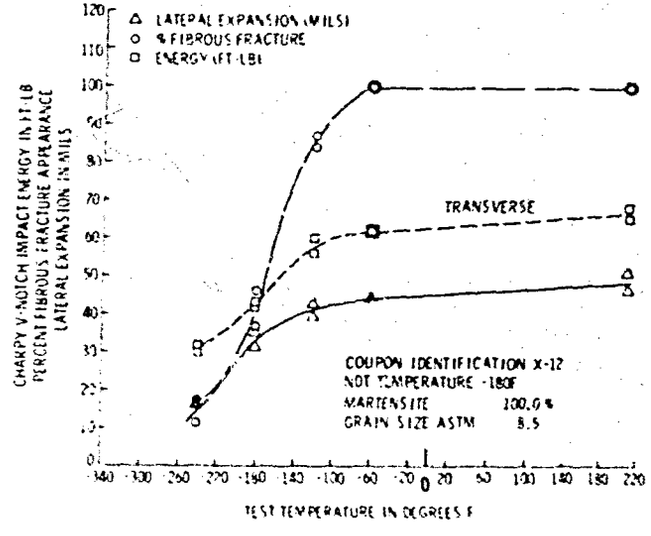

Figure D4 (Continued)

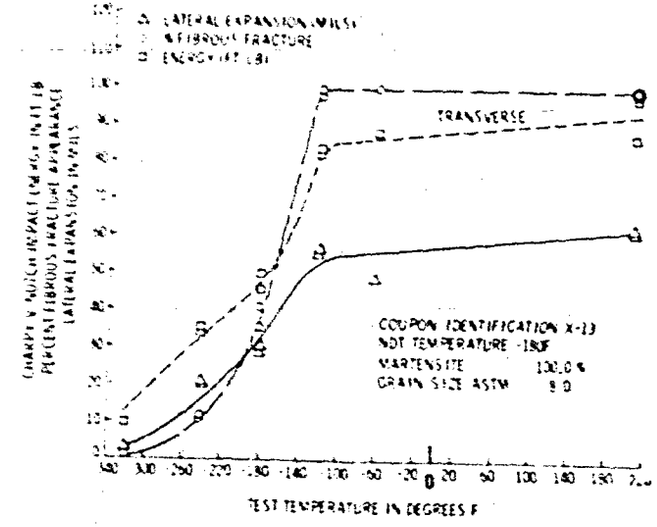

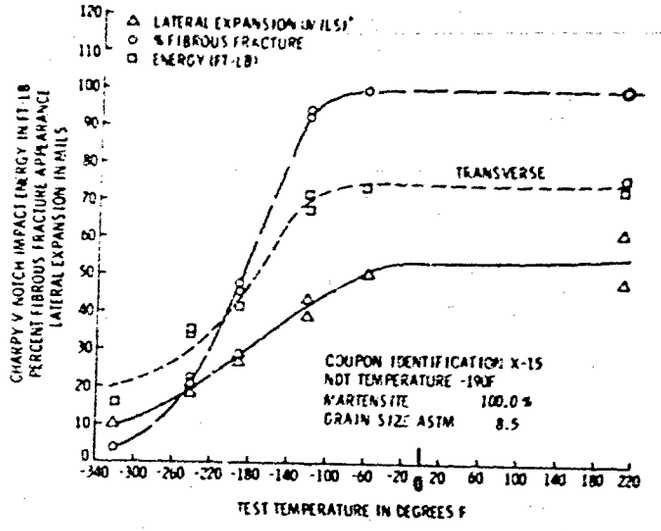

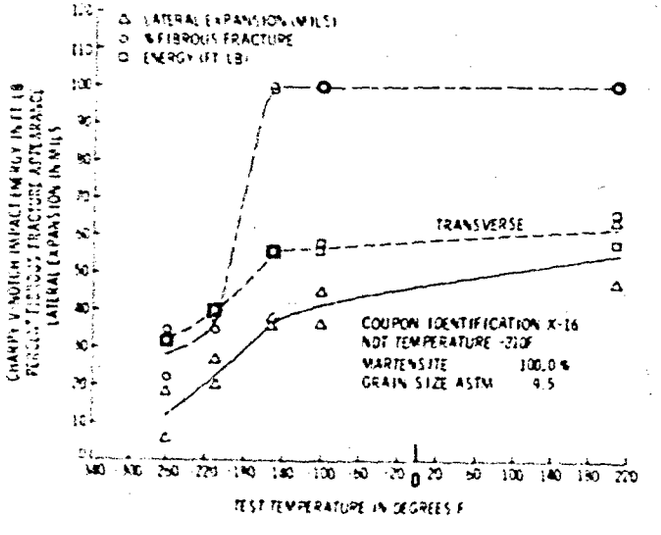

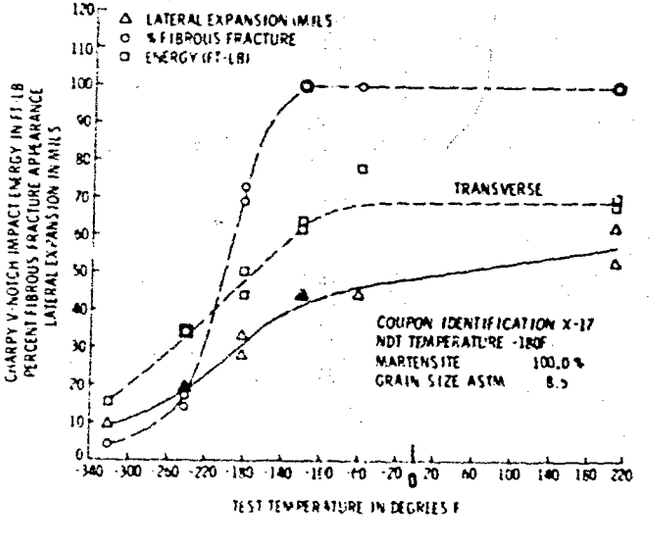

Figure D4 (Continued)

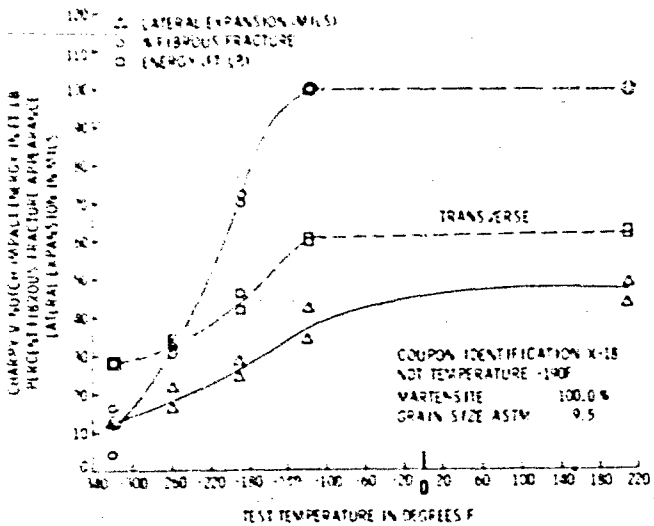

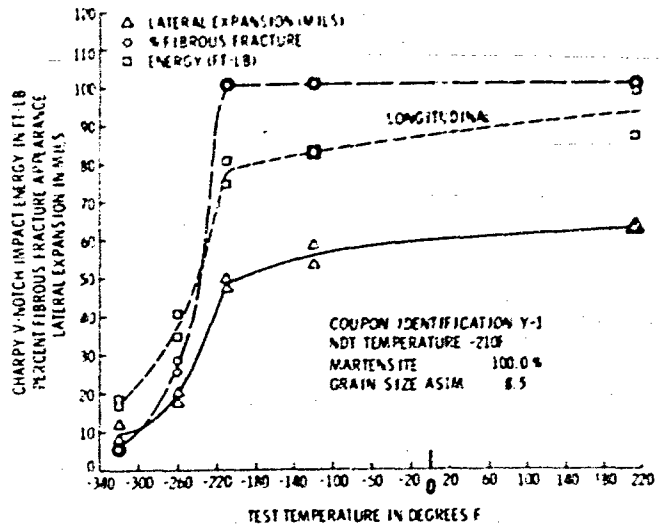

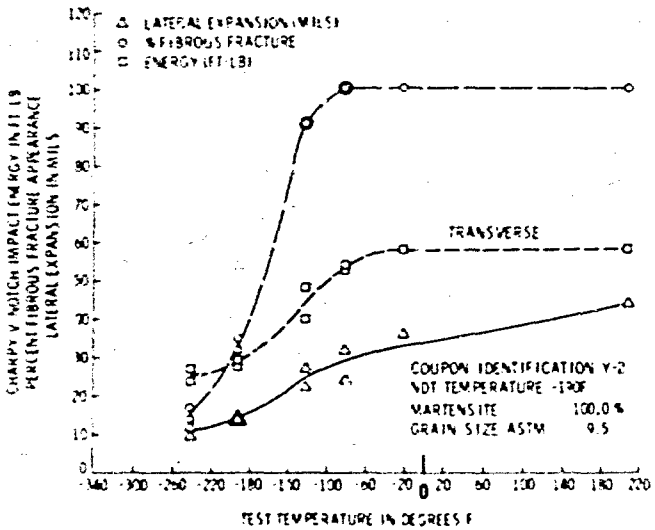

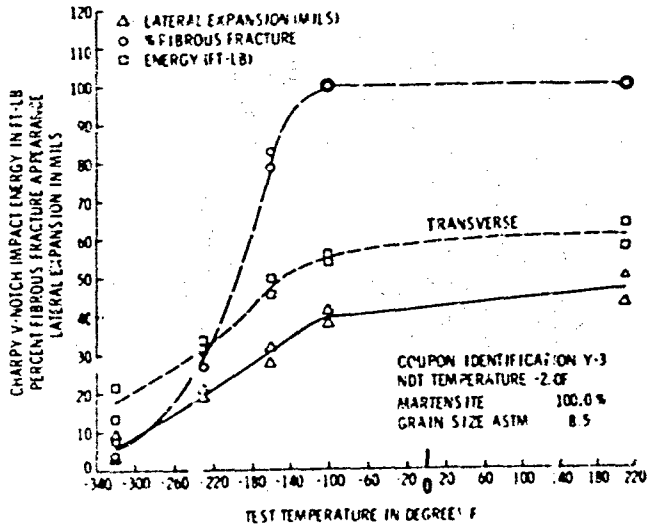

Figure D4 (Continued)

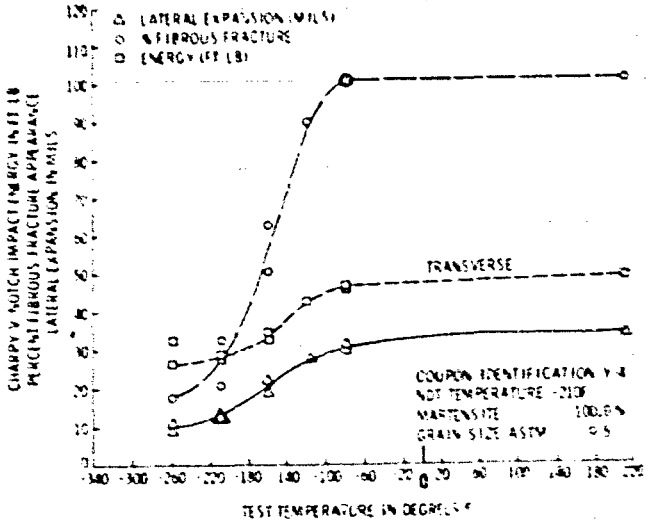

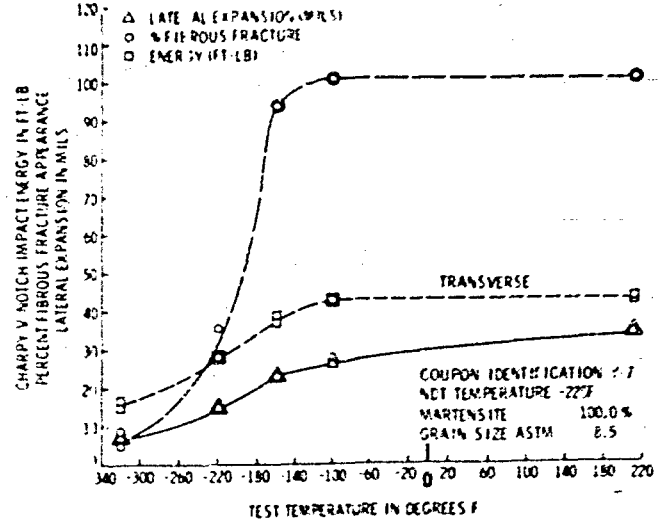

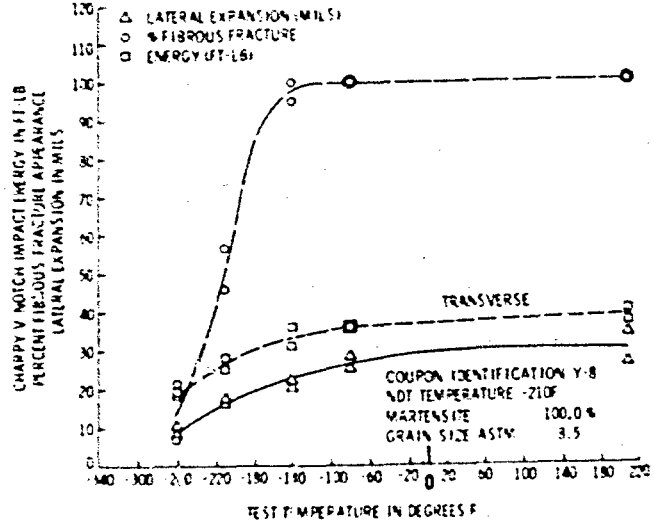

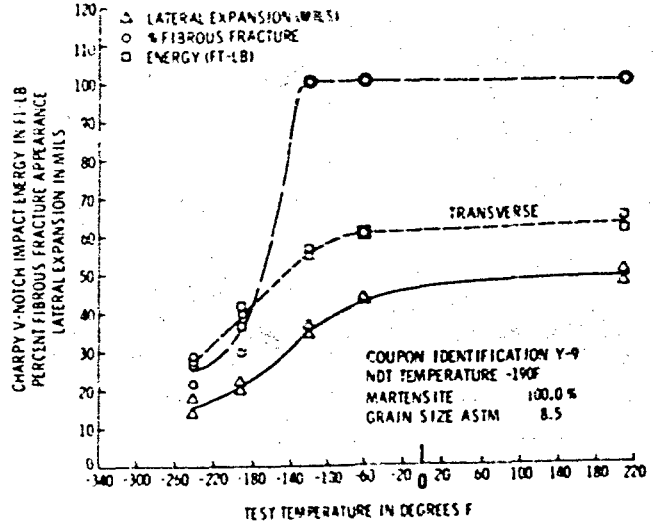

Figure D4 (Continued)

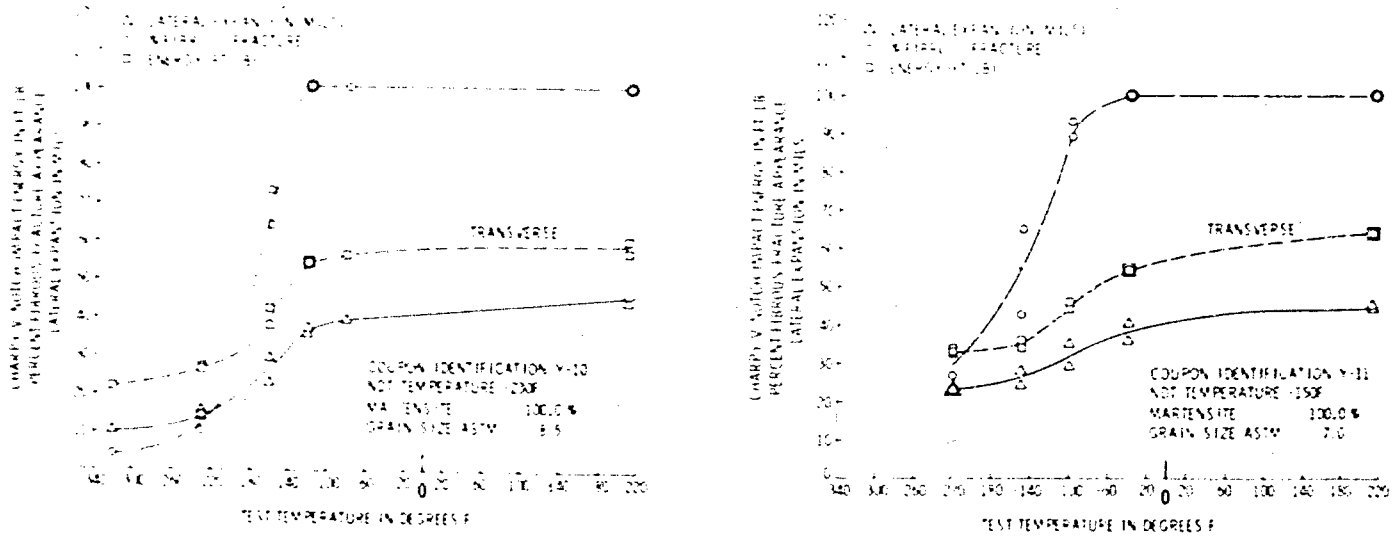

Figure D5 — Transverse Charpy V Notch Impact Data for Specimens Austenitized at 1640 F for 1/2 Hour, *Isothermally Treated at 1200 F for 8500 Seconds*, Water Quenched and Tempered at 1150 F for 1 Hour

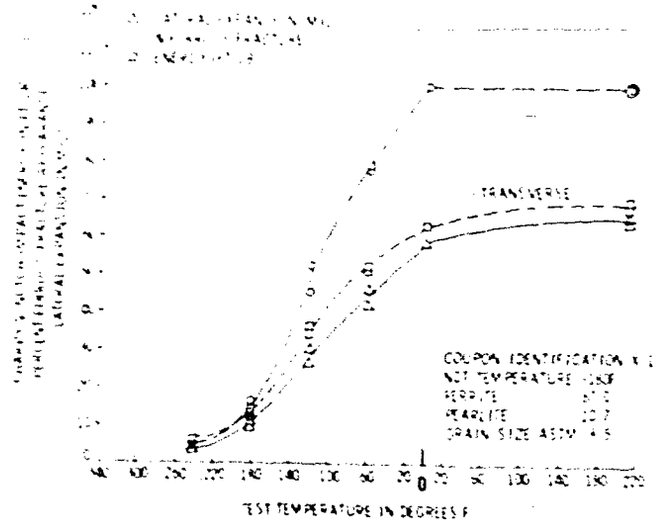

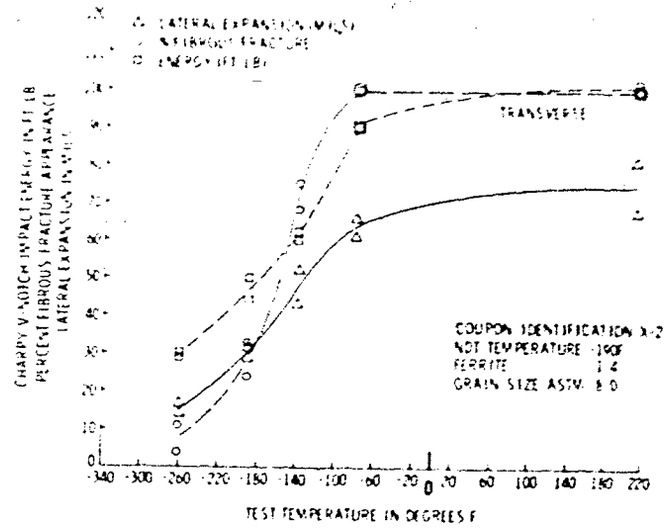

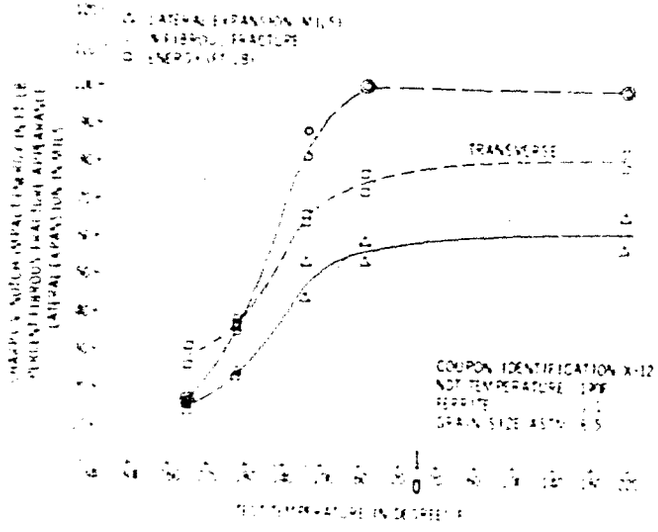

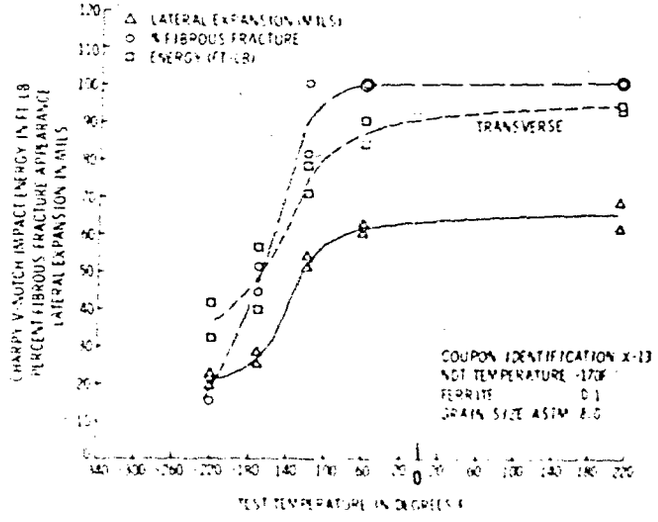

Figure D5 (Continued)

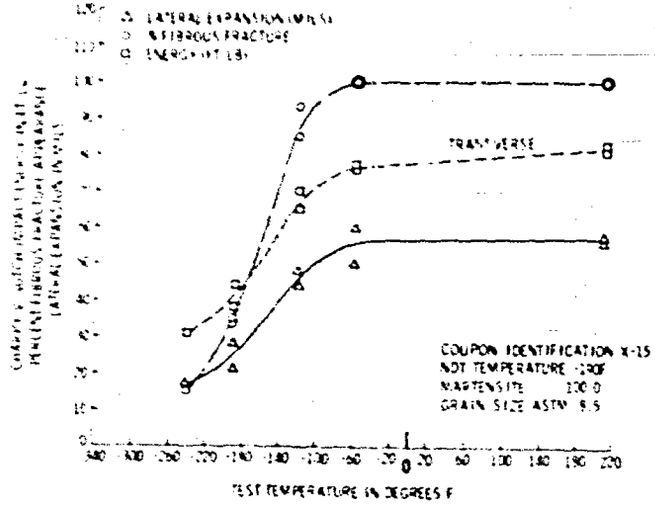

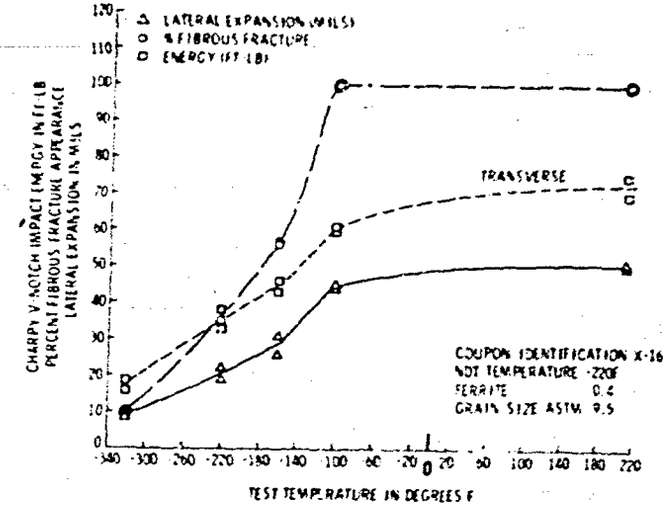

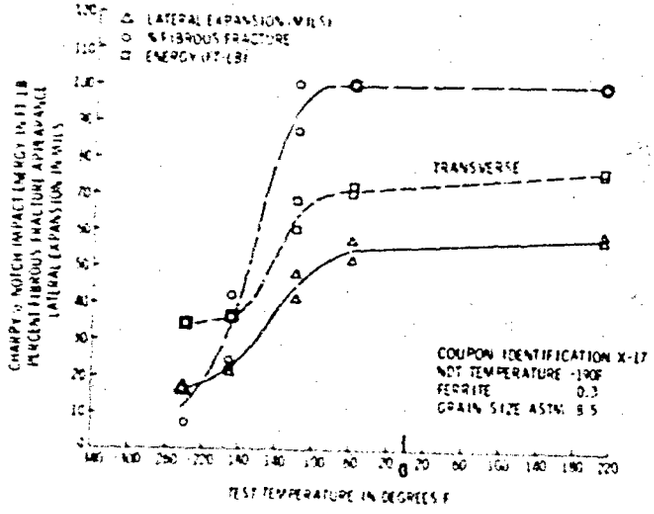

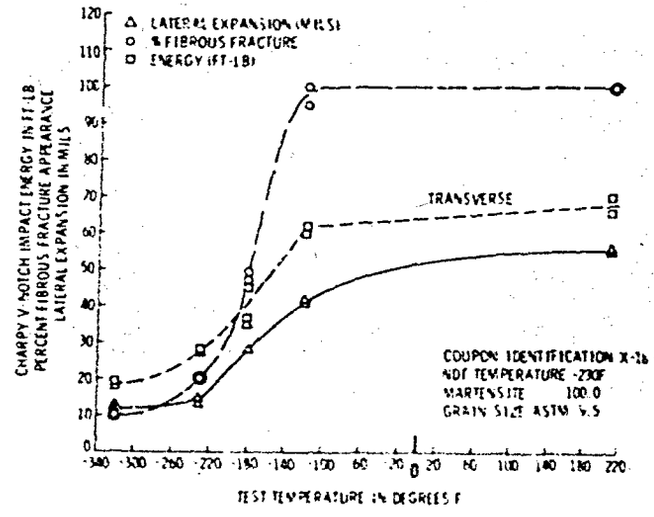

Figure D5 (Continued)

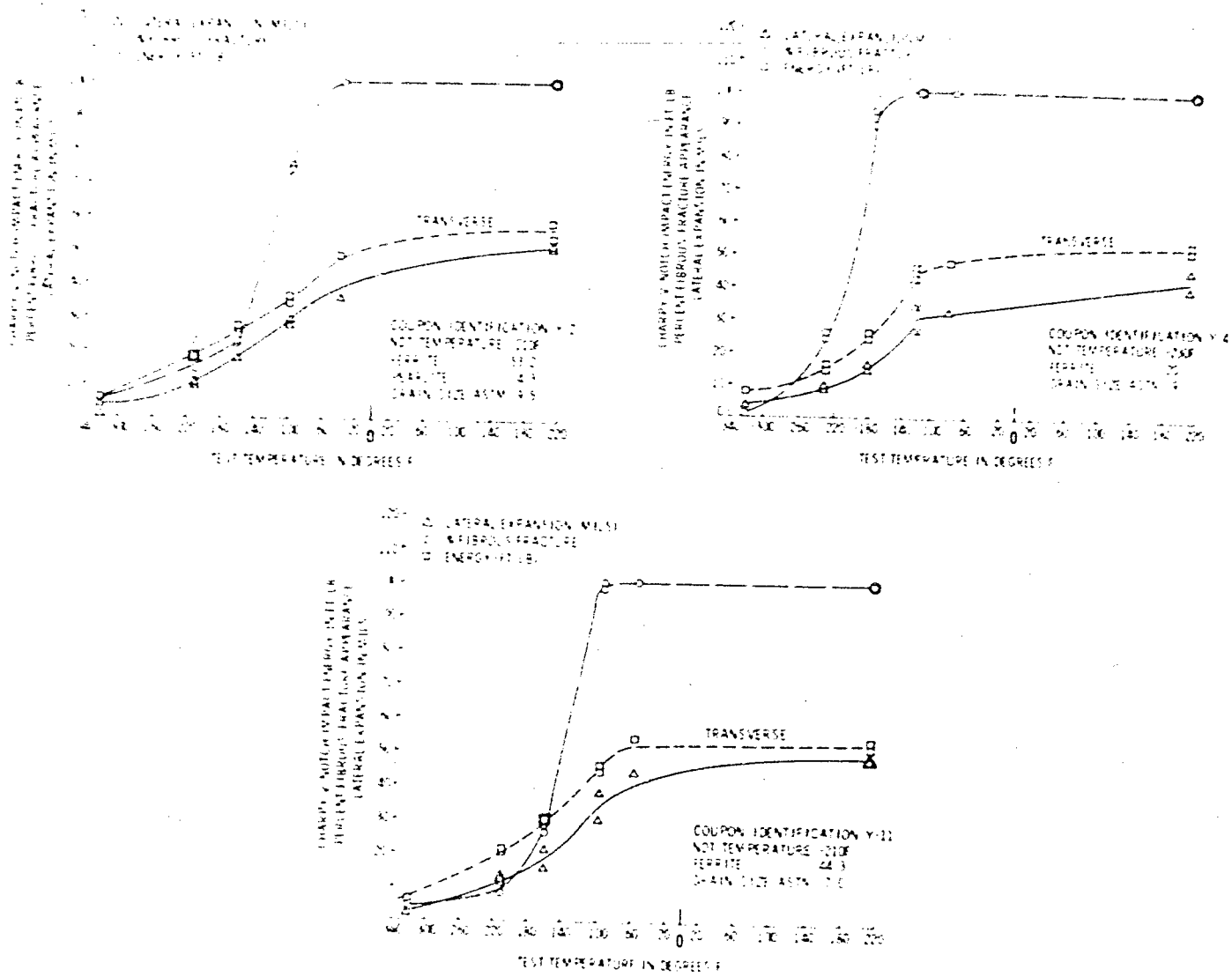

Figure D6 – Transverse Charpy V-Notch Impact Data for Specimens *Austenitized at 2000 F* for 1 Hour, Transferred to 1640 F for 5 Minutes Minimum, *Water Quenched* and Tempered at 1100 F for 1 Hour

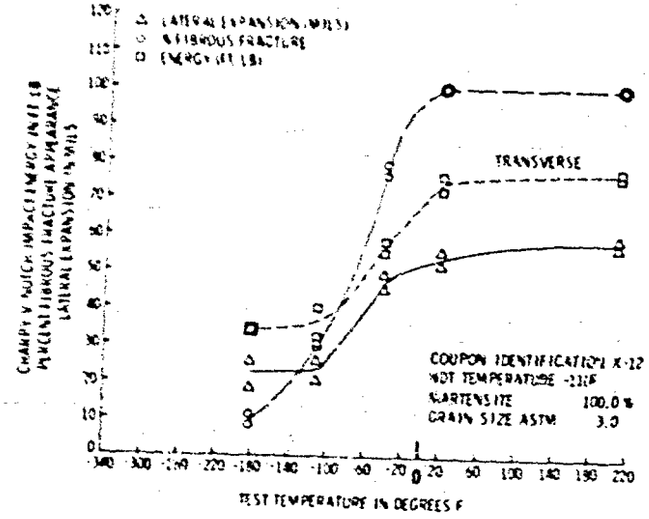

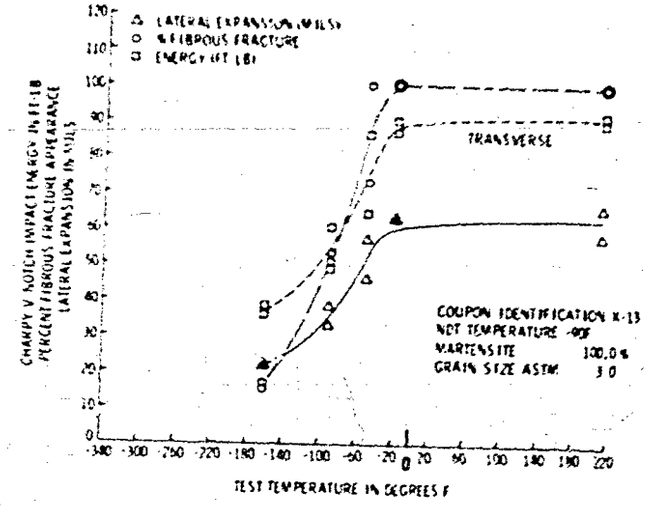

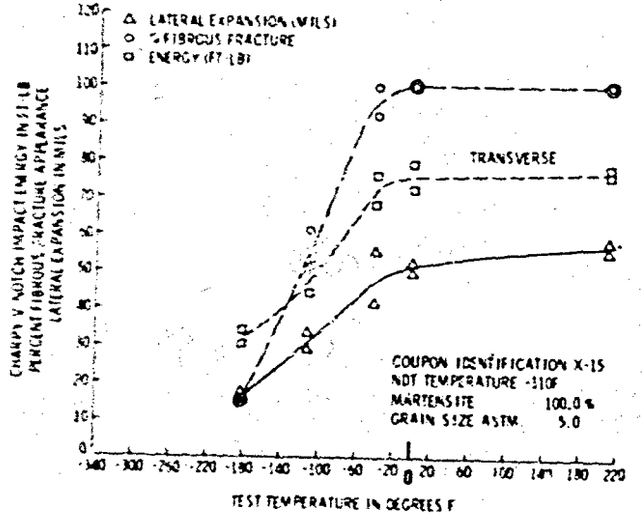

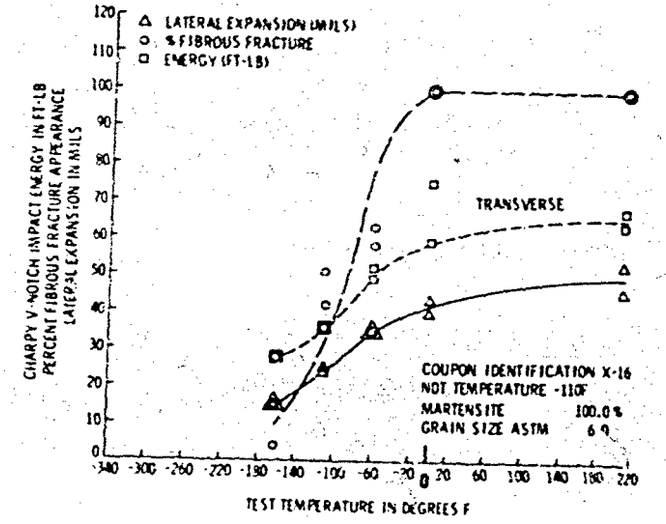

Figure D6 (Continued)

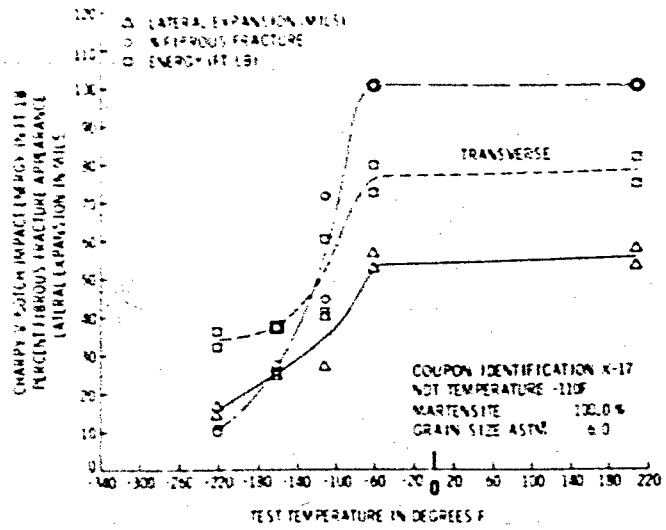

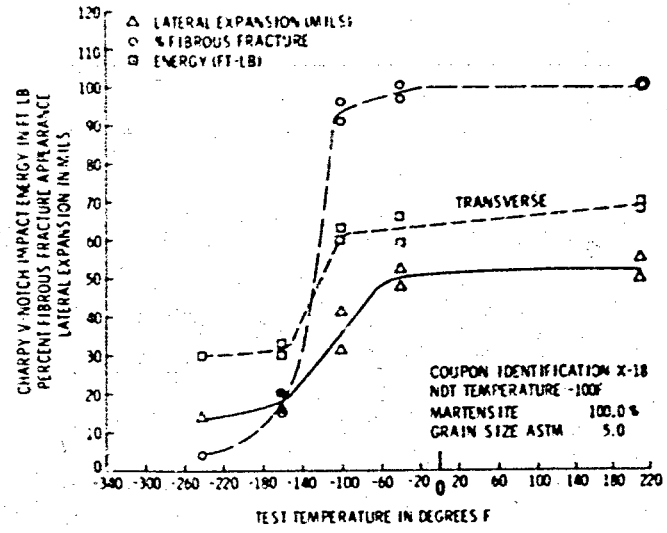

Figure D7 – Transverse Charpy V-Notch Impact Data for Specimens *Austenitized at 2000 F* for 1 Hour, Transferred to 1640 F for 5 Minutes Minimum, *Isothermally Treated at 875 F for 1600 Seconds*, Water Quenched and Tempered at 1150 F for 1 Hour

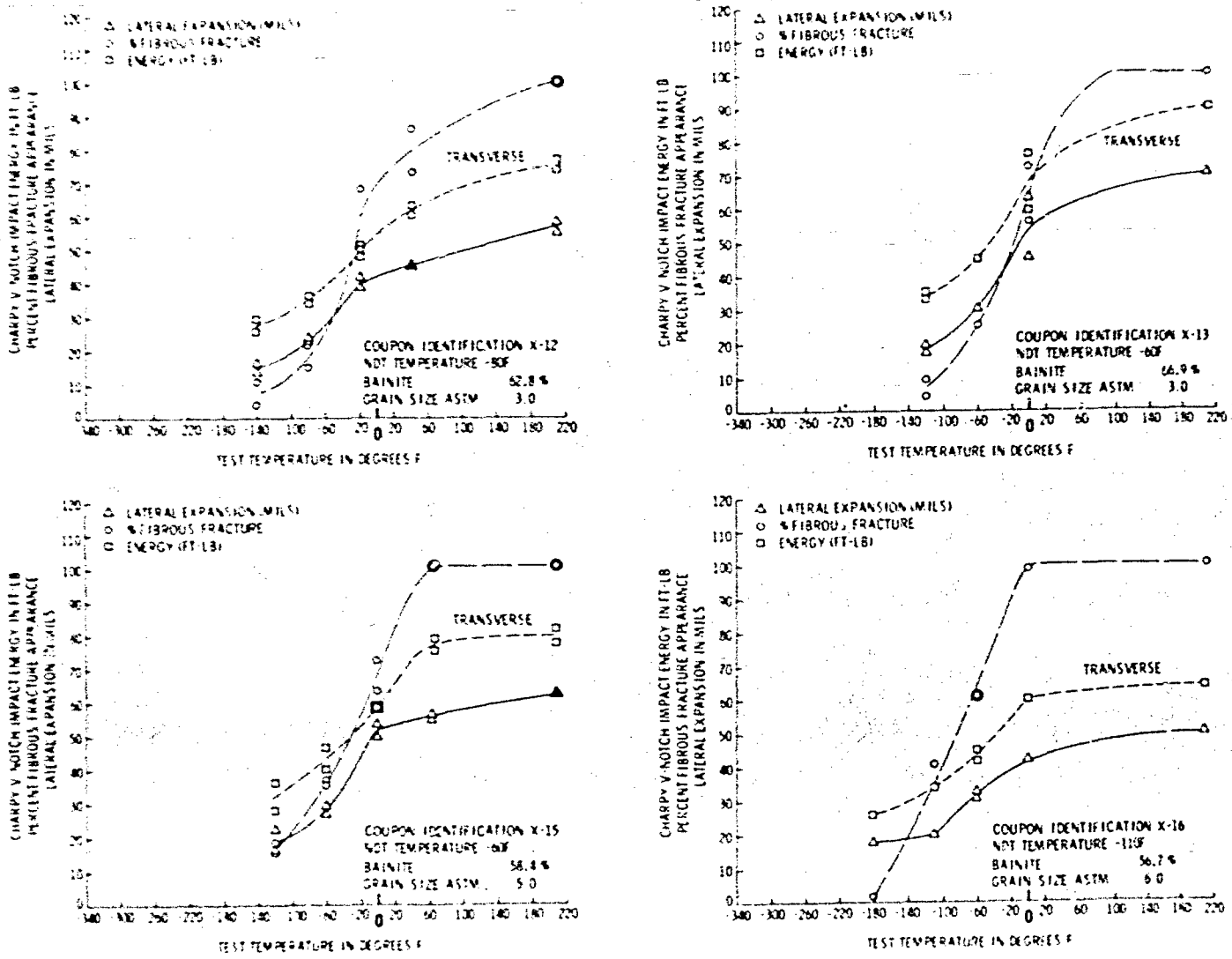

Figure D7 (Continued)

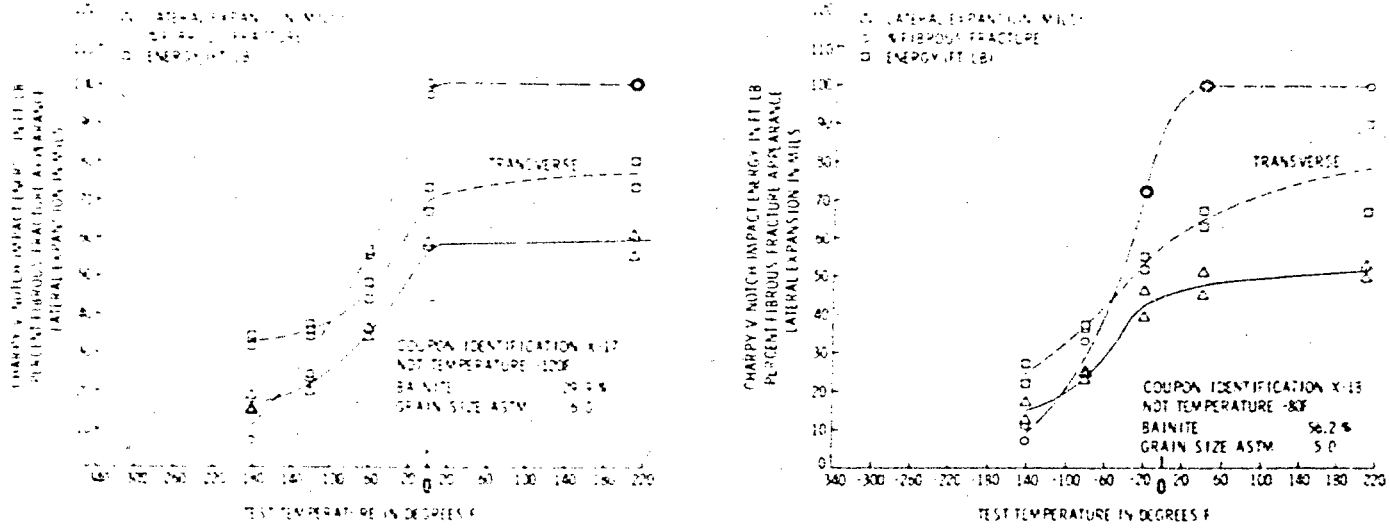

APPENDIX E

TIME-TEMPERATURE COOLING CURVES FOR DROP WEIGHT SPECIMENS WHEN TRANSFERRED FROM 1640 F FURNACE TO MOLTEN SALT BATHS AT EITHER 1200 F OR 875 F

INTRODUCTION

The actual time-temperature history was desired for the low-carbon Ni-Cr-Mo steel (5/8 x 2 x 5 in.) drop weight impact specimens used in these tests when they were transferred from a high temperature salt bath at 1640 F to a salt bath at either 1200 F or 875 F. In order to determine this thermal history a specimen was instrumented with a thermocouple at its center as recommended by Sinnott and Shyne[47] and the time-temperature history of the specimen and the bath were recorded at least every five seconds on a strip chart recorder. The experimental cooling curve is compared to the curve calculated using the method of Sinnott and Shyne.

SPECIMEN PREPARATION

A 0.087-inch diameter hole was drilled from one end, 2 1/2 inches deep into the center of the specimen. The hole was countersunk and tapped for 1/4--28 threads to a depth of 3/8 inch. A 7 inch length of 1/4 inch high pressure steel tubing was screwed tightly into the hole. An insulated 28-gauge Chromel-Alumel thermocouple was inserted in the tube and forced against the specimen at the bottom of the well. Another thermocouple was positioned in the low temperature salt bath adjacent to the specimen. Both thermocouples were attached to a multichannel recorder to alternately record the temperatures indicated by both thermocouples. The specimen was sand blasted between each run to remove all scale and salt and return it to a representative condition.

HEAT TREATMENT

The specimen was suspended vertically in a high temperature salt bath and allowed to come to 1640 F. It was held at 1640 F ±15 F for 30 minutes, minimum. The ±15 F bath temperature tolerance was used here and for the low temperature baths because it represented the tolerance of the commercial temperature controller used in this test as opposed to the closer ±5 F manual control used for the actual specimen heat treatments. From 4 to 5 inches of the thermocouple tubing was kept below the surface of the molten salt to minimize heat losses from the tube.

The specimen was transferred from the 1640 F bath to the low temperature bath within one or two seconds. The specimen was quenched vertically into the center of the low temperature bath and mildly agitated near the thermocouple recording the bath temperature. Multiple runs were made to allow for slight variations in the bath temperatures between runs.

RESULTS

The results of the cooling rate studies are plotted in Figure E1 and are compared to the salt-bath cooling rate predicted using the instantaneous film coefficient method of Sinnot and Shyne[47] with the following parameters:

Specimen Area	0.200 sq ft
Specimen Weight	1.771 lb
Mean Specific Heat, C_p*	
1640 to 1200 F	0.127 BTU/lb/F
1640 to 875 F	0.128 BTU/lb/F

Table E1 is a listing of the computer program used to predict cooling rates.

The variable names used in this program and their significance are given below:

ITB	Temperature of low temperature bath, 875, 900 or 1200 F.
ITS	Initial temperature of specimen, 1640 F
HF	Instantaneous film coefficient based on the difference between the average surface temperature of the specimen and the bath during the time interval THETA.
QTH	Average cooling rate in BTU/sec when cooling from MTS1 to MTS2.
THETA	Time to cool from a temperature MTS1 to MTS2, seconds
SUMTH	Total elapsed time to cool from ITS to MTS2, seconds.

The data shown in Figure E1 indicates reasonable agreement between experimental and predicted cooling rates. The low bath temperature experiments were run with an initial bath temperature of about 900 F rather than 875 F because of the characteristics of the commercial salt mix that was available in the salt bath when these tests were run.

The data show that it takes about 125 seconds for the center of the specimen to cool from 1640 F to 1210 F and about 140 seconds to cool from 1640 F to 885 F when a drop weight specimen is transferred to a 1200 F and an 875 F bath respectively.

*Based on data from U. S. Steel Corporation.

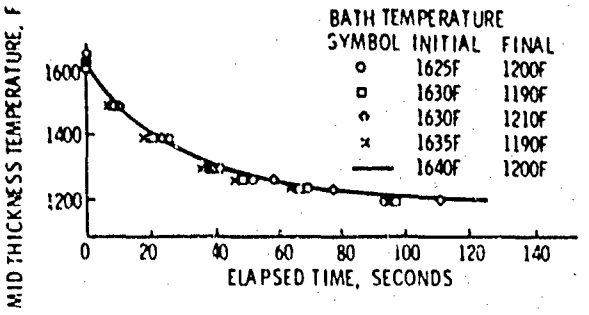

Figure E1a – Cooling Rate from 1640 F to 1200 F
(Average C_p = 0.127 BTU/lb/F)

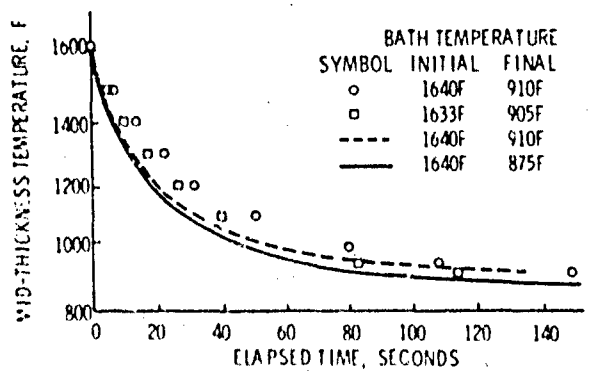

Figure E1b – Cooling Rate from 1640 F to 875 F
(Average C_p = 0.128 BTU/lb/F)

Figure E1 – Comparison of Actual Cooling Rates with Computed Cooling Rates for the Center of a 5/8 x 2 x 5 Inch Drop Weight Specimen

TABLE E1

Listing of a Computer Program Using the Instantaneous Film Coefficient Method of Sinnott and Shyne[47] to Predict the Instantaneous Cooling Rate and Time-Temperature Cooling Curve for a Low-Carbon Ni-Cr-Mo Alloy Steel Specimen 5/8 x 2 x 5 Inches When Transferred from a Neutral Salt Bath at 1640 F to a Neutral Salt Bath at 875 F

```
BUB

100 CP=.128
110 ITB=875.0
120 SUMTH=0.0
130 A=.19965
140 W=1.7708
150 ITS=1640.0
160 PRINT,"          *******  AGITATED BY HAND  *******"
170 PRINT,^
180 PRINT,"  MTS2          HF          QTH          THETA        SUMTH"
190 DØ 20 M=1,80
200 MTS2=ITS-M*10
210 IF(ITB-MTS2)15,20,20
220 15 MTS1=ITS-(M-1)*10
230 HF=93.0*EXP(0.0015*((MTS1+MTS2)*0.5)-ITB))
240 QTH=HF*A*(MTS1-ITB)/3600.0
250 THETA=(W*CP*(MTS1-MTS2)/QTH)
260 SUMTH=SUMTH+THETA
270 PRINT,MTS2,HF,QTH,THETA,SUMTH
280 20 CONTINUE
290 END
```

REFERENCES

1. Meklowitz, J., "The Effect of Temperature and Material Structure on the Fracture Properties of Medium-Carbon Steel," ASTM Proc., Vol. 49, pp. 602–617 (1949).

2. Hodge, J. M. et al., "The Effect of Ferritic Grain Size on Notch Toughness," Metals Transactions, pp. 233–240 (Mar 1949).

3. Sinclair, G. M. and Dolan, T. J., "Some Effects of Austenitic Grain Size and Metallurgical Structure on the Mechanical Properties of Steel," ASTM Proc., Vol. 50, pp. 587–616 (1950).

4. Geil, G. W. et al., "Influence of Nitrogen on the Notch Toughness of Heat-Treated 0.3 Percent-Carbon Steels at Low Temperatures," J. Res. of National Bureau of Standards, Vol. 48, No. 3, pp. 193–200 (Mar 1952).

5. Armstrong, T. N. et al., "Transition from Ductile to Brittle Behavior in Pressure Vessel Steels," Welding J., Vol. 31, pp. 371s–380s (Aug 1952).

6. Frazier, R. H. et al., "Influence of Heat Treatment on the Ductile-Brittle Transition Temperature of Semikilled Steel Plate," Trans. AIME, pp. 323–329 (Feb 1955).

7. Barrett, C. S., "Metallurgy at Low Temperatures – Edward DeMille Campbell Memorial Lecture," ASM Trans., Vol. 49, pp. 53–117 (1957).

8. Gross, J. H. and Stout, R. D., "Effect of Microstructure on Notch Toughness, Part II," Welding J., pp. 117s–122s (Mar 1955).

9. Schwartzbart, H. and Sheehan, J. P., "How Carbon Content Affects Impact Properties," Iron Age, pp. 85–89 (9 Aug 1956).

10. Schwartzbart, H. and Sheehan, J. P., "How Boron, Grain Size Affects Impact Properties," Iron Age, pp. 102–106 (16 Aug 1956).

11. Schwartzbart, H. and Sheehan, J. P., "How Fracture Type, Specimen Size Affect Impact Properties," Iron Age, pp. 107–110 (23 Aug 1956).

12. Mikus, E. B. and Siebert, C. A., "A Study of the Role of Carbon in Temper Embrittlement," Trans. ASM, Vol. 50, pp. 682–704 (1958).

13. Williams, M. L., "Correlation of Metallurgical Properties and Service Performance of Steel Plates from Fractures Ships," Welding J., pp. 445s–454s (Oct 1958).

14. Gross, J. H. and Stout, R. D., "The Effect of Microstructure on Notch Toughness – Part I," Welding J., Vol. 30, pp. 481s–485s (Oct 1951).

15. Rees, W. P., Hopkins, B. E., and Tipler, H. R., "Tensile and Impact Properties of Iron and Some Iron Alloys of High Purity," J. Iron and Steel Institute, Vol. 169, pp. 157–168 (Oct 1951).

16. Gross, J. H. and Stout, R. D., "The Effect of Microstructure on Notch Toughness – Part II," Welding J., Vol. 35, pp. 117s–122s (Mar 1955).

17. Gross, J. H. and Stout, R. D., "The Effect of Microstructure on Notch Toughness – Part III," Welding J., Vol. 36, pp. 72s–76s (Feb 1956).

18. Danko, J. C. and Stout, R. D., "The Effect of Sub-Boundaries and Carbide Distribution on the Notch Toughness of an Ingot Iron," Trans. ASM, Vol. 49, pp. 189–203 (1957).

19. Weaver, A. P., "Impact Characteristics and Mechanical Properties of Leaded and Nonleaded C-1050 and C-1141 Steels," Trans. ASM, Vol. 49, pp. 464–481 (1957).

20. Kottcamp, E. H. and Stout, R. D., "Effect of Microstructure on Notch Toughness – Part IV," Welding J., Vol. 38, pp. 435s–440s (Nov 1959).

21. Gross, J. H., "Comparison of Charpy V-Notch and Drop-Weight Tests for Structural Steels," Welding J., Vol. 39, pp. 59s–69s (Feb 1960).

22. Irvine, K. J., "The Development of High-Strength Steels," J. Iron and Steel Institute, Vol. 200, pp. 820–833 (Oct 1962).

23. Capus, J. M., "Austenite Grain Size and Temper Brittleness," J. Iron and Steel Institute, Vol. 200, pp. 922–927 (Nov 1962).

24. Boulger, F. W. and Hansen, W. R., "The Effect of Metallurgical Variables in Ship-Plate Steels on the Transition Temperatures in the Drop-Weight and Charpy V-Notch Tests," Ship Structure Committee Report SSC-145, AD 294827 (3 Dec 1962).

25. Gulyayev, A. P., "Effect of Chromium and Nickel on Toughness of Steel," Metal Science and Heat Treatment of Metals, pp. 491–493 (Nov–Dec 1962).

26. Newhouse, D. L., "Relationships Between Charpy Impact Energy, Fracture Appearance and Test Temperature in Alloy Steels," Welding J., Vol. 42, pp. 105s–111s (Mar 1963).

27. Irvine, K. J. and Pickering, F. B., "The Impact Properties of Low Carbon Bainitic Steels," J. Iron and Steel Institute, Vol. 201, pp. 518–531 (Jun 1963).

28. Irvine, K. J. and Pickering, F. B., "Low-Carbon Steels with Ferrite-Pearlite Structures," J. Iron and Steel Institute, Vol. 201, pp. 944–959 (Nov 1963).

29. Spektor, Y. I., Sarrak, V. I. and Entin, R. I., "Brittle Failure and the Fine Structure of Steel," Phys. Metal. Metallog., Vol. 18, n. 6, pp. 107–111 (1964).

30. Masubuchi, K., Monroe, R. E. and Martin, D. C., "Interpretative Report on Weld-Metal Toughness," Ship Structure Committee Report SSC-169 (Jul 1965).

31. Jolley, W. and Kottcamp, E. H., "A Study of the Toughness Differences Between Aluminum-Killed and Semikilled Steels," Trans. ASM, Vol. 59, pp. 439–456 (Sep 1966).

32. Roper, C. R. and Stout, R. D., "Weldability and Notch Toughness of Heat-Treated Carbon Steels," Welding J., pp. 385s–392s (Sep 1968).

33. Hollomon, J. H., Jaffe, L. D., McCarthy, D. E. and Norton, M. R., "The Effects of Microstructure on the Mechanical Properties of Steel," Trans. ASM, Vol. 38, pp. 807–844 (1947).

34. Taber, A. P., Thorlin, J. F. and Wallace, J. F., "Influence of Composition on Temper Brittleness in Alloy Steels," Trans. ASM, Vol. 42, pp. 1033–1055 (1950).

35. Irvine, K. J. and Pickering, F. B., "Low-Carbon Bainitic Steels," J. Iron and Steel Institute, pp. 292–309 (Dec 1957).

36. Steven, W., Balajiva, K., "The Influence of Minor Elements on the Isothermal Embrittlement of Steels," J. Iron and Steel Institute, Vol. 193, pp. 141–147 (Oct 1959).

37. Capus, J. M. and Mayer, G., "The Influence of Trace Elements on Embrittlement Phenomena in Low-Alloy Steels," Metallurgia, Vol. 62, pp. 133–138 (Oct 1960).

38. Pense, A. W., Stout, R. D. and Kottcamp, Jr., E. H., "A Study of Subcritical Embrittlement in Pressure Vessel Steels," Welding J., Vol. 42, n. 12, pp. 541s–546s (Dec 1963).

39. Baron, H. G. and Turner, S., "Effects of Residual Elements on Brittleness in Hardened and Tempered Forgings of Nickel-Chromium-Molybdenum Steel," J. Iron and Steel Institute, Vol. 203, pp. 1229–1236 (Dec 1965).

40. Lubahn, J. D. and Chu, H. P., "Optimum Carbon Content for Tempered Martensitic Steels," Trans. ASME, J. Basic Eng., pp. 1–7 (Mar 1968).

41. Low, Jr., J. R., Goodman, S. R. and Smith, C. L., "Grain Boundary Segregation of Impurities in Metals and Intergranular Brittle Fracture," Carnegie-Mellon University Report No. 031–727–1, ONR Tech. Report 1, (Mar 1969).

42. Hehemann, R. F., Luken, V. J., and Troiano, A. R., "The Influence of Bainite on Mechanical Properties," Trans. ASM, Vol. 49, pp. 409–426 (1957).

43. Salive, M. L. and Langley, R. J., "Documentation of XIRE – A Multivariable Tape Regression Analysis Program with Rule-of-Thumb Guides for Interpretation of Results by Non-Statisticians," NSRDC Report 3702 (Aug 1971).

44. Willner, A. R. and Salive, M. L., "The Effects of Tempered Nonmartensitic Products on the Notch Toughness and Mechanical Properties of an HY-80 Steel," David Taylor Model Basin Report 1605 (Jan 1965).

45. Willner, A. R. and Salive, M. L., "Effects of Tempering Above the Lower Critical Temperature A_{C1} on the Properties of an HY-80 Steel," David Taylor Model Basin Report 2140 (Jan 1966).

46. Dieter, G. E., Jr., "Mechanical Metallurgy," McGraw-Hill (1961) p. 121 and pp. 188–189.

47. Sinnott, M. J. and Shyne, J. C., "An Investigation of the Quenching Characteristics of Salt Bath," Trans. ASM, Vol. 44, pp. 758–774 (1952).

48. Seitz, F., "The Physics of Metals," McGraw-Hill, New York (1943).

49. Crafts, W. and Lamont, J. L., "Hardenability and Steel Selection," Sir Isaac Pitman and Sons, Ltd., London (1949).

50. Hollomon, J. H. and Jaffe, L. D., "Ferrous Metallurgical Design," J. Wiley and Sons, Inc., New York (1947).

51. Hall, A. M., "Nickel in Iron and Steel," J. Wiley and Sons, Inc., New York (1953).

52. Case, S. L. and VanHorn, K. R., "Aluminum in Iron and Steel," J. Wiley and Sons, Inc., New York (1953).

53. Comstock, G. F., "Titanium in Iron and Steel," J. Wiley and Sons, Inc., New York (1955).

54. Grange, R. A., Shortsleeve, F. J., and Hilty, D. C., Binder, W. O., Motock, G. S., and Offenhauer, C. M., "Boron, Calcium, Columbium and Zirconium in Iron and Steel," J. Wiley and Sons, Inc., New York (1957).